iScience

CellPress
OPEN ACCESS

Article

Anti-V2 antibodies virus vulnerability revealed by envelope V1 deletion in HIV vaccine candidates

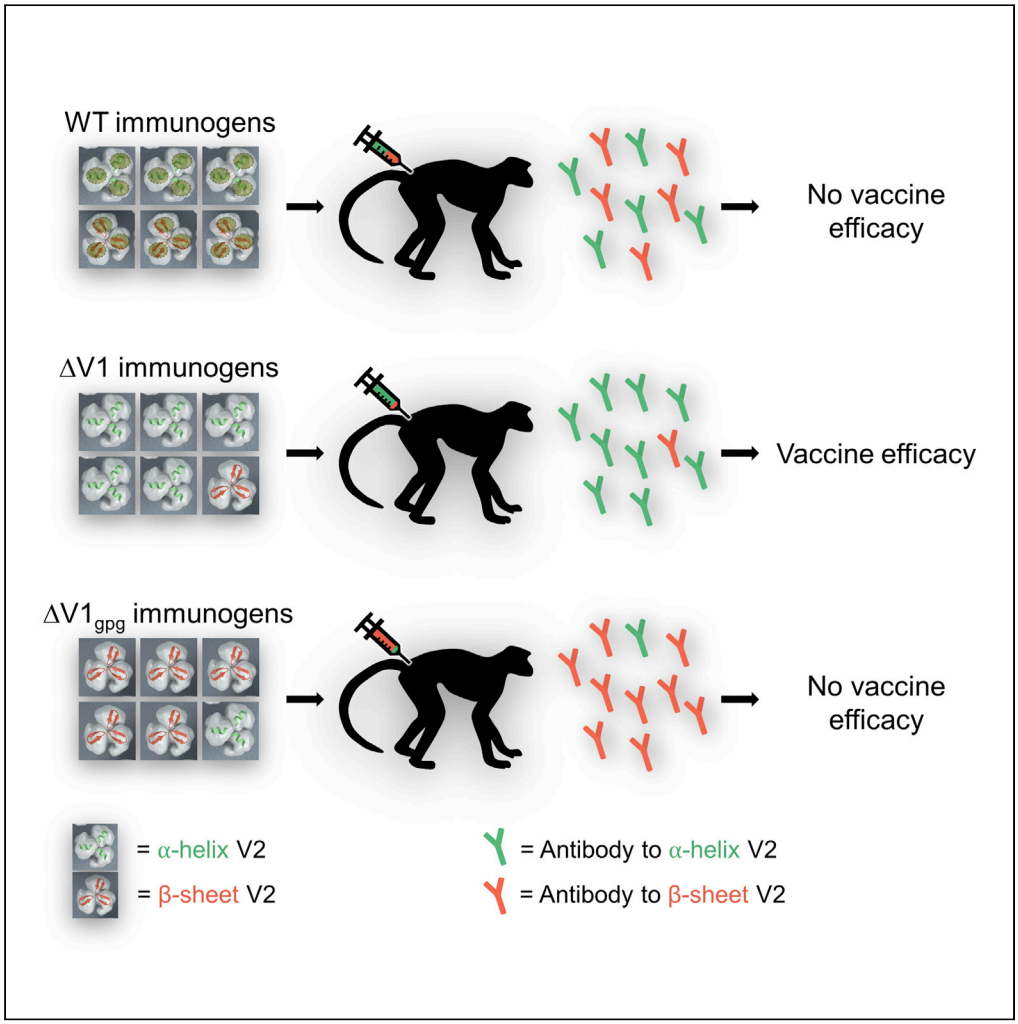

Isabela Silva de Castro, Giacomo Gorini, Rosemarie Mason, ..., Mangala Rao, Timothy J. Cardozo, Genoveffa Franchini

timothy.cardozo@nyulangone.org (T.J.C.)
franchig@mail.nih.gov (G.F.)

HIGHLIGHTS

HIV vaccine candidate protects against SIV_{mac251} acquisition

V1 deleted envelope immunogens with V2 in α-helical conformation are protective

V2-specific ADCC as correlate of risk

Anti-V1 antibodies interfere with V2-specific ADCC

Silva de Castro et al., iScience *24*, 102047
February 19, 2021 © 2021
https://doi.org/10.1016/j.isci.2021.102047

iScience

CellPress
OPEN ACCESS

Article

Anti-V2 antibodies virus vulnerability revealed by envelope V1 deletion in HIV vaccine candidates

Isabela Silva de Castro,[1,17] Giacomo Gorini,[1,17] Rosemarie Mason,[2,17] Jason Gorman,[3] Massimiliano Bissa,[1] Mohammad A. Rahman,[4] Anush Arakelyan,[5] Irene Kalisz,[6] Stephen Whitney,[6] Manuel Becerra-Flores,[7] Eric Ni,[7] Kristina Peachman,[8,9] Hung V. Trinh,[8,9] Michael Read,[9,18] Mei-Hue Liu,[10] Donald Van Ryk,[10] Dominic Paquin-Proulx,[8,9] Zhanna Shubin,[8,9] Marina Tuyishime,[11] Jennifer Peele,[11] Mohammed S. Ahmadi,[3] Raffaello Verardi,[3] Juliane Hill,[2] Margaret Beddall,[2] Richard Nguyen,[2] James D. Stamos,[1] Dai Fujikawa,[1] Susie Min,[10] Luca Schifanella,[1] Monica Vaccari,[1] Veronica Galli,[1] Melvin N. Doster,[1] Namal P.M. Liyanage,[1] Sarkis Sarkis,[1] Francesca Caccuri,[1] Celia LaBranche,[11] David C. Montefiori,[11] Georgia D. Tomaras,[12] Xiaoying Shen,[12] Margherita Rosati,[13] Barbara K. Felber,[14] George N. Pavlakis,[13] David J. Venzon,[15] William Magnanelli,[16] Matthew Breed,[16] Josh Kramer,[16] Brandon F. Keele,[16] Michael A. Eller,[8,9] Claudia Cicala,[10] James Arthos,[10] Guido Ferrari,[11] Leonid Margolis,[5] Marjorie Robert-Guroff,[4] Peter D. Kwong,[3] Mario Roederer,[2] Mangala Rao,[9] Timothy J. Cardozo,[7,*] and Genoveffa Franchini[1,19,*]

SUMMARY

The efficacy of ALVAC-based HIV and SIV vaccines in humans and macaques correlates with antibodies to envelope variable region 2 (V2). We show here that vaccine-induced antibodies to SIV variable region 1 (V1) inhibit anti-V2 antibody-mediated cytotoxicity and reverse their ability to block V2 peptide interaction with the $\alpha_4\beta_7$ integrin. SIV vaccines engineered to delete V1 and favor an α helix, rather than a β sheet V2 conformation, induced V2-specific ADCC correlating with decreased risk of SIV acquisition. Removal of V1 from the HIV-1 clade A/E A244 envelope resulted in decreased binding to antibodies recognizing V2 in the β sheet conformation. Thus, deletion of V1 in HIV envelope immunogens may improve antibody responses to V2 virus vulnerability sites and increase the efficacy of HIV vaccine candidates.

[1]Animal Models and Retroviral Vaccines Section, National Cancer Institute, Bethesda, MD 20892, USA

[2]ImmunoTechnology Section, Vaccine Research Center, National Institute of Allergy and Infectious Diseases, National Institutes of Health, Bethesda, MD 20892, USA

[3]Structural Biology Section, Vaccine Research Center, National Institute of Allergy and Infectious Diseases, National Institutes of Health, Bethesda, MD 20892, USA

[4]Immune Biology of Retroviral Infection Section, National Cancer Institute, Bethesda, MD 20892, USA

[5]Section on Intercellular Interactions, Eunice Kennedy-Shriver National Institute of Child Health and Human Development, National Institutes of Health, Bethesda, MD 20892, USA

[6]Advanced Bioscience Laboratories, Rockville, MD 20850, USA

[7]New York University School of Medicine, NYU Langone Health, New York, NY 10016, USA

[8]Henry M. Jackson Foundation for the Advancement of Military Medicine, Bethesda, MD 20817, USA

Continued

INTRODUCTION

The HIV recombinant canarypox-derived vector (ALVAC) and gp120-envelope proteins formulated in alum vaccine platform tested in the RV144 HIV vaccine trial was the first to reduce the risk of HIV acquisition in humans (31.2%) (Rerks-Ngarm et al., 2009). Serum IgG to the gp70-V1/V2 scaffold (Haynes et al., 2012) and to linear V2 peptides (Gottardo et al., 2013; Zolla-Pazner et al., 2014) have been identified as correlates of reduced risk of HIV acquisition. Sieve analysis further demonstrated genetic markers of immunologic pressure at positions 169 and 181 (Rolland et al., 2012) of V2, a region that binds to the $\alpha_4\beta_7$ integrin (Lertjuthaporn et al., 2018). V2 is structurally polymorphic and can adopt β strand or α-helical conformations. However, V2 interaction with the $\alpha_4\beta_7$ integrin is inhibited preferentially by antibodies recognizing its α-helical conformation (Lertjuthaporn et al., 2018).

The SIV_{mac251} macaque model, in which vaccinated animals are mucosally exposed to the highly pathogenic SIV_{mac251} at a dosage far in excess of HIV transmission in humans, recapitulated the modest vaccine efficacy observed in RV144 and identified antibodies to V2 as a correlate of reduced risk of SIV acquisition (Pegu et al., 2013; Vaccari et al., 2016). Furthermore, substitution of the alum adjuvant with MF59 (Vaccari et al., 2016) in the same animal model abolished the vaccine protection afforded by the ALVAC/gp120 vaccine platform, thereby predicting the recently announced lack of efficacy in the HVTN-702 HIV trial that used the MF59 adjuvant (Cohen, 2020).

The need to develop immunogens able to increase the efficacy of HIV vaccine candidates remains urgent. We found that antibodies to V1 interfere with the cytocidal function of antibodies to V2 and demonstrate here that the removal of V1, engineered to favor an α-helical conformation of V2, increases V2-specific cytocidal antibodies appearing to increase vaccine efficacy.

RESULTS

Antibodies to a V1 region adjacent to V2 (V1a) are associated with increased SIV_{mac251} acquisition

We investigated the serum antibody responses to V1 and V2 using linear peptide arrays in a cohort of 78 macaques immunized with four different vaccine regimens and exposed by the same route to the same dose of an identical SIV_{mac251} stock (Figure S1A). The gp120 protein bivalent boost was adjuvanted in alum in three regimens (ALVAC-SIV/gp120 + alum, DNA-SIV/ALVAC-SIV/gp120 + alum, and Ad26-SIV/ALVAC-SIV/gp120 + alum) and in MF59 in the fourth (ALVAC-SIV/gp120 + MF59) (Vaccari et al., 2016, 2018). The efficacy of these regimens was evaluated as the average per-challenge risk of SIV_{mac251} acquisition compared with unvaccinated controls following intrarectal exposure to repeated, low doses of the virus. For simplicity, we hereafter refer to ALVAC-SIV/gp120 + alum and the DNA-SIV/ALVAC-SIV/gp120 + alum (with respective vaccine efficacies of 44% and 52%; $p < 0.05$) as the *protective* regimens (Figures S1B and S1C), and to ALVAC-SIV/gp120 + MF59 and Ad26-SIV/ALVAC-SIV/gp120 + alum (vaccine efficacies of 9% and 13%; $p > 0.05$) as *non-protective* regimens (Figures S1D and S1E) (Vaccari et al., 2016, 2018).

The levels of sera antibody reactivity to overlapping linear V1 (Starcich et al., 1986) peptides 15–24 (Figure S1F) did not differ between *protective* and *non-protective* vaccines (Figure S1G). However, when all vaccinated macaques were analyzed, animals with above-median antibody levels to V1 had a trend toward increased risk of SIV_{mac251} acquisition ($p = 0.0658$; Figure S1H). Analysis of antibody responses to V1 peptides in *protective* and *non-protective* vaccine subgroups showed that anti-V1 antibodies were associated with an increased risk of SIV_{mac251} acquisition only in the *non-protective* group (Figures 1A and S1I). Antibody responses to V1 peptides 23 and 24, encompassing the amino acid segment NETSSCIAQNNCTGLEQEQMISCKF, revealed higher reactivity in the *non-protective* vaccine subgroup when compared with the *protective* group (Figure 1B). The region designated here as V1a (peptide 23 to 24) lies directly N-terminal to a cryptic $\alpha_4\beta_7$ integrin-binding site (Tassaneetrithep et al., 2014) in V2 (V2b), with both V1a and V2b being part of a continuous, exposed peptide segment at the extreme apex of the envelope trimer (Gorman et al., 2016; Julien et al., 2013; Liu et al., 2008; Pancera et al., 2014) (Figures 1C and 1D). V1a is also in tertiary contact with the V2 region (V2c) that contains the canonical tripeptide shown to bind to the $\alpha_4\beta_7$ integrin (Arthos et al., 2008; Nakamura et al., 2012), as depicted in Figure 1D in a 3D homology model of the SIV_{mac251} trimer based on the HIV BG505 cryo-EM structure. The V1/V2 domain of a related cryo-EM structure of SIVcpz*Ptt* is nearly identical (Andrabi et al., 2019). Based on these structural relationships, we hypothesized that antibodies to V1a may influence vaccine efficacy by interfering with antibody binding to V2 and tested different assays of anti-V1 and anti-V2-specific monoclonal antibodies (mAbs) cloned from vaccinated protected or vaccinated SIV-infected animals (Mason et al., 2016).

Antibody to V1a decreases anti-V2 antibody cytotoxicity and ability to inhibit gp120 binding to $\alpha_4\beta_7$

The mAbs (NCI09 and NCI05) cloned from the vaccinated and protected animal P770 (Vaccari et al., 2016) were cross-reactive with SIV_{mac251} and SIV_{smE543} gp120, V1/V2 scaffolds, and cyclic V2 peptides (Figures S2A–S2C). Linear peptide mapping (Figure S2D), peptide competition (Figures S2E and S2F), and crystallography (Figures S3 and S4; PDB: 6VRY) demonstrated that NCI09 recognized the TGLKRDKTKEY epitope in V2b. NCI05 did not bind to linear $SIV_{mac251\text{-}K6W}$ peptides (Figure S2C), but its binding to cyclic V2 was competed by peptides encompassing the SIV_{mac239}TGLKRDKKKEYNETWYSAD amino acid sequence (Figure S2F). From the same animal, we also obtained two V1-specific mAbs, NCI04 and NCI06, recognizing the CNKSETDRWGLTK epitope located N-terminal to V1a (Figures 1C and S2C). None of these mAbs neutralized tier 2 SIV_{mac251} or SIV_{SME660}. NCI05 neutralized tier 1 SIV_{SME660} but not tier 1 SIV_{mac251}. NCI06 and NCI09 had low neutralizing activity against tier 1 SIV_{mac251} (Figure S2G). Both NCI05 and NCI09 bound to gp120 on the surface of Gag-positive SIV_{mac239}-infected cells (Figures 1E, 1F, S5A, and S5B) and to SIV_{mac251} virions (Figure 1G). Functionally, NCI05 and NCI09 mAbs inhibited SIV gp120 binding to the $\alpha_4\beta_7$ integrin in a cell adhesion assay (Lertjuthaporn et al., 2018; Wibmer et al., 2018) (Figure 2A) and mediated antibody-dependent cell-mediated cytotoxicity (ADCC; Figure 2B). Of

[9]U.S. Military HIV Research Program, Walter Reed Army Institute of Research, Silver Spring, MD 20910, USA

[10]Laboratory of Immunoregulation, National Institute of Allergy and Infectious Diseases, National Institutes of Health, Bethesda, MD 20892, USA

[11]Division of Surgical Sciences, Duke University School of Medicine, Durham, NC 27701, USA

[12]Duke Human Vaccine Institute, Duke University, Durham, NC 27701, USA

[13]Human Retrovirus Section, National Cancer Institute, Frederick, MD 21702, USA

[14]Human Retrovirus Pathogenesis Section, National Cancer Institute, Frederick, MD 21702, USA

[15]Biostatistics and Data Management Section, Center for Cancer Research, National Cancer Institute, Bethesda, MD 20892, USA

[16]AIDS and Cancer Virus Program, Leidos Biomedical Research Inc., Frederick National Laboratory, Frederick, MD 21704, USA

[17]These authors contributed equally to this work.

[18]Present address: Vaccine Research Center, National Institute of Allergy and Infectious Diseases, National Institutes of Health, Bethesda, MD, USA.

[19]Lead contact

*Correspondence: timothy.cardozo@nyulangone.org (T.J.C.), franchig@mail.nih.gov (G.F.)

https://doi.org/10.1016/j.isci.2021.102047

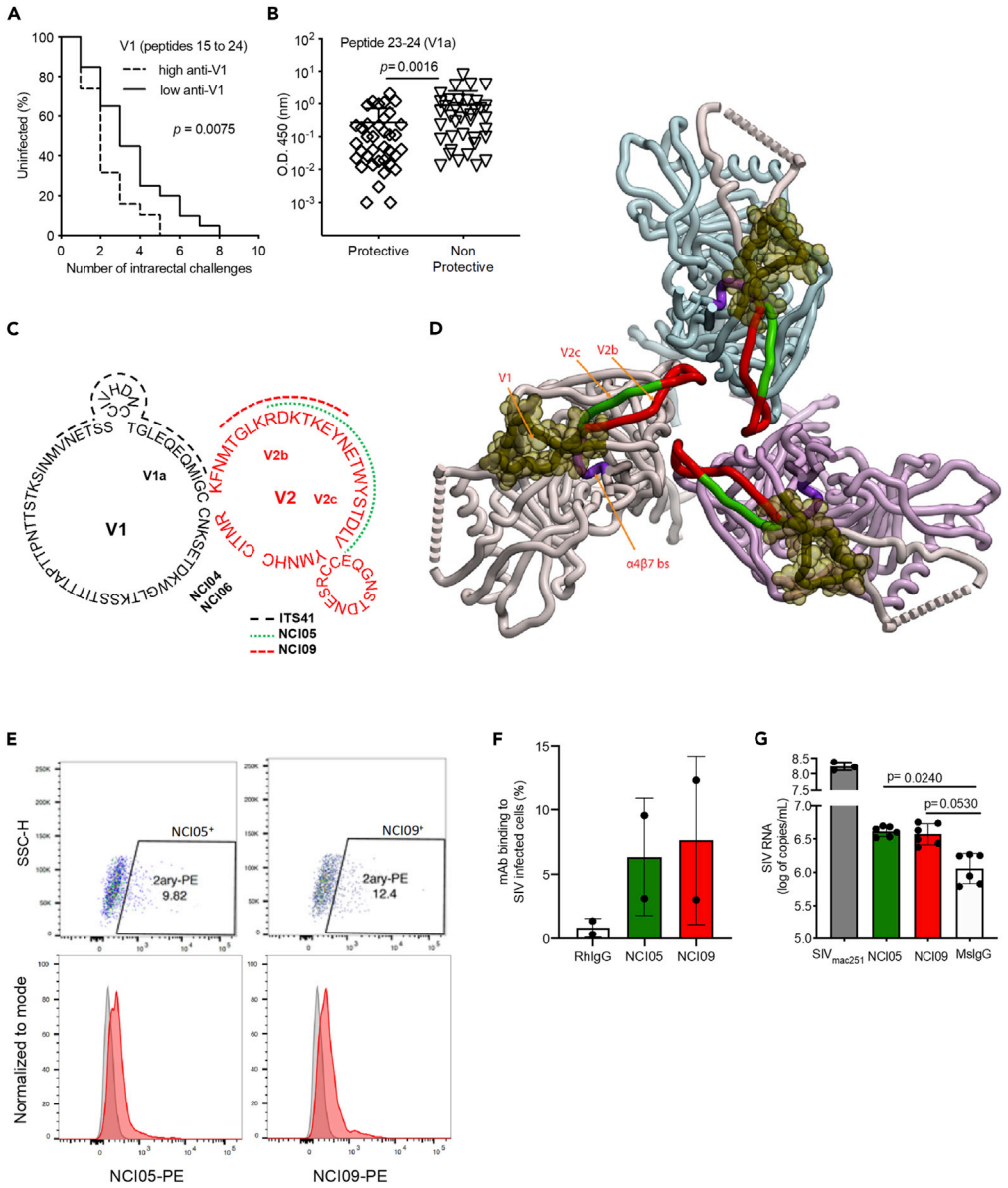

Figure 1. V1 Antibody levels are associated with increased risk of SIV_{mac251} acquisition

(A) Time of acquisition in macaques immunized with *non-protective* vaccines and mean O.D. sum of serum responses to V1 peptides 15–24 at week 27: high (n = 19) and low (n = 20) anti-V1 values.

(B) Serum antibody against peptides 23 and 24 (V1a) in animals vaccinated with *protective* (diamonds, n = 39) and *non-protective* (inverted triangles, n = 39) vaccines 3 weeks after the last immunization and 1 week before challenge (week 27), data shown as mean with SD.

(C) Amino acid sequence of V1 and V2 ($SIV_{mac251-K6W}$). Sequences are represented as follows: V1 (black); V1a (black dotted line); V2 (red); V2b (red dotted line; recognized by mAb NCI09); V2c (green dotted line; recognized by mAb NCI05). MAb ITS41 recognizes the V1a epitope, and NCI04 and NCI06 recognize amino acids in the N-terminal region of V1.

(D) Spatial relationship of V1 (olive), V2b (red), V2c (green), and the canonical V2 tripeptide, DLV, that binds the $\alpha_4\beta_7$ integrin (purple) in the gp120 trimer.

(E) NCI05 and NCI09 binding to SIV_{mac239}-infected A66 p24 Gag-positive cells in a representative experiment of staining of SIV_{mac251}-infected cells.

(F) The average percentage of Gag and NCI05 positive (green) or NCI09 positive (red, n = 2), data shown as mean with SD.

(G) SIV_{mac251} virion capture assay (n = 7 experiments, black dots): virion input (gray) or virion captured by beads coated with NCI05 (green), NCI09 (red), or mouse IgG (negative control) (Rhesus IgG isotype was also used as a negative control, with n = 3, mean = 5.09 SIV RNA in transformed log copies/mL and SD = 0.08. Both NCI05 and NCI09 mAb were

Figure 1. *Continued*

statistically higher than Rhesus IG control, data not shown). Data in the graph are shown as mean with SD. Statistical analyses comparing two groups was done using Mann-Whitney test; when comparing three groups or more Kruskal-Wallis test with Dunn's multiple comparison test was used, and the infection curves were analyzed using Log Rank (Mantel-Cox test).
See Figure S1.

interest, the mAb ITS41 recognizing V1a (Mason et al., 2016) inhibited binding of NCI09 to the gp120 on the surface of SIV_{mac251}-infected cells (Figure 2C), as well as the binding of NCI05 and NCI09 mAbs to gp120 $SIV_{mac251\text{-}M766}$ (Lertjuthaporn et al., 2018; Wibmer et al., 2018) (Figures 2D and 2E). Prebound NCI05 and NCI09 were not affected by ITS41, demonstrating asymmetric competition (Figures S5C and S5D). The NCI06 mAb, which recognizes a peptide distal to V1a not in contact with V2b or V2c in the 3D envelope structure (Figures 1C and 1D), did not interfere with NCI09 binding to gp120 (Figures S5E and S5F). In addition, increasing amounts of ITS41 reversed NCI09 inhibition of gp120 binding to the $\alpha_4\beta_7$ integrin (Figures 2F and S5G) and inhibited NCI05 and NCI09-mediated ADCC (Figures 2G and 2H). NCI04 did not affect NCI05 or NCI09-mediated ADCC (Figures 2I and 2J). Of interest, both ITS41 and NCI04 mediate ADCC to a much lower extent than NCI05 and NCI09 despite having the identical Fc region since all antibodies were cloned in an expression vector that joined variable regions with the same Fc scaffold. This result highlights the importance of Fab properties and epitope accessibility for ADCC.

V1-deleted immunogens designed to favor V2 α-helical conformation reduce the risk of SIV_{mac251} acquisition

The functional interference of ITS41 with NCI05 and NCI09 raised the hypothesis that deletion of V1 in SIV/HIV envelope immunogens could increase V2 accessibility, enhance the level of V2 functional antibodies, and increase vaccine efficacy. To test this, we designed V1-deleted gp120 proteins ($gp120_{\Delta V1}$) by symmetrically truncating V1 at its stem, since its origin and insertion (stem) to the V1/V2 domain connect the A and B β strands (McLellan et al., 2011). The V1/V2 domain remaining after deletion of the gp120 V1 ($gp120_{\Delta V1}$) was energy minimized as previously described (Abagyan and Totrov, 1994; Cardozo et al., 1995). The search predicted a stable, low-energy, partially α-helical V2 conformation in gp120 (Figure 3A and Table S1). As control, we designed another V1-deleted gp120 ($gp120_{\Delta V1gpg}$) by inserting the Gly-Pro-Gly β turn at the excision point with the purpose of minimizing disruption to the crystallographically visualized V1/V2 Greek key β sheet fold (Figures 3B and Table S2). We then expressed M766-based $gp120_{\Delta V1}$ and $gp120_{\Delta V1gpg}$ proteins in Chinese Hamster Ovary (CHO) cells together with wild-type gp120 ($gp120_{WT}$; Table S3). The purified monomeric $gp120_{\Delta V1}$ and $gp120_{\Delta V1gpg}$ proteins were stable and unrecognized by the anti-V1 NCI06 and ITS41 mAbs (Figure S5H), bound to NCI05 and NCI09 by ELISA (Figures 3C–3E), immune precipitation, and western blot better than $gp120_{WT}$ (Figures S5H and S5I). Of interest, $gp120_{\Delta V1}$ and $gp120_{\Delta V1gpg}$ also bound better to simian soluble CD4 than the $gp120_{WT}$ (Figure 3F). These data are consistent with increased exposure of V2 epitopes and the CD4-binding site in the $gp120_{\Delta V1}$ and $gp120_{\Delta V1gpg}$ antigens (Ching and Stamatatos, 2010).

We tested the efficacy of the V1-deleted immunogens using a DNA-SIV-prime/ALVAC-SIV/with gp120 protein + alum monovalent boost regimen followed by low-dose intrarectal exposures to SIV_{mac251}. We designed a modified vaccine regimen aimed at magnifying a possible difference in the efficacy of the wild type and ΔV1 immunogens. Here, we halved the amount of SIV Gag DNA in the prime and performed a single protein boost (rather than two) with ALVAC-SIV using the SIV_{mac251} $gp120_{M766}$ alone, omitting the two SIV_{SME543} $gp120_{GC7V}$ protein boosts (Vaccari et al., 2016, 2018). In previous studies, the association between antibodies to V2 and a decreased risk of SIV_{mac251} acquisition were notably revealed by SIV_{SME543} antigens but, curiously, not by SIV_{mac251} antigens.

We vaccinated three groups of 14 macaques each with two inoculations (weeks 0 and 4) of plasmid DNAs expressing SIV $gp160_{WT}$ (group 1; Table S4), SIV $gp160_{\Delta V1}$ (group 2; Table S5), or SIV $gp160_{\Delta V1gpg}$ (group 3; Table S6) together with SIV p57 Gag. All groups received one boost at week 8 with ALVAC-SIV expressing $gp120_{WT}$, and each group was administered a final boost at week 12 consisting of the same ALVAC-SIV together with the $SIV_{mac251\text{-}M766}$ $gp120_{WT}$ (group 1), $gp120_{\Delta V1}$ (group 2), or $gp120_{\Delta V1gpg}$ (group 3) protein adjuvanted with alum Alhydrogel (Figure 3G). Alongside a simultaneous control group of 18 naive macaques, the vaccinated macaques were exposed weekly to a total of 11 low doses of SIV_{mac251} by the intrarectal route, beginning at 5 weeks from the last immunization (week 17). A significant

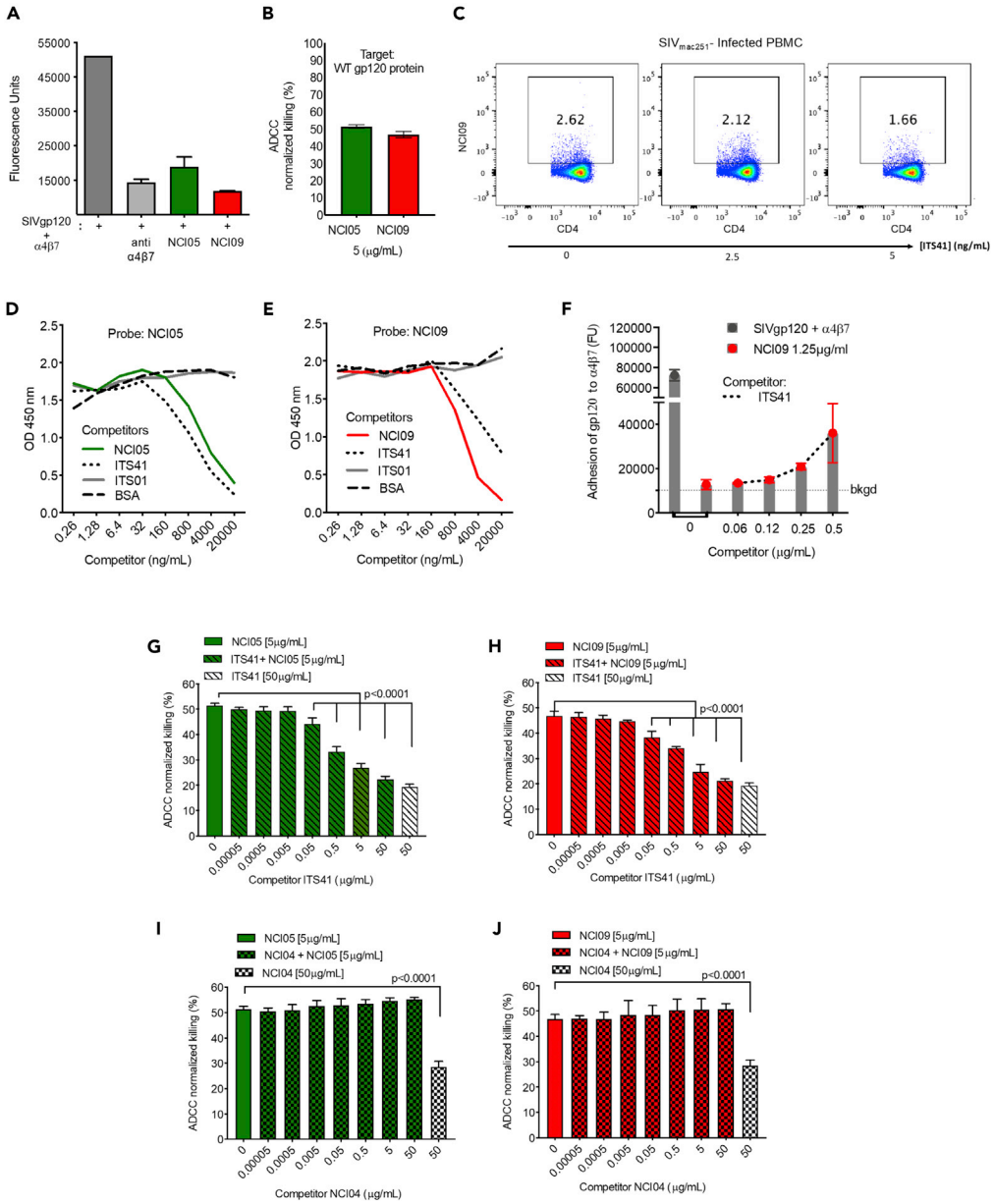

Figure 2. Functional activity of V1 and V2 mAbs

(A) Adhesion of gp120 $SIV_{mac251\text{-}M766}$ to the α4β7 integrin only (dark gray) in the presence of vedolizumab, a mAb anti-α4β7 integrin used as a positive control at a concentration of 0.5 μg/mL (light gray), or in the presence of NCI05 (green) and NCI09 (0.25 μg/mL; red). Data shown as mean with SEM.

(B) ADCC mediated by NCI05 and NCI09 in the CEM-based assay (n = 3), data shown as mean with SD.

(C) Competition of NCI09 binding to SIV_{mac251}-infected $CD4^+$ T cells by increasing amounts of ITS41 (0, 2.5, and 5 ng/mL). The dot plot displayed is of one representative experiment (n = 2).

(D and E) Inhibition of gp120 $SIV_{mac251\text{-}M766}$ binding to mAbs (D) NCI05 or (E) NCI09 by ITS41, or albumin and mAb ITS01 with CD4 binding specificity as controls.

(F) Adhesion of $SIV_{mac251\text{-}M766}$ to α4β7 integrin in the absence or presence of NCI09 (1.25μg/mL), or with increasing concentrations of prebound ITS41, followed by 1.25 μg/mL of NCI09. As the concentration of ITS41 is increased, the inhibitory activity of NCI09 is lost. Data shown as mean with SD.

(G) Inhibition of ADCC mediated by mAbs NCI05 and (H) NCI09 by increasing amounts of ITS41 (n = 3).

(I and J) NCI04 does not compete with (I) NCI05 or (J) NCI09-mediated ADCC (n = 3). Data shown as mean with SD.

Statistical analyses were performed using two-way ANOVA test with Dunnett's multiple comparison test.

See Figures S2–S5.

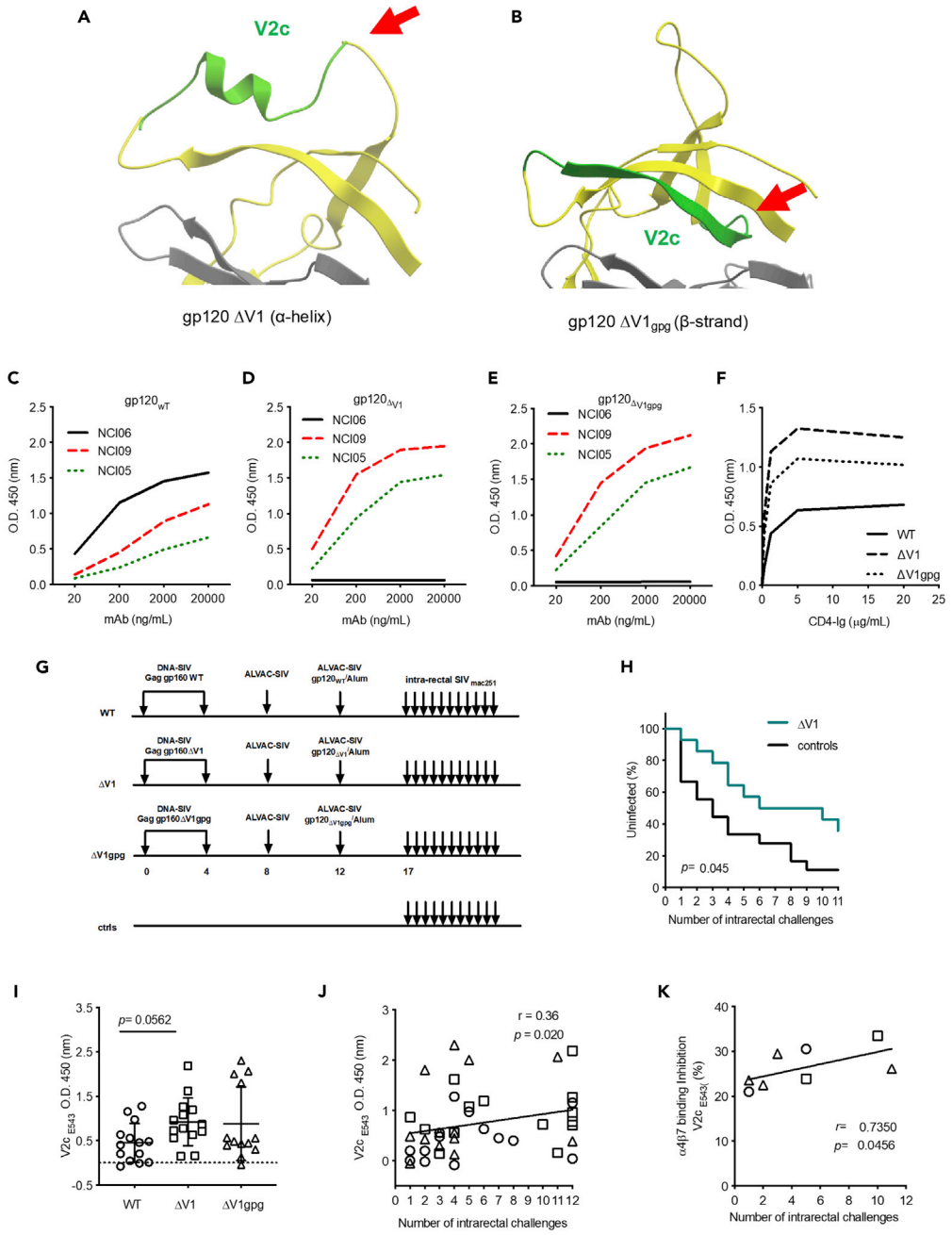

Figure 3. Vaccine design and virological outcome

(A) Model of the gp120$_{\Delta V1}$V2 α helix (green). The predicted α-helical structure of the V2c peptide was imposed on the V2c segment in gp120 and the local backbone energy minimized.

(B) Model of the gp120$_{\Delta V1gpg}$ β strand.

(C–E) ELISA binding of the purified (C) gp120$_{WT}$, (D), gp120$_{\Delta V1}$, and (E) gp120$_{\Delta V1gpg}$ with α-V2 mAbs NCI05 and NCI09 and the α-V1 mAb NCI06.

(F) Binding of simian CD4-Ig to gp120$_{WT}$, gp120$_{\Delta V1}$, and gp120$_{\Delta V1gpg}$.

(G) Schematic representation of the study design. Each vaccinated group included 14 young macaques, and the control group consisted of 18 naive young macaques. All animals were simultaneously exposed to weekly low doses of SIV$_{mac251}$ by the intrarectal route beginning at week 17.

(H) Risk of SIV$_{mac251}$ acquisition in animals immunized with ΔV1 envelope immunogens.

(I) Binding of week 17 (minus the baseline) serum to V2c$_{E543}$ peptide in immunized animals (WT, n = 14; ΔV1, n = 14; ΔV1gpg, n = 13), data shown as mean with SD.

Figure 3. *Continued*

(J) Correlation between serum antibodies to $V2c_{E543}$ and number of intrarectal challenges (WT, n = 14; ΔV1, n = 14; ΔV1gpg, n = 13).

(K) Correlation of serum inhibition of the $\alpha_4\beta_7$ integrin (expressed on RPMI8866 cells) to $V2c_{E543}$ and intrarectal challenges (WT, n = 2; ΔV1, n = 2; ΔV1gpg, n = 4). The correlation was performed only with data from animals that had inhibition above the assay cutoff. The infection curves were analyzed using Log Rank (Mantel-Cox test); data comparison between the three vaccinated groups was done with non-parametrical Kruskal-Wallis test with Dunn's multiple comparison test. The correlation analyses were performed using the non-parametric Spearman rank correlation method with the exact permutation two-tailed p-values calculated.

See Tables S1–S6 and Figures S5–S7.

decrease in the risk of SIV_{mac251} acquisition was observed following immunization with the $gp160_{\Delta V1}$ DNA and $gp120_{\Delta V1}$ protein immunogens engineered predominantly to favor the α-helical V2 conformation (vaccine efficacy 57%; p = 0.04; Figure 3H) but not following vaccination with wild-type envelope immunogens in group 1 or ΔV1gpg envelope immunogens in group 3 (Figures S6A and S6B). We observed no sustained, significant difference in the level of plasma viral RNA in animals that became infected in each vaccinated group compared with controls (Figures S6C–S6I) and only a transient trend of decreased SIV DNA levels in the rectal mucosa in group 2 (Figure S6J). The lack of vaccine efficacy in group 1 was not entirely unexpected given both the decreased amount of DNA used in the prime and, perhaps more importantly, the omission of the two SIV_{SME660} $gp120_{GC7V}$ boosts, as the antibody level to cyclic $V2_{E543}$ was a main correlate of reduced risk in two independent studies (Vaccari et al., 2016, 2018). The different outcomes in groups 2 and 3 compared with controls suggested that the inferred differences in the V2 conformation of the ΔV1 and ΔV1gpg immunogens might have quantitatively or qualitatively affected the antibody response to V2.

Antibodies inhibiting V2-$\alpha_4\beta_7$ interaction are associated with a decreased risk of SIV_{mac251} acquisition

Protection in RV144 correlated with a non-glycosylated V2 peptide that adopts an α-helical 3D conformation (Aiyegbo et al., 2017) and encompasses the canonical $\alpha_4\beta_7$ integrin-binding site in V2. In previous macaque studies, Ab binding to the V2 SIV_{SME543} peptide (but not SIV_{mac251}) was associated with a decreased risk of SIV_{mac251} acquisition (Vaccari et al., 2016, 2018). We therefore engineered an isolated V2 peptide ($V2c_{E543}$) corresponding to the V2c region of SIV_{SME543} (a clone of SIV_{SME660}) by identifying the beginning and ending amino acids between V2 positions 165 and 181 that adopt an α-helical conformation. Serum reactivity to the $V2c_{E543}$ peptide (DKKIEYNETWYSRD) was higher (trend) in animals immunized with the ΔV1 immunogens (Figure 3I) and correlated with a decreased risk of SIV_{mac251} acquisition (R = 0.36, p = 0.02; Figure 3J). Furthermore, the level of inhibition of $V2c_{E543}$ binding to the $\alpha_4\beta_7$ integrin in the eight animals that had values above the cutoff of the assay correlated with a decreased risk of SIV_{mac251} acquisition (R = 0.73, p = 0.046; Figures 3K and S7A). Reactivity to an equivalent SIV_{mac251} peptide did not reveal any association with risk of acquisition (data not shown). These animals were all immunized with SIV_{mac251}-based immunogens, suggesting that the $V2c_{E543}$ conformation is better able to capture antibodies associated with a decreased risk of SIV_{mac251} acquisition, in agreement with prior observations (Vaccari et al., 2016, 2018). Serum recognition of SIV_{mac251} V2 linear (Figures S7B–S7D) or cyclic peptide (Figure S7E), of the entire gp120 peptide array (sorted as responses to V4, C3, and C5, with responses to C3 and C5 being highest in animals immunized with the ΔV1 immunogens; Figures S7F–S7H), had no apparent association with a decreased risk of SIV_{mac251} acquisition.

ADCC to gp120-coated cells or SIV-infected cells correlates with a decreased risk of SIV_{mac251} acquisition

ADCC was a secondary correlate of reduced risk in individuals with low IgA levels in RV144 (Tomaras et al., 2013). ADCC activity mediated by the plasma from animals in the WT, ΔV1, and ΔV1gpg groups was performed using the target EGFP-CEM-NKr-CCR5-SNAP cells (Orlandi et al., 2016) (T lymphoblastoid cell line CEM-based assay) coated with purified $gp120_{WT}$, $gp120_{\Delta V1}$. Analysis of the coated cells demonstrated that NCI05 or NCI09 bound less well to CEM cells coated with $gp120_{WT}$ than those coated with $gp120_{\Delta V1}$ and $gp120_{\Delta V1gpg}$ (Figures S8A–S8D). However, ADCC measured with cells coated with the $gp120_{WT}$ did not differ among the animal groups (Figures 4A–4C), suggesting that V1 is not a major target of ADCC. Animals vaccinated with the ΔV1 immunogen (group 2) mounted significantly higher ADCC titers directed to ΔV1 than to the ΔV1gpg antigen (Figure 4B). Animals immunized with the ΔV1gpg immunogen (group 3) mounted lower ADCC titers directed to ΔV1gpg than to ΔV1 antigens (Figures 4C and Table S7). ADCC

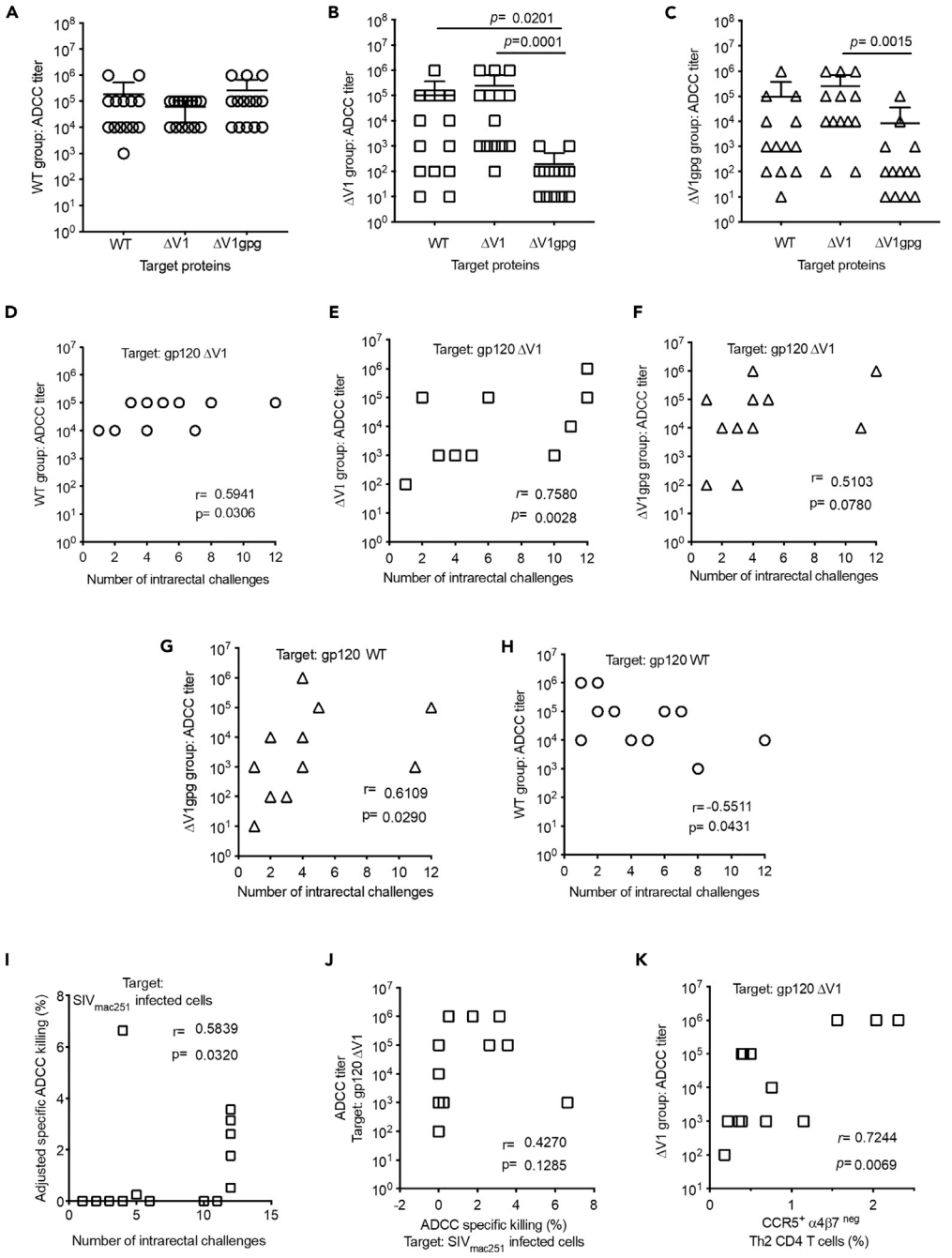

Figure 4. ADCC directed to ΔV1 gp120 associated with decreased risk of SIV_{mac251} acquisition

(A–C) CEM-based ADCC titers in animals immunized with (A) WT, (B) ΔV1, or (C) ΔV1gpg envelope immunogens on target cells coated with $gp120_{WT}$, $gp120_{\Delta V1}$, or $gp120_{\Delta V1gpg}$ (WT, n = 14; ΔV1, n = 14; ΔV1gpg, n = 13 animals). Data shown as mean with SD.

(D–F) Correlation of ADCC titers directed to the ΔV1 antigen in animals immunized with (D) WT, (E) ΔV1, or (F) ΔV1gpg envelope immunogens and time of SIV_{mac251} acquisition (WT, n = 14; ΔV1, n = 14; ΔV1gpg, n = 13 animals).

(G and H) Correlation of ADCC titers in animals immunized with (G) ΔV1gpg or (H) WT envelope immunogens on target cells coated with $gp120_{WT}$ and time of SIV_{mac251} acquisition (WT, n = 14; ΔV1gpg, n = 13 animals).

(I) Correlation of percentage of specific ADCC killing of SIV_{mac251}-infected cells in animals immunized with ΔV1 envelope immunogens and time of SIV_{mac251} acquisition.

(J) Correlation of ADCC titers on the CEM-based assay $gp120_{\Delta V1}$ and ADCC measured on SIV_{mac251}-infected cells in animals immunized with ΔV1 immunogens.

Figure 4. *Continued*

(K) Correlation of ADCC titers (week 17) on target CEM cells coated with $gp120_{\Delta V1}$ in animals immunized with ΔV1 immunogens and $CCR5^{+}\alpha_4\beta_7^{-}$ Th2 CD4 T cells (from PBMC collected at week 13; ΔV1, n = 14). Data comparison between the three vaccinated groups was done with non-parametrical Kruskal-Wallis test with Dunn's multiple comparison test, and the correlation analyses were performed using the non-parametric Spearman rank correlation method with exact permutation two-tailed p-values calculated.
See Table S7 and Figures S8.

was also performed using target cells infected with SIV_{mac251} (Lewis et al., 2019), and no differences were observed among the animal groups in this assay (Figure S8E). These data demonstrate that the two V1-deleted immunogens differ both in their ability to induce and to reveal cytotoxicity activity when used in the CEM-based ADCC assay.

We performed correlation analyses using the non-parametric Spearman test to assess the relationship of ADCC titers to the three antigens and the risk of SIV_{mac251} acquisition and found that ADCC directed to $gp120_{\Delta V1}$ protein is significantly correlated with a reduced acquisition risk in the WT and ΔV1-vaccinated groups, and a correlation (trend) was observed in the ΔV1gpg group (WT, R = 0.59, p = 0.03; ΔV1, R = 0.76, p = 0.003; ΔV1gpg, R = 0. 51, p = 0.08; Figures 4D–4F and Table S7), indicative of the ΔV1 antigen's ability to capture protective antibodies. In group 3, a correlation with decreased acquisition was also observed with ADCC directed to WT gp120 (R = 0. 61, p = 0.03; Figures 4G and Table S7). Strikingly, there was a correlation with ADCC directed to WT and an increased risk of SIV_{mac251} acquisition in animals immunized with the WT immunogens (R = −0.55; p = 0.04; Figures 4H and Table S7), suggesting that ADCC leading to a decreased risk of viral infection in all groups is better elicited and exhibited in the CEM-based ADCC assay by the ΔV1 protein.

ADCC activity measured on SIV_{mac251}-infected cells demonstrated no difference among the vaccinated groups (Figure S8E). However, the percentage of specific ADCC killing of SIV_{mac251}-infected cells correlated significantly with a decreased risk of SIV_{mac251} acquisition in the non-parametric Spearman test only in the ΔV1-immunized group (R = 0.58, p = 0.03; Figure 4I). In this group, the level of ADCC directed to CEM cells coated with the ΔV1 protein correlated (trend) with the ADCC measured against infected cells (R = 0.43, p = 0.13; Figure 4J) and the frequency of vaccine-induced T helper (Th) 2 cells (R = 0.72, p = 0.007; Figures 4K, S8F, and S8G), suggesting that Th2 cells promote protective ADCC activity.

V2-specific ADCC, but not neutralizing antibody titers, correlates with a decreased risk of SIV_{mac251} acquisition

Next, we examined the contribution of anti-V2 antibodies to the ADCC measured with the CEM-based assay by using purified NCI05 and NCI09 $F(ab')_2$ as competitor, since both antibodies proved equally capable of mediating ADCC against $gp120_{\Delta V1}$-coated cells (Figures 2A and 2B). Both the NCI05 and NCI09 $F(ab')_2$ competed approximately 40% of serum ADCC directed to the $gp120_{\Delta V1}$ antigen in animals immunized with this immunogen (group 2; Figures 5A and 5B and Figures S8H–S8K). Of importance, the V2-specific serum ADCC activity inhibited by NCI05 or NCI09 $F(ab')_2$ in the ΔV1-immunized group (NCI05 mean delta = 15.12% +/− 2.96; NCI09 = 14.09% +/− 5.21) correlated with a decreased risk of SIV_{mac251} acquisition (NCI05, R = 0.67, p = 0.01; NCI09, R = 0.54, p = 0.05; Figures 5C and 5D), whereas the remaining non-V2-specific ADCC activity did not (data not shown).

An identical analysis of the sera of animals immunized with the ΔV1gpg immunogen demonstrated approximately 20% inhibition by both mAbs F(ab') (NCI05 mean delta = 8.60% +/− 3.05; NCI09 = 8.74% +/− 3.18; Figures 5E, 5F, S8L, and S8M). We observed no correlation with V2-specific ADCC activity inhibited by NCI05 or NCI09 (delta) and the risk of SIV_{mac251} acquisition in this group (Figures 5G and 5H). The level of estimated V2-specific serum ADCC activity inhibited by either NCI05 or NCI09 $F(ab')_2$ was significantly higher in the ΔV1 than the ΔV1gpg group (NCI05: p = 0.0001; NCI09: p = 0.0040; Figures 5I and 5J). Extension of our analyses to antibody-dependent cellular phagocytosis (ADCP) and antibody-dependent neutrophil activation (ADNP) using beads coated with the $gp120_{\Delta V1}$ protein (Mahan et al., 2016) revealed that none of these responses correlated with SIV_{mac251} acquisition (Figures S8N and S8O and data not shown). Serum neutralizing antibody titers against the tier 2 $SIV_{mac251\text{-}CS41}$ were highest in the ΔV1 group as expected (Ching and Stamatatos, 2010) (Figure S8P) but did not correlate with the risk of infection (data not shown). Neutralizing titers to tier 1B $SIV_{mac251\text{-}M766}$ did not differ among the immunization groups (Figure S8Q), but strikingly, their levels correlate with an increased risk of SIV_{mac251} acquisition in the ΔV1 group

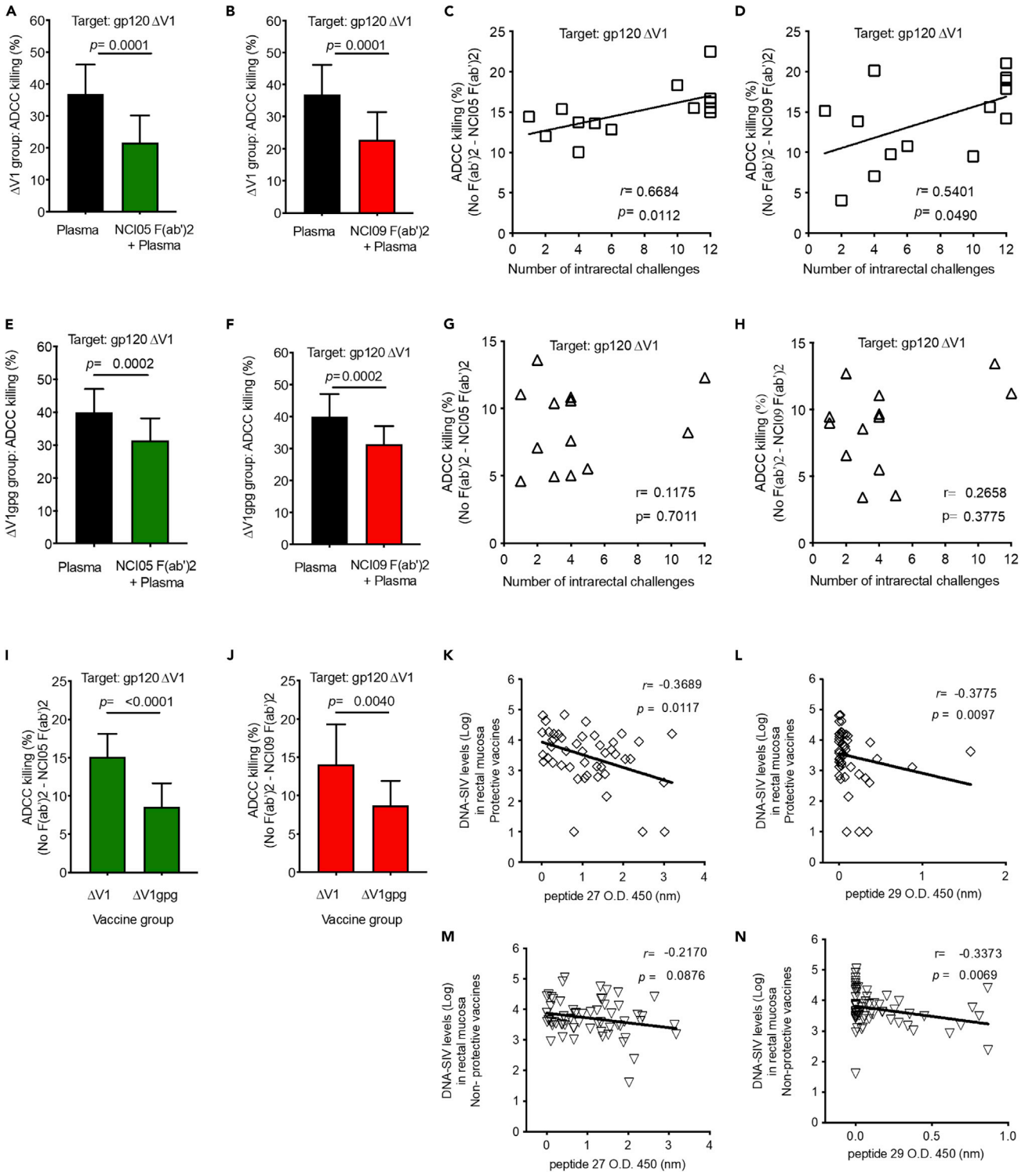

Figure 5. V2-specific ADCC associated with decreased risk of SIV_{mac251} acquisition

(A and B) ADCC killing percentage in animals immunized with ΔV1 immunogens on $gp120_{\Delta V1}$-coated target cells following pre-incubation of target cells with (A) NCI05 $F(ab')_2$ or (B) NCI09 F(ab') (ΔV1, n = 14).

(C and D) The V2-specific ADCC inhibited by (C) NCI05 or (D) NCI09 $F(ab')_2$ correlated with a decreased risk of SIV_{mac251} acquisition in the ΔV1 group (ΔV1, n = 14).

(E and F) ADCC killing percentage in animals immunized with ΔV1gpg immunogens on $gp120_{\Delta V1}$-coated target cells following pre-incubation of target cells with (E) NCI05 $F(ab')_2$ or (F) NCI09 F(ab') (ΔV1gpg, n = 13).

Figure 5. *Continued*

(G and H) Correlation of V2-specific ADCC inhibited by (G) NCI05 or (H) NCI09 F(ab')$_2$ in the ΔV1gpg group with risk of SIV$_{mac251}$ acquisition (ΔV1gpg, n = 14).
(I and J) Comparison of V2-specific ADCC revealed by (I) NCI05 F(ab')$_2$ or (J) NCI09 F(ab') competition in the ΔV1 and ΔV1gpg immunized animals.
(K and L) Correlation of serum reactivity at the end of the immunization to linear V2 peptides (K) 27 and (L) 29 (Figure S7B) and level of SIV DNA in rectal mucosa at 2 weeks after infection in animals vaccinated with *protective* vaccine regimens (including ΔV1) that became infected (n = 46).
(M and N) Correlation of serum reactivity at the end of the immunization to V2 peptides (M) 27 and (N) 29 and level of SIV DNA in rectal mucosa at 2 weeks after infection in animals vaccinated with *non-protective* vaccines (including the WT and ΔV1gpg immunized animals in the current study) that became infected (n = 60). Data represented as mean with SD. Data comparisons between two paired or unpaired groups were done with Wilcoxon signed-rank test and Mann-Whitney test, respectively. The correlation analyses were performed using the non-parametric Spearman rank correlation method with exact permutation two-tailed p-values calculated.
See Table S8 and Figures S1A–S1D, S6A–S6B, S7, and S8.

(Table S8 and Figure S8R). These data support the idea that the ΔV1 immunogen engineered to favor a V2 α-helical conformation to elicit qualitatively different V2-specific ADCC titers providing a plausible explanation for the difference in vaccine efficacy observed in groups 2 and 3.

Antibodies to V2 correlate with SIV DNA in the mucosa

We tested whether the cytocidal function of V2-specific antibody limits the early seeding of the virus in vaccinated animals that become infected. First, we measured serum reactivity to linear V2 peptides 27 and 29 (corresponding to V2b and V2c) in animals immunized with *protective* vaccines, including group 2 described in the current study (Figures 3H, S1B, and S1C), or with *non-protective* vaccines, including groups 1 and 3 of the current study (Figures S6A, S6B, S1D, and S1E). An inverse correlation with serum reactivity and the level of SIV DNA in the rectal mucosa was found in *protective* (peptide 27: R = – 0.37, p = 0.01; peptide 29: R = – 0.38, p = 0.01; Figures 5K and 5L) as well as *non-protective* vaccines (a trend for peptide 27: R = – 0.22, p = 0.09; peptide 29: R = – 0.34, p = 0.007; Figures 5M and 5N). Collectively, these data suggest that anti-V2 antibodies may inhibit infection by more than one mechanism.

V1 deletion in HIV A244 gp120 decreases V2 β sheet conformation

To address the potential for differences in HIV and SIV envelope structures, we tested the relevance of our finding to HIV by generating two V1-deleted HIV clade A/E A244 gp120 proteins. The first, A244ΔV1$_a$, was designed by deleting the LTNVNNRTNVSNIIGNITD peptide and leaving the natural nine-amino-acid loop in V1 (Table S10 and Figure S9A) with the intent of minimizing tension in the adjacent V2 loop. In the second construct, A244ΔV1$_b$, the nine-amino-acid loop was replaced with the corresponding nine amino acids of the SIV$_{mac251}$ΔV1 antigen already proven to favor an α-helical V2 structure eliciting cytocidal antibodies correlating with a decreased risk of SIV acquisition (Table S11 and Figure S9A). A244WT, A244ΔV1$_a$, and A244ΔV1$_b$ (Tables S9–S11) gp120 antigens expressed in 293 cells (Figures S9B–S9D) were probed in ELISA with mAb PG9, which recognizes V2 in a β sheet conformation, or CH58 and CH59, which recognize V2c in an α-helical conformation (Bonsignori et al., 2012; Gorny et al., 1994; Liao et al., 2013). The PG9 mAb bound better to gp120 A244$_{WT}$ than to both the gp120 A244$_{\Delta V1a}$ and gp120 A244$_{\Delta V1b}$ proteins (Figures 6A and 6B). The CH58 and CH59 mAbs had similar reactivity to A244 $_{WT}$ and the A244$_{\Delta V1a}$ and A244$_{\Delta V1b}$ proteins (Figures 6C–6F), suggesting that V1 deletion in the HIV gp120 A244ΔV1$_a$ and gp120 A244ΔV1$_b$ proteins shifts the structural equilibrium of V2 and reduces the V2 β sheet conformation (recognized by PG9) without affecting the V2 α-helical conformation (recognized by CH58 and CH59). These ΔV1 HIV immunogens therefore represent reagents matched to the V1-deleted SIV immunogens (that reduced the risk of virus acquisition) suitable to test whether focusing the antibody response to a V2 α-helical conformation improves the efficacy of HIV vaccine candidates.

DISCUSSION

We have herein demonstrated that antibodies to the V1 region, exposed at the apex of the virion envelope trimer and adjacent to a conserved V2 region, have opposing effects on SIV$_{mac251}$ acquisition in vaccinated macaques. Anti-V2 antibodies bound to infected cells and virions inhibited V2 binding to $\alpha_4\beta_7$ and mediated ADCC, whose level and function correlated with a decreased risk of virus acquisition. In contrast, anti-V1 antibodies interfered with the ability of anti-V2 antibodies to bind gp120, mediate ADCC, and inhibit gp120 and $\alpha_4\beta_7$ integrin interaction and furthermore correlated with an increased risk of virus acquisition. Whether antibodies to V1 affect V2 recognition by rendering specific V2 Ab-targeted epitopes less accessible by steric hindrance (competitive) or by stabilizing V1/V2 in a Greek-key β sheet fold through allosteric (non-competitive) inhibition remains to be determined. These mechanisms

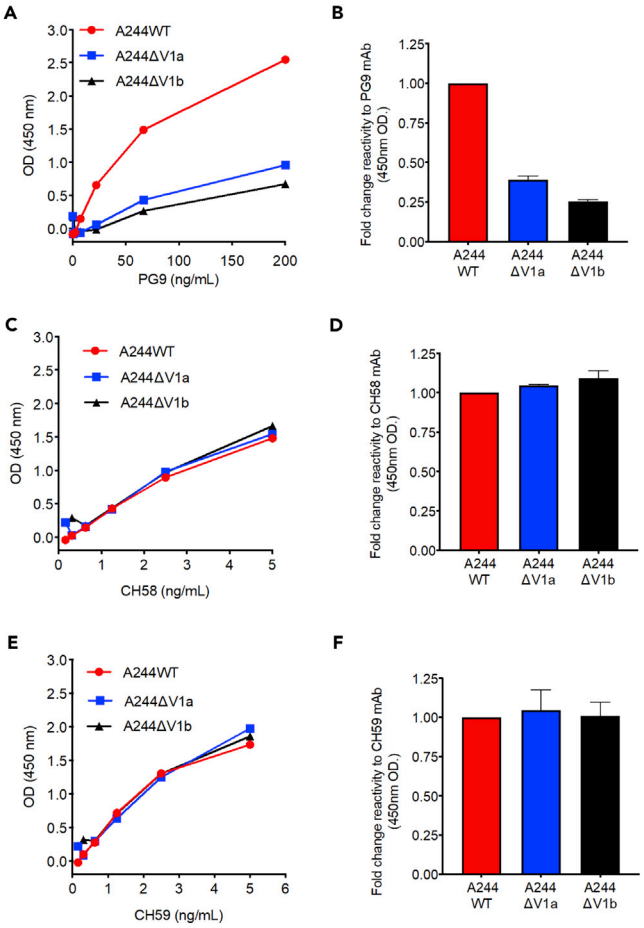

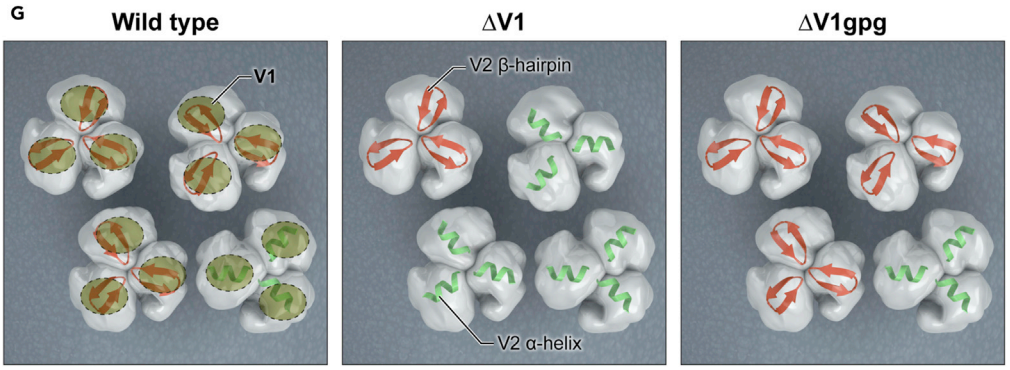

Figure 6. HIV A244ΔV1 gp120 immunogens are preferentially recognized by human antibodies binding to V2 in α-helix conformation

(A, C and E) ELISA kinetic of HIV gp120 A244 WT, gp120 $\Delta V1_a$, and gp120 $\Delta V1_b$ reactivity to (A) PG9 (anti-V2 antibody that recognizes V2 β Barrel conformation), (C) CH58, and (E) CH59 (anti-V2 antibodies recognizing V2 α-helical conformation).

(B, D and F) Average antibody binding in two experiments at the highest concentration of (B) PG9, (D) CH58, and (F) CH59 antibodies.

(G) Pictorial representation of the hypothesized abundance of the α-helical and β sheet V2 conformations in the WT gp120 (left), ΔV1 (center), and ΔV1gpg (right) apex trimers (not to scale). Data represented as mean with SD.

See Tables S9–11 and Figure S9.

are not mutually exclusive in the context of polyclonal antibody responses. We demonstrate here that vaccination with the ΔV1 immunogens engineered to favor the V2 α-helical conformation (Figure 6G, center) elicited higher cytocidal V2 antibodies correlating with vaccine efficacy than immunogens with V2 in a β sheet conformation (Figure 6G, right) that afforded no vaccine efficacy. Overall, the results presented here are consistent with the finding of an alternative, unconstrained V2 α-helical conformation, distinct from that visualized in most envelope crystallographic structures, that was targeted by antibodies from the sera of volunteers in RV144 (Aiyegbo et al., 2017). This raises the hypothesis that V1 may not only decrease V2 accessibility to the immune system by direct masking but may also enforce a constrained V2 β strand conformation less accessible to the antibodies mediating ADCC via a non-competitive mechanism. Indeed, we demonstrate here that the SIV ΔV1 and ΔV1gpg antigens differed in their epitope accessibility. It is notable that the structure adopted by the isolated peptide V2c used in our studies differs significantly from the β strand form found in both the HIV-1 prefusion-closed trimer derived from stabilized gp120-gp41 linked by artificial disulfide bond (SOS) in combination with isoleucine-to-proline (IP) change in the gp41 (SOSIP) trimers (Medina-Ramírez et al., 2017) and the scaffolded V2 structures bound to HIV-1 bNAbs (Jiang et al., 2016). The structure inferred in our study is instead closer to that identified in co-crystals of HIV V2 peptides in complex with mAbs derived from an uninfected RV144 vaccinee (Liao et al., 2013), suggesting that the SIV V2 can adopt an α-helical structure analogous to the structure of V2 in HIV that has previously been linked to a reduced risk of HIV acquisition in humans (Lertjuthaporn et al., 2018).

The V2 envelope region is important in viral transmission and seeding gut inductive sites, as inferred by studies on transmitted HIV variants (Cavrois et al., 2014; Chohan et al., 2005; Jiang et al., 2016; Ritola et al., 2004; Rong et al., 2007; Sagar et al., 2006; Smith et al., 2016). Our findings here suggest that antibodies to V2 may interfere at different steps of viral transmission, from disrupting the interaction of the α-helical conformation of V2 with $\alpha_4\beta_7$ during the establishment of infection to inhibiting virus spread by ADCC. Indeed, a recent study by Goes et al., 2020 demonstrated that V2 interaction with $\alpha_4\beta_7$ provides a co-stimulatory signal that increases activation and proliferation of $CD4^+$ cells and consequent HIV replication, suggesting that V2 may make gut resident T cells more receptive for viral infection. Furthermore, this phenotype was inhibited by antibodies recognizing the HIV α helix but not the β sheet conformation. Similar results were also obtained for SIV using the NCI09 mAb that was instrumental in our studies to reveal V2-specific ADCC responses correlating with a decreased risk of SIV_{mac251} acquisition (Figure 5D).

It is likely that the V1 of gp120 has evolved in SIV and HIV to counteract antibodies targeting the vulnerable V2 α-helical conformation. Antibody interference to HIV gp41 has been observed (Verrier et al., 2001), but interfering antibodies that target the apical gp120 domains and the V1/V2 have not been previously described. Interfering antibodies have been described in other viruses as well, including the Western equine encephalitis, polio, hepatitis C, and influenza viruses and the SARS-coronavirus (Dulbecco et al., 1956; Nicasio et al., 2012; Sautto et al., 2012; To et al., 2012; Tripp et al., 2005; Zhong et al., 2009).

The V1 deletion strategy employed here is relevant to the HIV vaccine design as removal of V1 from the A244 gp120 envelope decreases mAb PG9 binding to the protein, as we have demonstrated. Of particular significance is that this detrimental V1 element remains a component of most current Env-based vaccine candidates, suggesting that these candidates may exhibit improved efficacy with V1 deletion.

In summary, we have demonstrated that antibodies to V1 counteract functional antibody responses to viral vulnerability sites in V2. Minimizing the confounding role of V1, by its deletion or other means, presents a new opportunity to understand the biochemical basis of V2-associated viral vulnerability toward developing a fully efficacious vaccine for HIV.

Limitations of the study

The current study demonstrates that SIV envelope immunogens with the V1 region deleted (ΔV1) to favor the V2 α-helical conformation induced significant vaccine protection, whereas deletion of V1 to favor the V2 β sheet conformation, or V1 repleted (Wild Type) SIV immunogens, were not protective. Although the ΔV1 immunogens were engineered to assume these different conformations, we were unable to confirm their conformation experimentally. It was encouraging, however, that V1 deletion in the HIV A244 envelope,

engineered to favor the V2 α-helical conformation, resulted in the loss of binding to monoclonal antibodies recognizing V2 in a β sheet conformation. In addition, the level and interference activity of V1-specific antibodies may vary depending on the HIV clade (Shen et al., 2015). Lastly, the predictive value of our preclinical study in Indian rhesus macaques for humans remains unclear. It is noteworthy, however, that the identical SIV_{mac251} macaque model recapitulated and predicted (Vaccari et al., 2016) the efficacy of the RV144 human trial (performed in more than 16,000 volunteers in Thailand) and the lack of efficacy of the HVTN702 trial (more than 5,000 volunteers in South Africa), respectively.

Resource availability

Lead contact

Further information and requests for resources and reagents should be directed to and will be fulfilled by Dr. Genoveffa Franchini (franchig@mail.nih.gov).

Materials availability

All unique/stable reagents generated in this study are available from the Lead Contact with a completed Materials Transfer Agreement.

Data and code availability

The accession number for the structural analysis of the NCI09 antibody reported in this paper is PDB: 6VRY. All other data can be made available upon request.

METHODS

All methods can be found in the accompanying Transparent methods supplemental file.

SUPPLEMENTAL INFORMATION

Supplemental information can be found online at https://doi.org/10.1016/j.isci.2021.102047.

ACKNOWLEDGMENTS

We thank D. Ahern for editorial assistance, K. Saunders for providing the vector for antibody expression, and J. Heeney, G. Alter, and S. Phogat for helpful discussion. We also thank Sanofi Pasteur for the ALVAC-SIV vaccine. Funding: This work was supported with federal funds from the National Cancer Institute Intramural Program and the Office of AIDS research, National Institutes of Health (to G.F.) and under contract No. HHSN261200800001E (to B.F.K.); the National Institute on Drug Abuse (DA036478 to T.C.); the National Institute of Allergy and Infectious Diseases Extramural Program (R01AI084119 to T.C. and 5 T32-AI007392-30 to M.T.; the Intramural Program of the Vaccine Research Center (to P.D.K. and M.R.) and funding from the DOD and MHRP (to M.R. and M.A.E). The contents of this publication do not necessarily reflect the views or policies of the Department of Health and Human Services, the positions of the US Army, or the Department of Defense, nor does mention of trade names, commercial products, or organization imply endorsement.

AUTHOR CONTRIBUTIONS

G. Franchini conceived the study in consultation with T.C.; G. Franchini wrote the paper, with contributions from all authors; T.C. designed the immunogens and diagnostic peptides, and M.B.-F and E.N. performed confirmatory molecular modeling; I.S.d.C. and M. Bissa coordinated and performed the macaque studies with J.K., M. Breed, and W.M., and cellular immune assays with M.V., L.S., F.C., N.P.M.L., M.N.D., and V.G.; I.K., S.W., D.F., and J.D.S. expressed and characterized the ΔV1 immunogens with I.S.d.C.; G.G., R.M., J.H., R.V., M. Beddall, R.N., and M. Roederer cloned and characterized simian monoclonal antibodies and performed antigenicity studies; M.B.-F. performed serological assays with peptides; A.A. and L.M. performed SIV capture assays and analyzed data; C.L., H.V.T., K.P., M. Read, and M. Rao performed serological and α4β7 functional assays; M.L., D.V.R., C.C., S.M., and J.A. performed peptide competition assays; T.C., J.G., M.S.A., and P.D.K. analyzed peptide/antibody structures; M.A.R. and M.R-G. performed ADCC assays; M.A.E., D.P.P., and Z.S. performed ADCP and ADNP assays; D.C.M. and C.L. performed neutralization assays; G.D.T. and X.S. performed mucosal antibody assays; G. Ferrari, M.T, and J.P. performed assays of NCI05 and NCI09 binding to SIV-infected cells and plasma ADCC targeting SIV-infected cells; S.S. performed western blot for env and gag proteins; D.J.V. performed statistical analysis of the data; B.F.K.

CellPress
OPEN ACCESS

analyzed the viral variants; M. Rosati., B.K.F., and G.N.P. provided the SIV_{WT} gp160 and the p27 Gag DNA vaccines.

DECLARATION OF INTERESTS

The US Government has filed a patent on the V1-deleted immunogens with G.F., T.C., I.S.d.C., M.B.-F., M. Bissa., and R.M.A as inventors.

Received: September 14, 2020
Revised: November 23, 2020
Accepted: January 6, 2021
Published: February 19, 2021

REFERENCES

Abagyan, R., and Totrov, M. (1994). Biased probability Monte Carlo conformational searches and electrostatic calculations for peptides and proteins. J. Mol. Biol. *235*, 983–1002.

Aiyegbo, M.S., Shmelkov, E., Dominguez, L., Goger, M., Battacharya, S., deCamp, A.C., Gilbert, P.B., Berman, P.W., and Cardozo, T. (2017). Peptide targeted by human antibodies associated with HIV vaccine-associated protection assumes a dynamic alpha-helical structure. PLoS One *12*, e0170530.

Andrabi, R., Pallesen, J., Allen, J.D., Song, G., Zhang, J., de Val, N., Gegg, G., Porter, K., Su, C.Y., Pauthner, M., et al. (2019). The chimpanzee SIV envelope trimer: structure and deployment as an HIV vaccine template. Cell Rep. *27*, 2426–2441 e2426.

Arthos, J., Cicala, C., Martinelli, E., Macleod, K., Van Ryk, D., Wei, D., Xiao, Z., Veenstra, T.D., Conrad, T.P., Lempicki, R.A., et al. (2008). HIV-1 envelope protein binds to and signals through integrin alpha4beta7, the gut mucosal homing receptor for peripheral T cells. Nat. Immunol. *9*, 301–309.

Bonsignori, M., Pollara, J., Moody, M.A., Alpert, M.D., Chen, X., Hwang, K.K., Gilbert, P.B., Huang, Y., Gurley, T.C., Kozink, D.M., et al. (2012). Antibody-dependent cellular cytotoxicity-mediating antibodies from an HIV-1 vaccine efficacy trial target multiple epitopes and preferentially use the VH1 gene family. J. Virol. *86*, 11521–11532.

Cardozo, T., Totrov, M., and Abagyan, R. (1995). Homology modeling by the ICM method. Proteins *23*, 403–414.

Cavrois, M., Neidleman, J., Santiago, M.L., Derdeyn, C.A., Hunter, E., and Greene, W.C. (2014). Enhanced fusion and virion incorporation for HIV-1 subtype C envelope glycoproteins with compact V1/V2 domains. J. Virol. *88*, 2083–2094.

Ching, L., and Stamatatos, L. (2010). Alterations in the immunogenic properties of soluble trimeric human immunodeficiency virus type 1 envelope proteins induced by deletion or heterologous substitutions of the V1 loop. J. Virol. *84*, 9932–9946.

Chohan, B., Lang, D., Sagar, M., Korber, B., Lavreys, L., Richardson, B., and Overbaugh, J. (2005). Selection for human immunodeficiency virus type 1 envelope glycosylation variants with shorter V1-V2 loop sequences occurs during transmission of certain genetic subtypes and may impact viral RNA levels. J. Virol. *79*, 6528–6531.

Cohen, J. (2020). Another HIV vaccine strategy fails in large-scale study. Science. https://doi.org/10.1126/science.abb1480. https://www.sciencemag.org/news/2020/02/another-hiv-vaccine-strategy-fails-large-scale-study.

Dulbecco, R., Vogt, M., and Strickland, A.G. (1956). A study of the basic aspects of neutralization of two animal viruses, western equine encephalitis virus and poliomyelitis virus. Virology *2*, 162–205.

Goes, L.R.S., Sivro, A.A., Olowojesiku, R., Ray, J., Perrone, I., Yolitz, J., Girard, A., Leyre, L., Winmer, C.K., et al. (2020). The V2 loop of HIV delivers costimulatory signals to CD4+ T cells through integrin a4b7 and promotes cellular activation and infection. Proc. Natl. Acad. Sci. USA *117*, 32566–32573.

Gorman, J., Soto, C., Yang, M.M., Davenport, T.M., Guttman, M., Bailer, R.T., Chambers, M., Chuang, G.Y., DeKosky, B.J., Doria-Rose, N.A., et al. (2016). Structures of HIV-1 Env V1V2 with broadly neutralizing antibodies reveal commonalities that enable vaccine design. Nat. Struct. Mol. Biol. *23*, 81–90.

Gorny, M.K., Moore, J.P., Conley, A.J., Karwowska, S., Sodroski, J., Williams, C., Burda, S., Boots, L.J., and Zolla-Pazner, S. (1994). Human anti-V2 monoclonal antibody that neutralizes primary but not laboratory isolates of human immunodeficiency virus type 1. J. Virol. *68*, 8312–8320.

Gottardo, R., Bailer, R.T., Korber, B.T., Gnanakaran, S., Phillips, J., Shen, X., Tomaras, G.D., Turk, E., Imholte, G., Eckler, L., et al. (2013). Plasma IgG to linear epitopes in the V2 and V3 regions of HIV-1 gp120 correlate with a reduced risk of infection in the RV144 vaccine efficacy trial. PLoS One *8*, e75665.

Haynes, B.F., Gilbert, P.B., McElrath, M.J., Zolla-Pazner, S., Tomaras, G.D., Alam, S.M., Evans, D.T., Montefiori, D.C., Karnasuta, C., Sutthent, R., et al. (2012). Immune-correlates analysis of an HIV-1 vaccine efficacy trial. N. Engl. J. Med. *366*, 1275–1286.

Jiang, X., Totrov, M., Li, W., Sampson, J.M., Williams, C., Lu, H., Wu, X., Lu, S., Wang, S., Zolla-Pazner, S., et al. (2016). Rationally designed immunogens targeting HIV-1 gp120 V1V2 induce distinct conformation-specific antibody responses in rabbits. J. Virol. *90*, 11007–11019.

Julien, J.P., Cupo, A., Sok, D., Stanfield, R.L., Lyumkis, D., Deller, M.C., Klasse, P.J., Burton, D.R., Sanders, R.W., Moore, J.P., et al. (2013). Crystal structure of a soluble cleaved HIV-1 envelope trimer. Science *342*, 1477–1483.

Lertjuthaporn, S., Cicala, C., Van Ryk, D., Liu, M., Yolitz, J., Wei, D., Nawaz, F., Doyle, A., Horowitch, B., Park, C., et al. (2018). Select gp120 V2 domain specific antibodies derived from HIV and SIV infection and vaccination inhibit gp120 binding to alpha4beta7. PLoS Pathog. *14*, e1007278.

Lewis, G.K., Ackerman, M.E., Scarlatti, G., Moog, C., Robert-Guroff, M., Kent, S.J., Overbaugh, J., Reeves, R.K., Ferrari, G., and Thyagarajan, B. (2019). Knowns and unknowns of assaying antibody-dependent cell-mediated cytotoxicity against HIV-1. Front.Immunol. *10*, 1025.

Liao, H.X., Bonsignori, M., Alam, S.M., McLellan, J.S., Tomaras, G.D., Moody, M.A., Kozink, D.M., Hwang, K.K., Chen, X., Tsao, C.Y., et al. (2013). Vaccine induction of antibodies against a structurally heterogeneous site of immune pressure within HIV-1 envelope protein variable regions 1 and 2. Immunity *38*, 176–186.

Liu, J., Bartesaghi, A., Borgnia, M.J., Sapiro, G., and Subramaniam, S. (2008). Molecular architecture of native HIV-1 gp120 trimers. Nature *455*, 109–113.

Mahan, A.E., Jennewein, M.F., Suscovich, T., Dionne, K., Tedesco, J., Chung, A.W., Streeck, H., Pau, M., Schuitemaker, H., Francis, D., et al. (2016). Antigen-specific antibody glycosylation is regulated via vaccination. PLoS Pathog. *12*, e1005456.

Mason, R.D., Welles, H.C., Adams, C., Chakrabarti, B.K., Gorman, J., Zhou, T., Nguyen, R., O'Dell, S., Lusvarghi, S., Bewley, C.A., et al. (2016). Targeted isolation of antibodies directed against major sites of SIV env vulnerability. PLoS Pathog. *12*, e1005537.

McLellan, J.S., Pancera, M., Carrico, C., Gorman, J., Julien, J.P., Khayat, R., Louder, R., Pejchal, R., Sastry, M., Dai, K., et al. (2011). Structure of HIV-1 gp120 V1/V2 domain with broadly neutralizing antibody PG9. Nature *480*, 336–343.

Medina-Ramírez, M., Garces, F., Escolano, A., Skog, P., de Taeye, S.W., Del Moral-Sanchez, I., McGuire, A.T., Yasmeen, A., Behrens, A.J.,

Ozorowski, G., et al. (2017). Design and crystal structure of a native-like HIV-1 envelope trimer that engages multiple broadly neutralizing antibody precursors in vivo. J. Exp. Med. *214*, 2573–2590.

Nakamura, G.R., Fonseca, D.P., O'Rourke, S.M., Vollrath, A.L., and Berman, P.W. (2012). Monoclonal antibodies to the V2 domain of MN-rgp120: fine mapping of epitopes and inhibition of α4β7 binding. PLoS One *7*, e39045.

Nicasio, M., Sautto, G., Clementi, N., Diotti, R.A., Criscuolo, E., Castelli, M., Solforosi, L., Clementi, M., and Burioni, R. (2012). Neutralization interfering antibodies: a "novel" example of humoral immune dysfunction facilitating viral escape? Viruses *4*, 1731–1752.

Orlandi, C., Flinko, R., and Lewis, G.K. (2016). A new cell line for high throughput HIV-specific antibody-dependent cellular cytotoxicity (ADCC) and cell-to-cell virus transmission studies. J. Immunol. Methods *433*, 51–58.

Pancera, M., Zhou, T., Druz, A., Georgiev, I.S., Soto, C., Gorman, J., Huang, J., Acharya, P., Chuang, G.Y., Ofek, G., et al. (2014). Structure and immune recognition of trimeric pre-fusion HIV-1 Env. Nature *514*, 455–461.

Pegu, P., Vaccari, M., Gordon, S., Keele, B.F., Doster, M., Guan, Y., Ferrari, G., Pal, R., Ferrari, M.G., Whitney, S., et al. (2013). Antibodies with high avidity to the gp120 envelope protein in protection from simian immunodeficiency virus SIV(mac251) acquisition in an immunization regimen that mimics the RV-144 Thai trial. J. Virol. *87*, 1708–1719.

Rerks-Ngarm, S., Pitisuttithum, P., Nitayaphan, S., Kaewkungwal, J., Chiu, J., Paris, R., Premsri, N., Namwat, C., de Souza, M., Adams, E., et al. (2009). Vaccination with ALVAC and AIDSVAX to prevent HIV-1 infection in Thailand. N. Engl. J. Med. *361*, 2209–2220.

Ritola, K., Pilcher, C.D., Fiscus, S.A., Hoffman, N.G., Nelson, J.A., Kitrinos, K.M., Hicks, C.B., Eron, J.J., and Swanstrom, R. (2004). Multiple V1/V2 env variants are frequently present during primary infection with human immunodeficiency virus type 1. J. Virol. *78*, 11208–11218.

Rolland, M., Edlefsen, P.T., Larsen, B.B., Tovanabutra, S., Sanders-Buell, E., Hertz, T., deCamp, A.C., Carrico, C., Menis, S., Magaret, C.A., et al. (2012). Increased HIV-1 vaccine efficacy against viruses with genetic signatures in Env V2. Nature *490*, 417–420.

Rong, R., Gnanakaran, S., Decker, J.M., Bibollet-Ruche, F., Taylor, J., Sfakianos, J.N., Mokili, J.L., Muldoon, M., Mulenga, J., Allen, S., et al. (2007). Unique mutational patterns in the envelope alpha 2 amphipathic helix and acquisition of length in gp120 hypervariable domains are associated with resistance to autologous neutralization of subtype C human immunodeficiency virus type 1. J. Virol. *81*, 5658–5668.

Sagar, M., Wu, X., Lee, S., and Overbaugh, J. (2006). Human immunodeficiency virus type 1 V1-V2 envelope loop sequences expand and add glycosylation sites over the course of infection, and these modifications affect antibody neutralization sensitivity. J. Virol. *80*, 9586–9598.

Sautto, G., Mancini, N., Diotti, R.A., Solforosi, L., Clementi, M., and Burioni, R. (2012). Anti-hepatitis C virus E2 (HCV/E2) glycoprotein monoclonal antibodies and neutralization interference. Antivir. Res *96*, 82–89.

Shen, X., Duffy, R., Howington, R., Cope, A., Sadagopal, S., Park, H., Pal, R., Kwa, S., Ding, S., Yang, O.O., et al. (2015). Vaccine-induced linear epitope-specific antibodies to simian immunodeficiency virus SIVmac239 envelope are distinct from those induced to the human immunodeficiency virus type 1 envelope in nonhuman primates. J. Virol. *89*, 8643–8650.

Smith, S.A., Burton, S.L., Kilembe, W., Lakhi, S., Karita, E., Price, M., Allen, S., Hunter, E., and Derdeyn, C.A. (2016). Diversification in the HIV-1 envelope hyper-variable domains V2, V4, and V5 and higher probability of transmitted/founder envelope glycosylation favor the development of heterologous neutralization breadth. PLoS Pathog. *12*, e1005989.

Starcich, B.R., Hahn, B.H., Shaw, G.M., McNeely, P.D., Modrow, S., Wolf, H., Parks, E.S., Parks, W.P., Josephs, S.F., and Gallo, R.C. (1986). Identification and characterization of conserved and variable regions in the envelope gene of HTLV-III/LAV, the retrovirus of AIDS. Cell *45*, 637–648.

Tassaneetrithep, B., Tivon, D., Swetnam, J., Karasavvas, N., Michael, N.L., Kim, J.H., Marovich, M., and Cardozo, T. (2014). Cryptic determinant of alpha4beta7 binding in the V2 loop of HIV-1 gp120. PLoS One *9*, e108446.

To, K.K., Zhang, A.J., Hung, I.F., Xu, T., Ip, W.C., Wong, R.T., Ng, J.C., Chan, J.F., Chan, K.H., and Yuen, K.Y. (2012). High titer and avidity of nonneutralizing antibodies against influenza vaccine antigen are associated with severe influenza. Clin.Vaccin. Immunol. *19*, 1012–1018.

Tomaras, G.D., Ferrari, G., Shen, X., Alam, S.M., Liao, H.X., Pollara, J., Bonsignori, M., Moody, M.A., Fong, Y., Chen, X., et al. (2013). Vaccine-induced plasma IgA specific for the C1 region of the HIV-1 envelope blocks binding and effector function of IgG. Proc. Natl. Acad. Sci. U S A *110*, 9019–9024.

Tripp, R.A., Haynes, L.M., Moore, D., Anderson, B., Tamin, A., Harcourt, B.H., Jones, L.P., Yilla, M., Babcock, G.J., Greenough, T., et al. (2005). Monoclonal antibodies to SARS-associated coronavirus (SARS-CoV): identification of neutralizing and antibodies reactive to S, N, M and E viral proteins. J. Virol. Methods *128*, 21–28.

Vaccari, M., Fourati, S., Gordon, S.N., Brown, D.R., Bissa, M., Schifanella, L., Silva de Castro, I., Doster, M.N., Galli, V., Omsland, M., et al. (2018). HIV vaccine candidate activation of hypoxia and the inflammasome in CD14(+) monocytes is associated with a decreased risk of SIVmac251 acquisition. Nat. Med. *24*, 847–856.

Vaccari, M., Gordon, S.N., Fourati, S., Schifanella, L., Liyanage, N.P., Cameron, M., Keele, B.F., Shen, X., Tomaras, G.D., Billings, E., et al. (2016). Adjuvant-dependent innate and adaptive immune signatures of risk of SIVmac251 acquisition. Nat. Med. *22*, 762–770.

Verrier, F., Nadas, A., Gorny, M.K., and Zolla-Pazner, S. (2001). Additive effects characterize the interaction of antibodies involved in neutralization of the primary dualtropic human immunodeficiency virus type 1 isolate 89.6. J. Virol. *75*, 9177–9186.

Wibmer, C.K., Richardson, S.I., Yolitz, J., Cicala, C., Arthos, J., Moore, P.L., and Morris, L. (2018). Common helical V1V2 conformations of HIV-1 Envelope expose the alpha4beta7 binding site on intact virions. Nat. Commun. *9*, 4489.

Zhong, L., Haynes, L., Struble, E.B., Tamin, A., Virata-Theimer, M.L., and Zhang, P. (2009). Antibody-mediated synergy and interference in the neutralization of SARS-CoV at an epitope cluster on the spike protein. Biochem.Biophys. Res. Commun. *390*, 1056–1060.

Zolla-Pazner, S., deCamp, A., Gilbert, P.B., Williams, C., Yates, N.L., Williams, W.T., Howington, R., Fong, Y., Morris, D.E., Soderberg, K.A., et al. (2014). Vaccine-induced IgG antibodies to V1V2 regions of multiple HIV-1 subtypes correlate with decreased risk of HIV-1 infection. PLoS One *9*, e87572.

iScience, Volume *24*

Supplemental Information

Anti-V2 antibodies virus vulnerability revealed by envelope V1 deletion in HIV vaccine candidates

Isabela Silva de Castro, Giacomo Gorini, Rosemarie Mason, Jason Gorman, Massimiliano Bissa, Mohammad A. Rahman, Anush Arakelyan, Irene Kalisz, Stephen Whitney, Manuel Becerra-Flores, Eric Ni, Kristina Peachman, Hung V. Trinh, Michael Read, Mei-Hue Liu, Donald Van Ryk, Dominic Paquin-Proulx, Zhanna Shubin, Marina Tuyishime, Jennifer Peele, Mohammed S. Ahmadi, Raffaello Verardi, Juliane Hill, Margaret Beddall, Richard Nguyen, James D. Stamos, Dai Fujikawa, Susie Min, Luca Schifanella, Monica Vaccari, Veronica Galli, Melvin N. Doster, Namal P.M. Liyanage, Sarkis Sarkis, Francesca Caccuri, Celia LaBranche, David C. Montefiori, Georgia D. Tomaras, Xiaoying Shen, Margherita Rosati, Barbara K. Felber, George N. Pavlakis, David J. Venzon, William Magnanelli, Matthew Breed, Josh Kramer, Brandon F. Keele, Michael A. Eller, Claudia Cicala, James Arthos, Guido Ferrari, Leonid Margolis, Marjorie Robert-Guroff, Peter D. Kwong, Mario Roederer, Mangala Rao, Timothy J. Cardozo, and Genoveffa Franchini

a

Groups	Relative VE	*p*
ALVAC-SIV+gp120 alum	44%	0.025
DNA-SIV+ALVAC-SIV+gp120 alum	52%	0.029
ALVAC-SIV+gp120 MF59	9%	ns
Ad26+SIV+ALVAC-SIV+gp120 alum	13%	ns

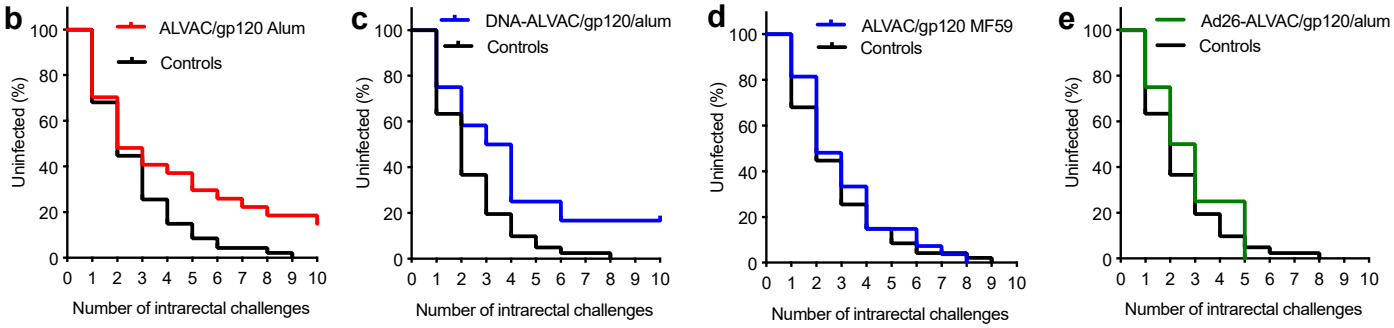

f V1 overlapping peptides

```
Peptide 15 PCVKLSPLCITMRCNKSETD
Peptide 16       PLCITMRCNKSETDRWGLTK
Peptide 17             RCNKSETDRWGLTKSSTTIT
Peptide 18                   TDRWGLTKSSTTITTAAPTS
Peptide 19                         TKSSTTITTAAPTSAPVSEK
Peptide 20                               ITTAAPTSAPVSEKIDMVNE
Peptide 21                                     TSAPVSEKIDMVNETSSCIA
Peptide 22                                           EKIDMVNETSSCIAQNNCTG
Peptide 23                                                 NETSSCIAQNNCTGLEQEQM
Peptide 24                                                       IAQNNCTGLEQEQMISCKFT
```

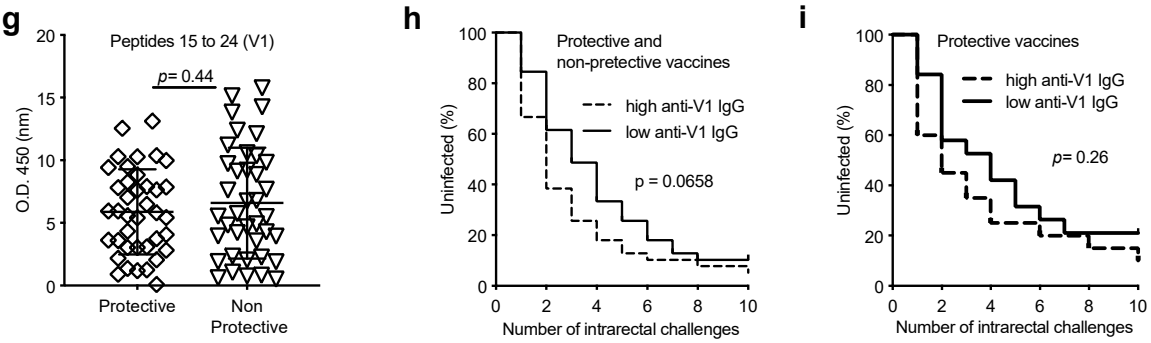

Figure S1. V1 response in protective vaccines, Related to Figures 1 and 5. (A) Vaccine efficacy (VE) measured as average per exposure risk of SIV_{mac251} acquisition in animals immunized with different vaccine regimens measured as rate of SIV_{mac251} acquisition compared to unimmunized controls. (B) Acquisition curves in animals vaccinated with ALVAC-SIV/gp120+alum (n = 27), (C) DNA-SIV/ALVAC-SIV/gp120+alum (n = 12), (D) ALVAC-SIV/gp120+MF59 (n = 27), and (E) Ad26-SIV /ALVAC-SIV/gp120+alum (n = 12). (F) V1 overlapping peptides from $SIV_{mac251\text{-}K6W}$ (Franchini et al., 1987). (G) Reactivity of sera to V1 (peptides 15 – 24) in an ELISA assay obtained from animals immunized with *protectiv*e (n = 39) and *non-protective* (n = 39) vaccines at week 27 (3 weeks after the last immunization, 1 week before challenge), data represented as mean with SD. (H) Association (trend) of SIV_{mac251} acquisition in animals immunized with *protective* and *non-protective* vaccines that had above (n = 39) or below average (n = 39) serum antibodies to V1 at week 27 (3 weeks after the last immunization and 1 week before challenge). (I) No significant difference in SIV_{mac251} acquisition in animals immunized with *protective* vaccines that had above (n = 20) or below average (n = 19) serum antibodies to V1 at week 27 (3 weeks after the last immunization 1 week before challenge). Statistical analyses comparing two groups was done using Mann-Whitney test. The infection curves were analyzed using Log-Rank (Mantel-Cox test).

a

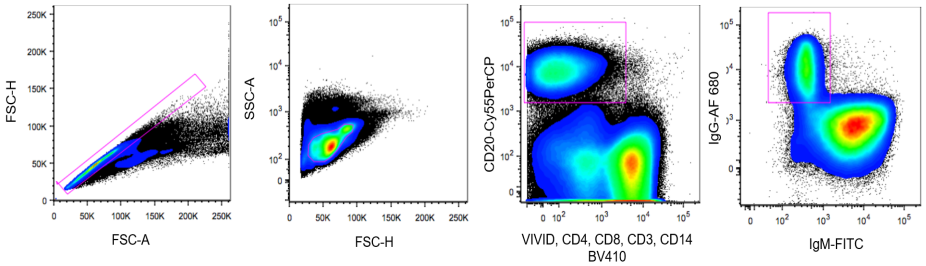

b

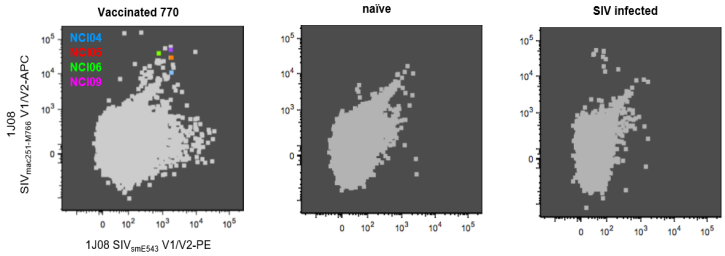

C

Monoclonal Antibody Binding

	NCI05	NCI09	NCI04	NCI06	ITS09	ITS41
SIVmac251 M766 gp120	++	++	++	++	++	++
SIVsmE660.CR54 gp140	++	++	-	++	++	-
SIVsmE543 1J08 V1V2	++	++	-	++	ND	ND
SIVmac251 1J08 V1V2	++	++	++	++	ND	ND
SIVmac239 1J08 V1V2	++	++	+	++	ND	ND
SIVsmE543 cV2	++	++	-	-	ND	ND
SIVmac251 cV2	~ ¶	++	-	-	ND	ND
V1 peptide	-	-	PLCITMRCNKSETDRWGLTK	RCNKSETDRWGLTK	ND	ND
V2 peptide	-	TGLKRDKTKEY	-	-	TGLKRDKKKEY	EQEQMISCKFNMTGL

++	OD450 ≥ 2
+	1 ≤ OD450 < 2
-	OD450 < 0.5
¶	borderline 0.5 ≤ OD450 < 1
ND	No data

d

SIV_{mac239} Peptides

```
Peptide 41 EQEQMISCKFNMTGL
Peptide 42     MISCKFNMTGLKRDK
Peptide 43         KFNMTGLKRDKKKEY
Peptide 44             TGLKRDKKKEYNETW
Peptide 45                 RDKKKEYNETWYSAD
Peptide 46                   KEYNETWYSADLVCE
Peptide 47                       ETWYSADLVCEQGNN
Peptide 48                           SADLVCEQGNNTGNE
```

e

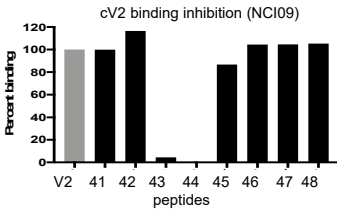

f

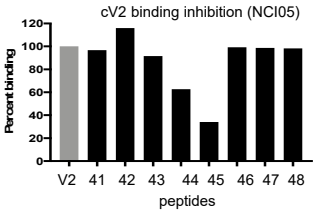

g

Monoclonal Antibody Neutralization

	NCI05	NCI09	NCI04	NCI06
SIVsmE660.CP3C (Tier 1)	4.449 *	>50†	>50†	>50†
SIVsmE660.CR54 (Tier 2)	>50†	>50†	>50†	>50†
SIVmac251.H9 (Tier 1)	>50	0.412 **	>50	0.024 ***
SIVmac251.30 (Tier 2)	>50†	>50†	>50†	>50†

* 1 - 9.99 μg/ml

** 0.01 - 0.099 μg/ml

*** 0.1 - 0.99 μg/ml

† curve plateaued below 50%

Figure S2. Generation and characterization of monoclonal Abs to V2, Related to Figure 2. We sourced B cells from animal P770. P770 was protected against 10 SIV_{mac251} challenge exposures, immunized with ALVAC-SIV/gp120+alum nine times over a four-year interval, and remained protected after exposure to 10 additional SIV_{mac251} challenges (data not shown). (A) Staining strategy on PBMCs to identify B cells positive for 1J08 SIV_{smE543} and/or SIV_{mac251} V1/V2 scaffolds in animal P770. Sorting memory B cells from animal P770 with the 1J08 SIV_{smE543} and SIV_{mac251} V1/V2 scaffolds yielded ~0.78% of the memory cells and 0.13% of the total B cells in blood. (B) Retrospective color identification of B cells that produced mAbs NCI04, NCI05, NCI06, and NCI09 isolated from the B cells of animal P770. (C) Summary of NCI04, NCI05, NCI06, and NCI09 monoclonal antibody binding in ELISA characterized using multiple SIV antigens, and of ITS09 and ITS41 described by Mason *et. al* (Mason et al., 2016). (D) Overlapping peptides (SIV_{mac239}) used in the competition assay of (E) NCI09 or (F) NCI05 binding to cyclic V2 in ELISA. (G) Neutralization potency of NCI mAbs, expressed by IC50. Cloned V1 or V2 -specific mAbs were tested for neutralization against tier 1 and tier 2 SIV_{mac251} and SIV_{smE660} pseudoviruses.

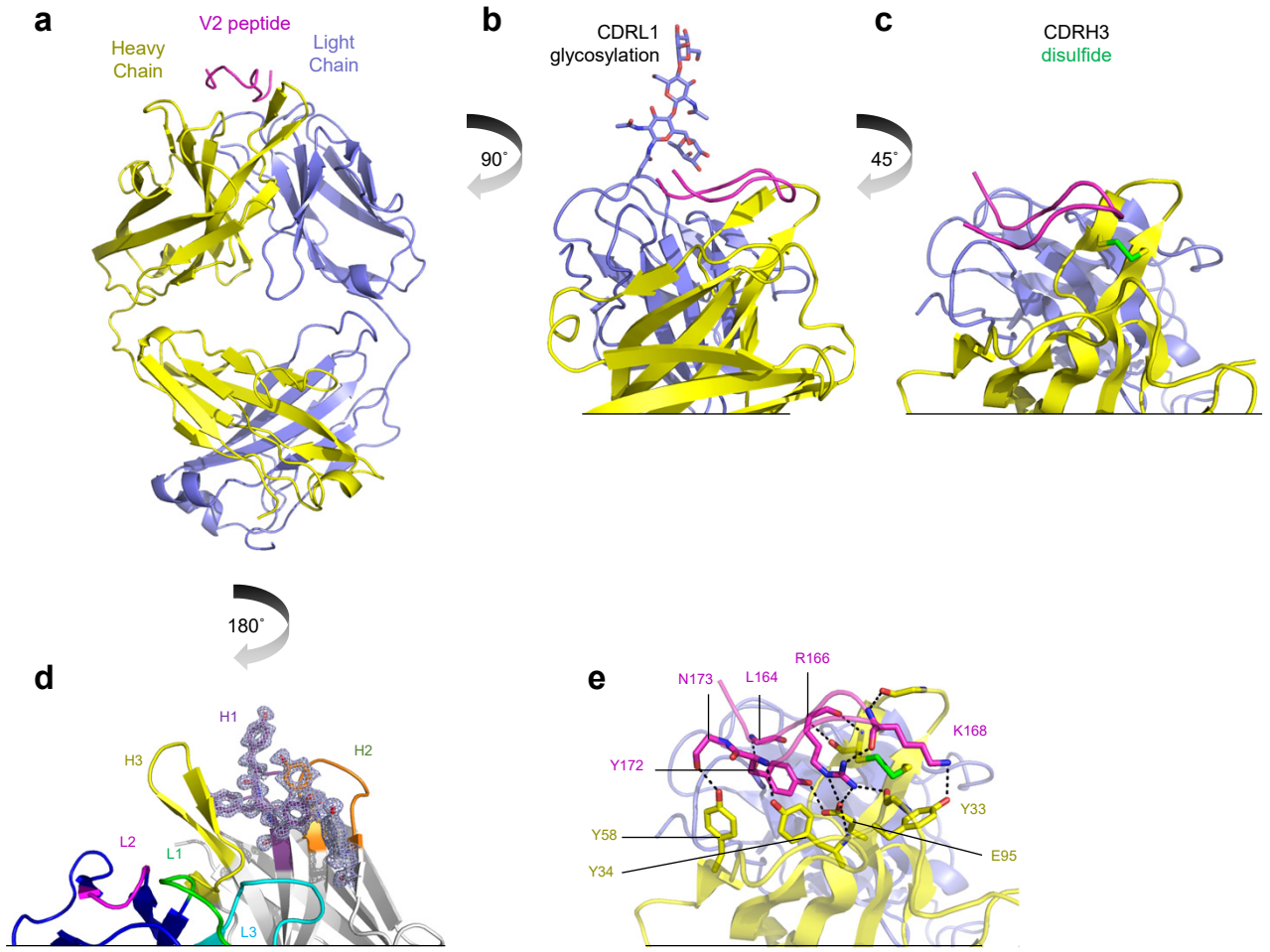

f

Heavy

```
IGHV4-2*01 QLQLQESGPGLVKPSETLSLTCAVSGGSISSN-YWSWIRQPPGKGLEWIGRISGSGGSTDYNPSLKSRVTISTDTSKNQFSLKLSSVTAADTAVYYCAR
NCI09      .V.........................DYY..N....F.........N.Y.KSA..Y.........S..K.......F..................EYCIGSTCYPILDSWGQGAVVTVSS
```

Light

```
IGKV3-2*01 EIVMTQSPATLSLSPGERATLSCRASQSVSSSLAWYQQKPGQAPRLLIYGASSRATGIPDRFSGSGSGTEFTLTISSLEPEDFAVYYCQQYSNWP
NCI09      ........V....................A.................D..T....................S...............H.F...TTFGGGTKVEIK
```

H-bond side chain ● H-bond main chain ○ Salt-bridge side chain ●
H-bond side chain & main chain ✷ Salt-bridge side chain & H-bond main chain ●

Figure S3. Crystal Structure of NCI09 Fab in complex with V2 peptide, Related to Figure 2. (A) Overall structure of NCI09 in complex with a SIV_{mac251} linear peptide. The peptide sequence of consensus SIV_{mac251} (KFTMTGLKRDKTKEYN, magenta) in complex with antibody NCI09 Fab is shown. The N-terminal 5 residues were not ordered in the structure. The NCI09 heavy and light chains are displayed as yellow and blue ribbons, respectively. (B) The light chain maturation introduced a sequon into the CDRL1 with density observed for several carbohydrate moieties. (C) The CDRH3 includes a disulfide bond stabilizing the hairpin structure of the loop. (D) The CDR regions of the heavy and light chain are highlighted with the peptide removed. Electron density is displayed for residues buried by the V2 peptide (2Fo-Fc, σ1). (E) Detailed interactions are highlighted with stick representation of residues forming H-bonds or salt bridges (dashed lines). (F) Heavy and light chain maturation is represented. Residues within 5 Å of the peptide are highlighted in magenta. The introduced sequon is highlighted in green. The heavy chain provides six H-bonds and one salt bridge, and the light chain provides an additional H-bond with a combined total buried surface area of 726 $Å^2$.

a

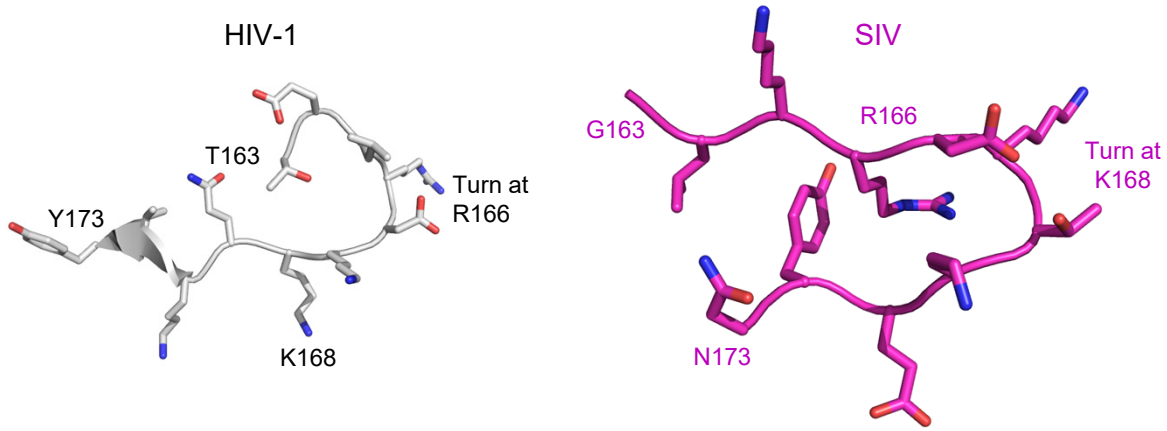

b

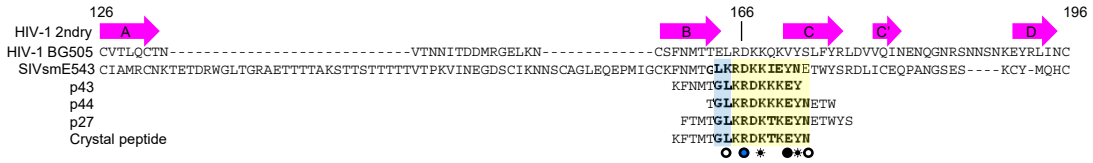

H-bond side chain ● H-bond main chain ○ Salt-bridge side chain ●
H-bond side chain & main chain ✳ Salt-bridge side chain & H-bond main chain ◉
Heavy chain proximal
Light chain proximal

Figure S4. Comparison of V1/V2 regions of HIV and SIV, Related to Figure 2. (A) The same structural region of the HIV-1 trimer (BG505, 4TVP) is compared to that of the SIV peptide, revealing an alteration in overall structure and location of the turn. (B) The sequences of V1/V2 for HIV-1 is aligned with that of SIV_{smE543}. The secondary structure of HIV-1 V1/V2 in the trimer context is displayed above. Structural details for that of SIV are unknown. Overlapping peptides in the crystal structure are shown below. Residues with density are bolded and highlighted by color according to their proximity to the heavy (yellow) or light (blue) chain. Interaction details for H-bonds or electrostatic contacts are indicated.

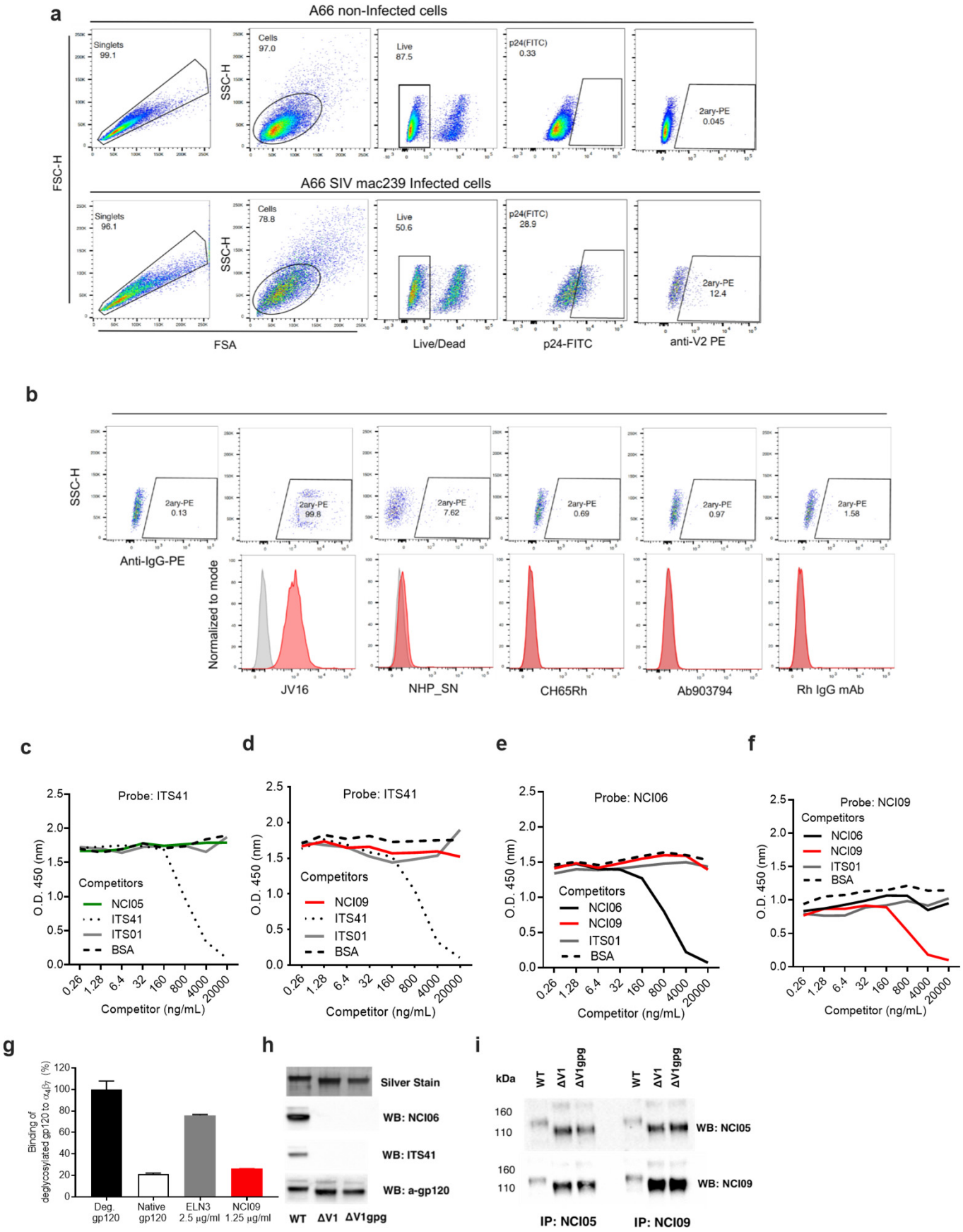
a
A66 non-Infected cells
Singlets 99.1
Cells 97.0
Live 87.5
p24(FITC) 0.33
2ary-PE 0.045
A66 SIV mac239 Infected cells
Singlets 96.1
Cells 78.8
Live 50.6
p24(FITC) 28.9
2ary-PE 12.4
FSC-H
SSC-H
FSA
Live/Dead
p24-FITC
anti-V2 PE
b
2ary-PE 0.13
2ary-PE 99.8
2ary-PE 7.62
2ary-PE 0.69
2ary-PE 0.97
2ary-PE 1.58
Anti-IgG-PE
Normalized to mode
JV16
NHP_SN
CH65Rh
Ab903794
Rh IgG mAb
c
Probe: ITS41
Competitors
NCI05
ITS41
ITS01
BSA
O.D. 450 (nm)
Competitor (ng/mL)
d
Probe: ITS41
Competitors
NCI09
ITS41
ITS01
BSA
e
Probe: NCI06
Competitors
NCI06
NCI09
ITS01
BSA
f
Probe: NCI09
Competitors
NCI06
NCI09
ITS01
BSA
g
Binding of deglycosylated gp120 to α4β7 (%)
Deg. gp120
Native gp120
ELN3 2.5 μg/ml
NCI09 1.25 μg/ml
h
Silver Stain
WB: NCI06
WB: ITS41
WB: a-gp120
WT
ΔV1
ΔV1gpg
i
kDa
WT
ΔV1
ΔV1gpg
WB: NCI05
WB: NCI09
IP: NCI05
IP: NCI09

Figure S5. Characterization of the ΔV1 immunogens, Related to Figures 2 and 3. (A) Gating strategy to evaluate NCI05 and NCI09 antibodies binding to A66 SIV_{mac239} infected cells. (B) Representative plot and histogram of the positive (JV16 antibody: SIV_{mac239} infected pigtail polyclonal serum) and negative controls (NHP-SN: negative-control serum from a naïve rhesus macaque; CH65: a human anti-Flu mAb with engineered NHP Fc region; Ab903793: rhesus mAb isolated from HIV-1 immunized NHP; Rh IgG mAb: a rhesus monoclonal IgG isotype) for cytometry analysis of A66 SIV_{mac239} infected cells. (C) ELISA profiles of anti-V1 ITS41 probe competed by NCI05, ITS41, ITS01, and BSA. (D) ELISA profiles of anti-V1 ITS41 probe competed by NCI09, ITS41, ITS01, and BSA. (E) ELISA profiles of anti-V1 NCI06 probe competed by NCI09, ITS01, NCI06, and BSA. (F) ELISA profiles of anti-V2 NCI09 probe competed by NCI06, NCI09, ITS01, and BSA. Competition assays were performed with $SIV_{mac251\text{-}M766}$ $gp120_{WT}$ protein. (G) NCI09-mediated inhibition of human $\alpha_4\beta_7$ binding to native or deglycosylated $SIV_{mac251\text{-}M766}$ gp120 alone or in the presence of the competitor ELN3 at 2.5 µg/ml (an inhibitory molecule of $\alpha_4\beta_7$), or NCI09 at 1.25 µg/ml. (H) Analysis of $SIV_{mac251\text{-}M766}$ $gp120_{WT}$, $gp120_{\Delta V1}$, and $gp120_{\Delta V1gpg}$ integrity by silver stain, western blot with NCI06, ITS41, and a rabbit polyclonal serum to SIV gp120 (top to bottom). (**I**) Western blot of immune precipitates with NCI05 and NCI09 reacted with NCI05 (left) or NCI09 (right).

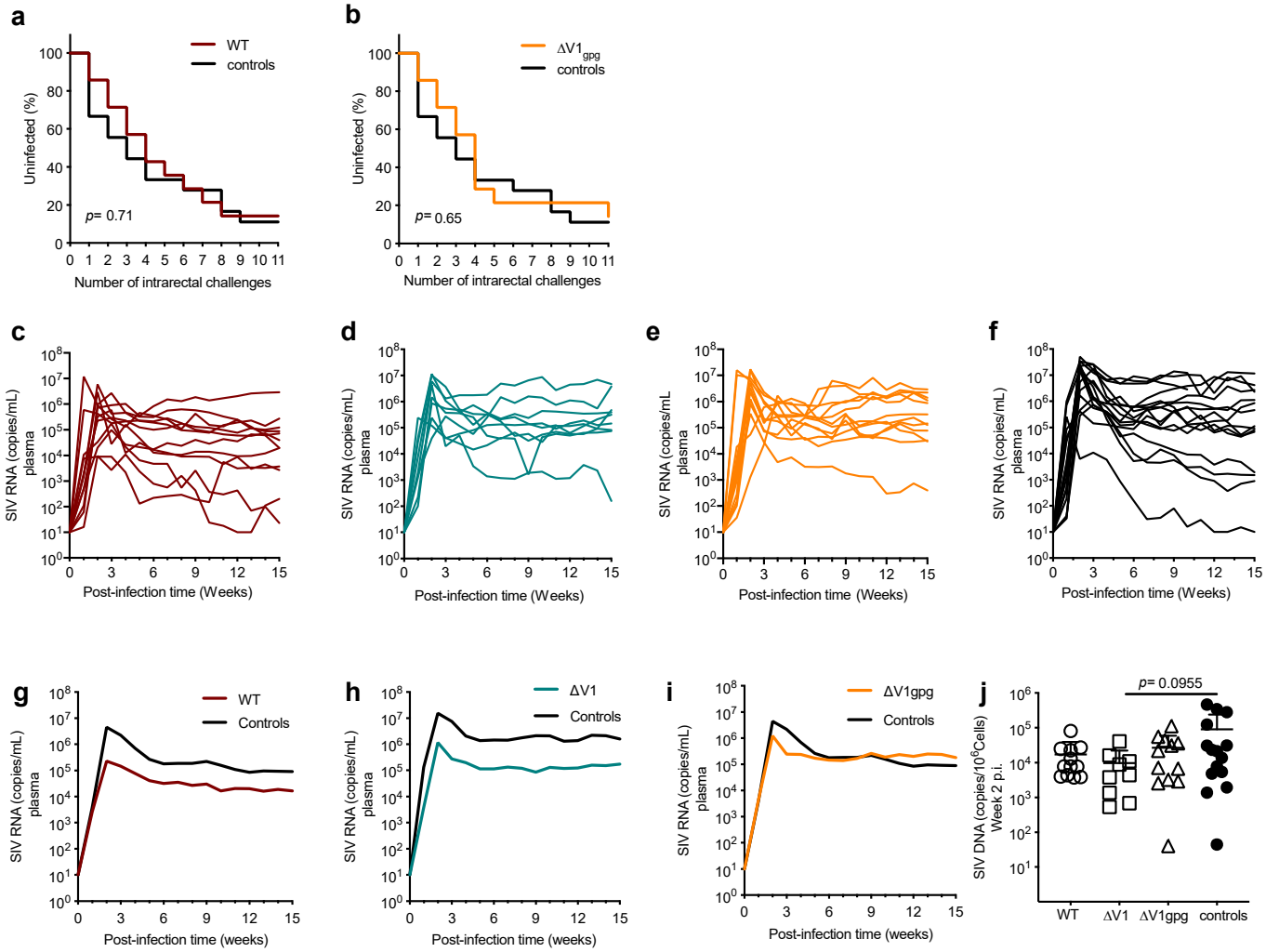
a
WT
controls
Uninfected (%)
p= 0.71
Number of intrarectal challenges
b
ΔV1gpg
controls
Uninfected (%)
p= 0.65
Number of intrarectal challenges
c
SIV RNA (copies/mL) plasma
Post-infection time (Weeks)
d
SIV RNA (copies/mL) plasma
Post-infection time (Weeks)
e
SIV RNA (copies/mL) plasma
Post-infection time (Weeks)
f
SIV RNA (copies/mL) plasma
Post-infection time (Weeks)
g
WT
Controls
SIV RNA (copies/mL) plasma
Post-infection time (weeks)
h
ΔV1
Controls
SIV RNA (copies/mL) plasma
Post-infection time (weeks)
i
ΔV1gpg
Controls
SIV RNA (copies/mL) plasma
Post-infection time (weeks)
j
p= 0.0955
SIV DNA (copies/10^6Cells) Week 2 p.i.
WT
ΔV1
ΔV1gpg
controls

Figure S6. SIV_{mac251} acquisition and plasma virus levels, Related to Figure 3. Risk of SIV_{mac251} acquisition in infected animals immunized with (A) wild type envelope immunogens (n = 14) or (B) ΔV1gpg envelope immunogens (n = 14). Plasma SIV RNA copies in animals immunized with (C) WT (magenta; n = 12), (D) ΔV1 (teal; n = 9), or (E) ΔV1gpg (yellow; n = 12) immunogens, and (F) control animals (black; n = 16). Comparison of mean plasma virus levels among control animals (n = 16) and animals immunized with (G) WT (n = 12), (H) ΔV1 (n = 9), or (I) ΔV1gpg (n = 12). (J) SIV DNA copies in rectal mucosa two weeks following infection in all animals that became infected, data represented as mean with SD. The infection curves were analyzed using Log-Rank (Mantel-Cox test). Data comparison between multiple groups was done with non-parametrical Kruskal-Wallis test with Dunn's multiple comparison test. Data comparison between ΔV1 and control group (J) was done with non-parametrical Mann-Whitney test.

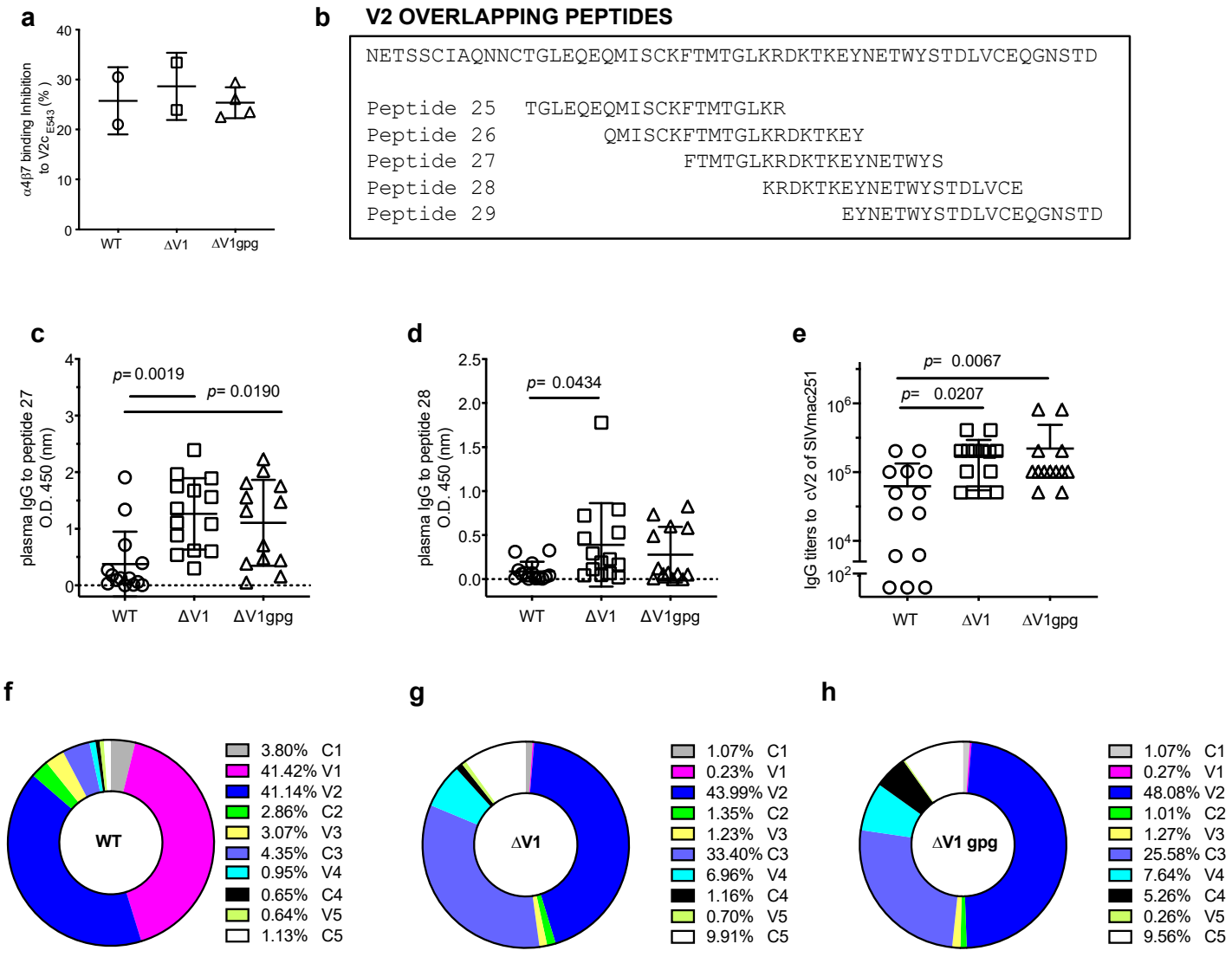
a
α4β7 binding Inhibition to V2c E543 (%)
40
30
20
10
0
WT
ΔV1
ΔV1gpg
b
V2 OVERLAPPING PEPTIDES
NETSSCIAQNNCTGLEQEQMISCKFTMTGLKRDKTKEYNETWYSTDLVCEQGNSTD
Peptide 25 TGLEQEQMISCKFTMTGLKR
Peptide 26 QMISCKFTMTGLKRDKTKEY
Peptide 27 FTMTGLKRDKTKEYNETWYS
Peptide 28 KRDKTKEYNETWYSTDLVCE
Peptide 29 EYNETWYSTDLVCEQGNSTD
c
plasma IgG to peptide 27 O.D. 450 (nm)
p= 0.0019
p= 0.0190
4
3
2
1
0
WT
ΔV1
ΔV1gpg
d
plasma IgG to peptide 28 O.D. 450 (nm)
p= 0.0434
2.5
2.0
1.5
1.0
0.5
0.0
WT
ΔV1
ΔV1gpg
e
IgG titers to cV2 of SIVmac251
p= 0.0067
p= 0.0207
10^6
10^5
10^4
10^2
WT
ΔV1
ΔV1gpg
f
WT
3.80% C1
41.42% V1
41.14% V2
2.86% C2
3.07% V3
4.35% C3
0.95% V4
0.65% C4
0.64% V5
1.13% C5
g
ΔV1
1.07% C1
0.23% V1
43.99% V2
1.35% C2
1.23% V3
33.40% C3
6.96% V4
1.16% C4
0.70% V5
9.91% C5
h
ΔV1 gpg
1.07% C1
0.27% V1
48.08% V2
1.01% C2
1.27% V3
25.58% C3
7.64% V4
5.26% C4
0.26% V5
9.56% C5

Figure S7. Antibodies to V2 in immunized animal sera, Related to Figures 3 and 5. (A) Serum inhibition of the $\alpha_4\beta_7$ integrin (expressed on RPMI8866 cells) binding to $V2c_{E543}$ (WT, n = 2; ΔV1, n = 2; ΔV1gpg, n = 4). Data of only 8 animals above the cut-off of the assay are represented in the graph (cut-off is defined here as 15% of inhibition). (B) Amino acid sequence of overlapping V2 peptides 25 – 29 from $SIV_{mac251\text{-}K6W}$ (Franchini et al., 1987). Serum recognition (ELISA) of V2 peptides (C) 27 and (D) 28 in immunized animals and of (E) cyclic v2 of SIV_{mac251} (delta of week 17 and baseline) in the immunized animals. Percent recognition of peptides encompassing the entire gp120 peptide array in animals vaccinated with (F) WT (n = 14), (G) ΔV1 (n = 14), or (H) ΔV1gpg (n = 13) immunogens. The constant (C) and variable (V) regions are defined by Starcich *et al.* (Starcich et al., 1986). Data represented as mean with SD. Comparison between multiple groups was done with non-parametrical Kruskal-Wallis test with Dunn's multiple comparison test.

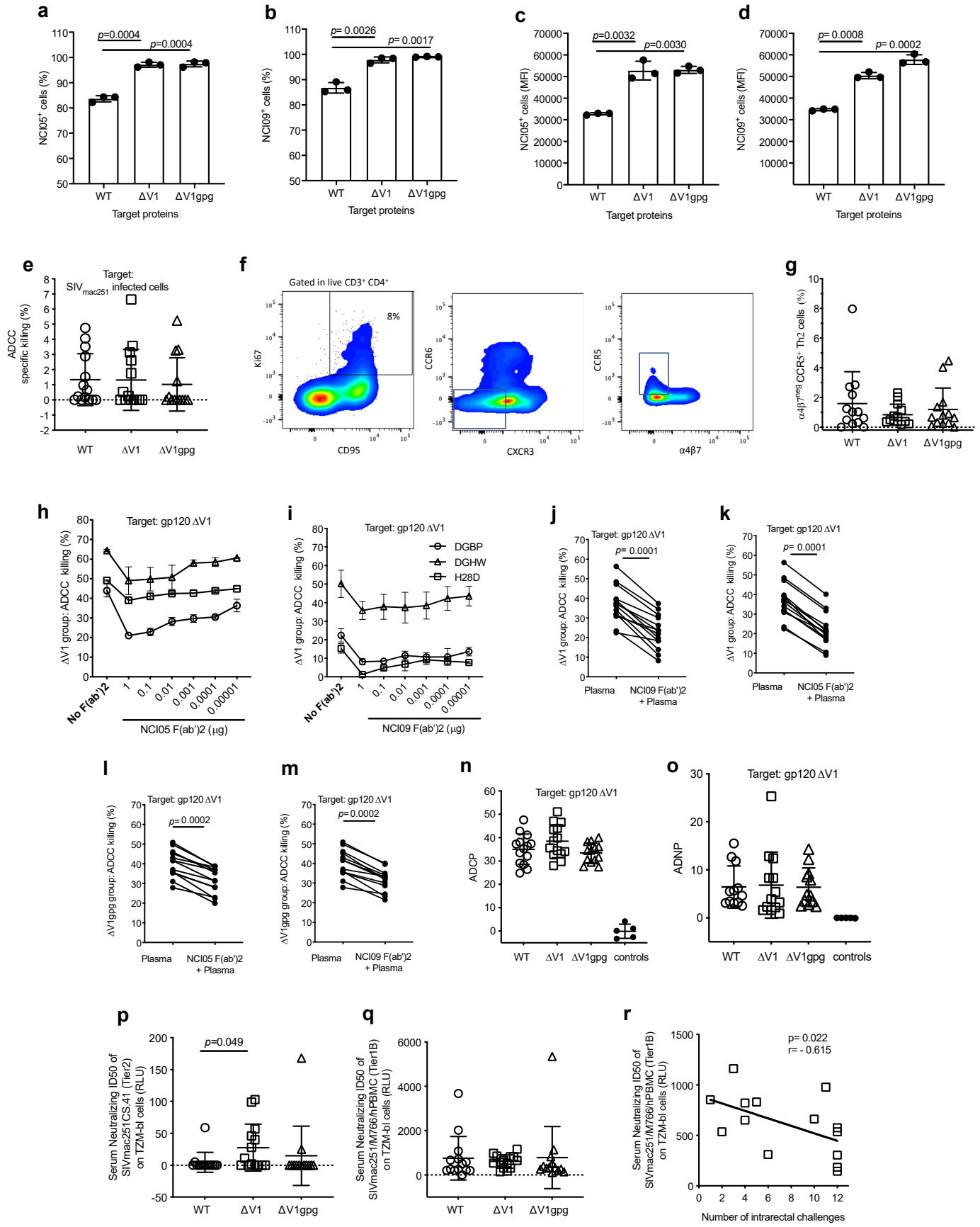
a
p=0.0004
p=0.0004
NCI05+ cells (%)
WT
ΔV1
ΔV1gpg
Target proteins
b
p= 0.0026
p= 0.0017
NCI09+ cells (%)
Target proteins
c
p=0.0032
p=0.0030
NCI05+ cells (MFI)
Target proteins
d
p= 0.0008
p= 0.0002
NCI09+ cells (MFI)
Target proteins
e
Target:
SIVmac251 infected cells
ADCC specific killing (%)
f
Gated in live CD3+ CD4+
8%
Ki67
CD95
CCR6
CXCR3
CCR5
α4β7
g
α4β7neg CCR5+ Th2 cells (%)
h
Target: gp120 ΔV1
ΔV1 group: ADCC killing (%)
No F(ab')2
NCI05 F(ab')2 (μg)
i
Target: gp120 ΔV1
DGBP
DGHW
H28D
NCI09 F(ab')2 (μg)
j
Target: gp120 ΔV1
p= 0.0001
Plasma
NCI09 F(ab')2 + Plasma
k
Target: gp120 ΔV1
p= 0.0001
NCI05 F(ab')2 + Plasma
l
Target: gp120 ΔV1
p=0.0002
ΔV1gpg group: ADCC killing (%)
NCI05 F(ab')2 + Plasma
m
Target: gp120 ΔV1
p=0.0002
NCI09 F(ab')2 + Plasma
n
Target: gp120 ΔV1
ADCP
controls
o
Target: gp120 ΔV1
ADNP
p
p=0.049
Serum Neutralizing ID50 of SIVmac251CS.41 (Tier2) on TZM-bl cells (RLU)
q
Serum Neutralizing ID50 of SIVmac251/M766/hPBMC (Tier1B) on TZM-bl cells (RLU)
r
p= 0.022
r= - 0.615
Serum Neutralizing ID50 of SIVmac251/M766/hPBMC (Tier1B) on TZM-bl cells (RLU)
Number of intrarectal challenges

Figure S8. Characterization of antibody responses to V2 in immunized animals, Related to Figures 4 and 5. We tested the percentage of CEM that reacted with the anti-V2 (A) NCI05 and (B) NCI09 mAbs coated with the gp120 immunogens and found that both mAbs stained a significantly lower percentage of cells coated with $gp120_{WT}$ than $gp120_{\Delta V1}$ and $gp120_{\Delta V1gpg}$, consistent with the improved binding of V1-deleted immunogens to CD4 shown in Figure 1F. Similarly, the Mean Fluorescent Intensity was also significantly lower in cells coated with WT than with V1-deleted immunogens following staining with (C) NCI05 and (D) and NCI09, consistent with the better accessibility of V2 epitopes in the absence of V1. (E) Percentage of specific ADCC killing in immunized animals (WT, n = 14; ΔV1, n = 14; ΔV1gpg; n = 13) on SIV_{mac251} infected cells. (F) CD4 Th2 cells Gating strategy. (G) Percentage of vaccine-induced ($Ki67^+$) $\alpha_4\beta_7^-$ $CCR5^+$ Th2 cells collected at week 13 (one week after the last immunization; WT, n = 13; ΔV1, n = 13; ΔV1gpg, n = 13). The mean is represented by a horizontal black line. To perform ADCC inhibition assays, we selected sera from 3 animals (DGBP, DGHW, and H28D) immunized with the ΔV1 envelope immunogen that had the highest ADCC titers (10^6) and used them at a 1:1000 dilution in ADCC assay with cells coated in $gp120_{\Delta V1}$. Both NCI05 and NCI09 $F(ab')_2$ inhibited ADCC in a dose-dependent manner, and inhibition was most effective at a dose of 1 µg per well (5µg/mL). (H–I) Dose-dependent inhibition of ADCC by (H) NCI05 $F(ab')_2$ and (I) NCI09 $F(ab')_2$ in the sera of the three animals immunized with the ΔV1 immunogens. We next used 1 µg each of NCI05 and NCI09 $F(ab')_2$ to compete ADCC activity directed to the ΔV1 gp120 in 1:1000 dilution of sera from animals immunized with the ΔV1 and ΔV1gpg immunogens. Inhibition of ADCC activity with 5µg/mL of (J) NCI05 $F(ab')_2$ and (K) NCI09 $F(ab')_2$ of the sera of all animals in the ΔV1 group at a 1:1000 dilution (n = 14), and (L) NCI05 $F(ab')_2$ and (M) NCI09 $F(ab')_2$ of the sera of animals in the ΔV1 gpg group (n = 13). (N) Phagocytic score using $gp120_{\Delta V1}$-coated beads (WT, n = 14; ΔV1, n = 14; ΔV1gpg, n = 13). (O) Neutrophil phagocytosis (WT, n = 12; ΔV1, n = 13; ΔV1gpg, n = 12). Serum neutralizing antibodies to (P) $SIV_{mac251\text{-}CS41}$ and to (Q) $SIV_{mac251\text{-}M766}$ in Relative Luminescence Unit (RLU; WT, n = 14; ΔV1, n = 14; ΔV1gpg: n = 13). (R) Correlation of serum neutralizing antibodies to $SIV_{mac251\text{-}M766}$ in animals immunized with ΔV1 envelope immunogens and intrarectal challenges (n = 14). Data represented as mean with SD. Data Comparisons between two paired or unpaired groups were performed using Wilcoxon signed-rank test or Mann-Whitney test, respectively. Comparisons between the three vaccinated groups was done with non-parametrical Kruskal-Wallis test with Dunn's multiple comparison test. Comparisons between three paired groups was done with two-way ANOVA test with

Tukey's multiple comparisons test. The correlation analyses were performed using the non-parametric Spearman rank correlation method with exact permutation two-tailed P values calculated.

a

A244 WT - …CTNANLTKANLTNVNNRTNVSNIIGNITDEVRNCSFN…
A244 ΔV1a - …CTNANL----------EVRNCSFN…
A244 ΔV1b - …CNKSET----------QMIGCSFN…

b

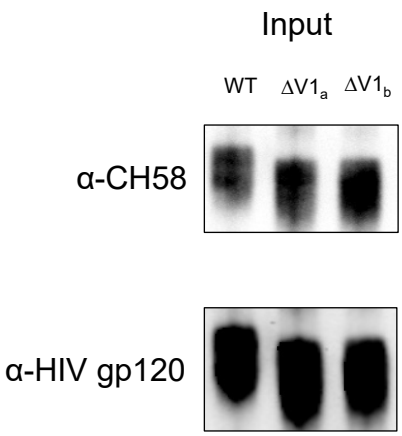

c

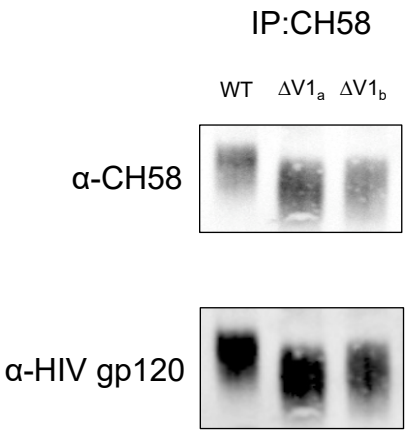

d

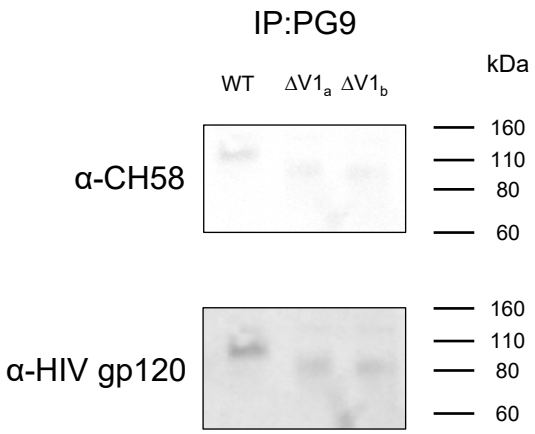

Figure S9. Expression of HIV clade A/E A244 ΔV1 immunogens, Related to Figure 6. (A) Amino acid sequence of the V1 boundaries in the HIV AE.A244 D11gp120 WT and HIV AE.A244 D11gp120 ΔV1 proteins. The 9 residual V1 amino acids in the A244ΔV1$_a$ and the equivalent 9 amino acids from SIV$_{mac251}$ in the A244ΔV1$_b$ construct are depicted. The A244ΔV1 constructs were expressed in 293 cells and subjected to immune precipitation (IP) with CH58 or PG9 and western blot with the same antibodies. (B) The input proteins used were readily detected by WB using CH58 and a polyclonal serum recognizing gp120. (C) Both the CH58 and polyclonal anti-gp120 Abs recognized the immune precipitates of CH58, whereas (D) PG9 immune precipitates were weakly reactive to both antibody preparation.

Supplemental Table 1

```
1                   10                  20                  30                  40                  50                  60                  70                  80
ATG GAT GCA ATG AAG AGA GGG CTC TGC TGT GTG CTG CTG CTG TGT GGA GCA GTC TTC GTT ACT ACC ACA GAG GCT AGC ATC TAC TGC
M   D   A   M   K   R   G   L   C   C   V   L   L   L   C   G   A   V   F   V   T   T   T   E   A   S   I   Y   C

90                  100                 110                 120                 130                 140                 150                 160                 170
ACC CAG TAC GTG ACC GTG TTC TAC GGC GTG CCA GCT TGG AGA AAC GCC ACC ATT CCA CTG TTC TGC GCC ACC AAG AAC AGG GAC ACC
T   Q   Y   V   T   V   F   Y   G   V   P   A   W   R   N   A   T   I   P   L   F   C   A   T   K   N   R   D   T

180                 190                 200                 210                 220                 230                 240                 250                 260
TGG GGA ACA ACC CAG TGC CTG CCA GAC AAT GGC GAT TAC TCT GAG CTG GCC CTG AAC GTG ACC GAG TCT TTC GAT GCC TGG GAG AAC
W   G   T   T   Q   C   L   P   D   N   G   D   Y   S   E   L   A   L   N   V   T   E   S   F   D   A   W   E   N

270                 280                 290                 300                 310                 320                 330                 340
ACC GTG ACC GAA CAG GCC ATT GAG GAC GTG TGG CAG CTG TTC GAA ACC TCC ATC AAG CCC TGC GTG AAG CTG TCC CCA CTG TGC ATC
T   V   T   E   Q   A   I   E   D   V   W   Q   L   F   E   T   S   I   K   P   C   V   K   L   S   P   L   C   I

350                 360                 370                 380                 390                 400                 410                 420                 430
ACC ATG AGG TGC AAC AAG TCC GAA ACC}{CAG ATG ATC GGC TGC AAG TTC AAC ATG ACC GGC CTG AAG AGG GAC AAG ACC AAA GAG TAC
T   M   R   C   N   K   S   E   T   Q   M   I   G   C   K   F   N   M   T   G   L   K   R   D   K   T   K   E   Y

440                 450                 460                 470                 480                 490                 500                 510                 520
AAC GAA ACC TGG TAC TCC ACC GAC CTC GTG TGC GAG CAG GGA AAC TCT ACC GAC AAC GAG TCC AGG TGC TAC ATG AAC CAC TGC AAC
N   E   T   W   Y   S   T   D   L   V   C   E   Q   G   N   S   T   D   N   E   S   R   C   Y   M   N   H   C   N

530                 540                 550                 560                 570                 580                 590                 600
ACC AGC ATC ATC CAA GAG TCC TGC GAC AAG CAC TAC TGG GAC ACC ATC AGG TTC AGA TAC TGC GCC CCA CCA GGA TAC GCC CTG CTG
T   S   I   I   Q   E   S   C   D   K   H   Y   W   D   T   I   R   F   R   Y   C   A   P   P   G   Y   A   L   L

610                 620                 630                 640                 650                 660                 670                 680                 690
AGA TGC AAC GAC ACC AAC TAC TCC GGC TTC ATG CCC AAG TGC TCC AAG GTG GTG GTG TCC TCC TGC ACC AGG ATG ATG GAA ACC CAG
R   C   N   D   T   N   Y   S   G   F   M   P   K   C   S   K   V   V   V   S   S   C   T   R   M   M   E   T   Q

700                 710                 720                 730                 740                 750                 760                 770                 780
ACC TCC ACT TGG TTT GGC TTC AAC GGC ACC AGG GCC GAG AAC AGG ACC TAC ATC TAC TGG CAC GGC AGG GAC AAC AGG ACC ATC ATC
T   S   T   W   F   G   F   N   G   T   R   A   E   N   R   T   Y   I   Y   W   H   G   R   D   N   R   T   I   I

790                 800                 810                 820                 830                 840                 850                 860                 870
TCC CTG AAC AAG TAC TAC AAC CTG ACC ATG AAG TGC AGA AGG CCC GGC AAC AAA ACC GTG CTG CCA GTG ACC ATC ATG TCC GGC CTG
S   L   N   K   Y   Y   N   L   T   M   K   C   R   R   P   G   N   K   T   V   L   P   V   T   I   M   S   G   L

880                 890                 900                 910                 920                 930                 940                 950
GTG TTT CAC AGC CAG CCA GTG AAC GAA AGG CCC AAC CAG GCT TGG TGT TGG TTC GGC GGA AAT TGG AAG GAC GCC ATC AAA GAA GTG
V   F   H   S   Q   P   V   N   E   R   P   N   Q   A   W   C   W   F   G   G   N   W   K   D   A   I   K   E   V

960                 970                 980                 990                 1,000               1,010               1,020               1,030               1,040
AAG CAG ACC ATC GTG AAG CAC CCC AGA TAC ACC GGC ACC AAC AAC ACC GAC AAG ATC AAC CTG ACA GCC CCA AGA GGC GGA GAT CCC
K   Q   T   I   V   K   H   P   R   Y   T   G   T   N   N   T   D   K   I   N   L   T   A   P   R   G   G   D   P

1,050               1,060               1,070               1,080               1,090               1,100               1,110               1,120               1,130
GAA GTG ACC TTT ATG TGG ACC AAC TGC AGG GGC GAG TTC CTG TAC TGC AAG ATG AAC TGG TTC CTG AAC TGG GTC GAA GAT AGG GAC
E   V   T   F   M   W   T   N   C   R   G   E   F   L   Y   C   K   M   N   W   F   L   N   W   V   E   D   R   D

1,140               1,150               1,160               1,170               1,180               1,190               1,200               1,210
CTG ACC ACA CAG AGG CCC AAA GAG AGG CAT AGA AGA AAC TAC GTG CCC TGC CAC ATC AGG CAG ATC ATC AAC ACC TGG CAC AAA GTG
L   T   T   Q   R   P   K   E   R   H   R   R   N   Y   V   P   C   H   I   R   Q   I   I   N   T   W   H   K   V

1,220               1,230               1,240               1,250               1,260               1,270               1,280               1,290               1,300
GGC AAG AAC GTG TAC CTG CCA CCT AGA GAG GGC GAC CTG ACC TGC AAT TCT ACC GTG ACC AGC CTG ATC GCT AAC ATC GAC TGG ACC
G   K   N   V   Y   L   P   P   R   E   G   D   L   T   C   N   S   T   V   T   S   L   I   A   N   I   D   W   T

1,310               1,320               1,330               1,340               1,350               1,360               1,370               1,380               1,390
GAC GGC AAC CAG ACC AAT ATC ACC ATG TCT GCC GAG GTG GCC GAG CTG TAC AGA CTG GAA CTG GGA GAC TAC AAG CTG GTG GAA ATC
D   G   N   Q   T   N   I   T   M   S   A   E   V   A   E   L   Y   R   L   E   L   G   D   Y   K   L   V   E   I

1,400               1,410               1,420               1,430               1,440               1,450               1,460               1,467
ACC CCA ATC GGA CTG GCC CCA ACC GAC GTG AAA AGA TAT ACC ACC GGC GGC ACC TCC AGA AAC AAG AGA TGA TGA
T   P   I   G   L   A   P   T   D   V   K   R   Y   T   T   G   G   T   S   R   N   K   R   *   *
```

Supplemental Table 2

```
1                   10                  20                  30                  40                  50                  60                  70                  80
ATG GAT GCA ATG AAG AGA GGG CTC TGC TGT GTG CTG CTG CTG TGT GGA GCA GTC TTC GTT ACT ACC ACA GAG GCT AGC ATC TAC TGC
M   D   A   M   K   R   G   L   C   C   V   L   L   L   C   G   A   V   F   V   T   T   T   E   A   S   I   Y   C

90                  100                 110                 120                 130                 140                 150                 160                 170
ACC CAG TAC GTG ACC GTG TTC TAC GGC GTG CCA GCT TGG AGA AAC GCC ACC ATT CCA CTG TTC TGC GCC ACC AAG AAC AGG GAC ACC
T   Q   Y   V   T   V   F   Y   G   V   P   A   W   R   N   A   T   I   P   L   F   C   A   T   K   N   R   D   T

180                 190                 200                 210                 220                 230                 240                 250                 260
TGG GGA ACA ACC CAG TGC CTG CCA GAC AAT GGC GAT TAC TCT GAG CTG GCC CTG AAC GTG ACC GAG TCT TTC GAT GCC TGG GAG AAC
W   G   T   T   Q   C   L   P   D   N   G   D   Y   S   E   L   A   L   N   V   T   E   S   F   D   A   W   E   N

270                 280                 290                 300                 310                 320                 330                 340
ACC GTG ACC GAA CAG GCC ATT GAG GAC GTG TGG CAG CTG TTC GAA ACC TCC ATC AAG CCC TGC GTG AAG CTG TCC CCA CTG TGC ATC
T   V   T   E   Q   A   I   E   D   V   W   Q   L   F   E   T   S   I   K   P   C   V   K   L   S   P   L   C   I

350                 360                 370                 380                 390                 400                 410                 420                 430
ACC ATG AGG TGC AAC AAG TCC GAA ACC}GGA CCA GGC{CAG ATG ATC GGC TGC AAG TTC AAC ATG ACC GGC CTG AAG AGG GAC AAG ACC
T   M   R   C   N   K   S   E   T}G   P   G{Q   M   I   G   C   K   F   N   M   T   G   L   K   R   D   K   T

440                 450                 460                 470                 480                 490                 500                 510                 520
AAA GAG TAC AAC GAA ACC TGG TAC TCC ACC GAC CTC GTG TGC GAG CAG GGA AAC TCT ACC GAC AAC GAG TCC AGG TGC TAC ATG AAC
K   E   Y   N   E   T   W   Y   S   T   D   L   V   C   E   Q   G   N   S   T   D   N   E   S   R   C   Y   M   N

530                 540                 550                 560                 570                 580                 590                 600
CAC TGC AAC ACC AGC ATC ATC CAA GAG TCC TGC GAC AAG CAC TAC TGG GAC ACC ATC AGG TTC AGA TAC TGC GCC CCA CCA GGA TAC
H   C   N   T   S   I   I   Q   E   S   C   D   K   H   Y   W   D   T   I   R   F   R   Y   C   A   P   P   G   Y

610                 620                 630                 640                 650                 660                 670                 680                 690
GCC CTG CTG AGA TGC AAC GAC ACC AAC TAC TCC GGC TTC ATG CCC AAG TGC TCC AAG GTG GTG GTG TCC TCC TGC ACC AGG ATG ATG
A   L   L   R   C   N   D   T   N   Y   S   G   F   M   P   K   C   S   K   V   V   V   S   S   C   T   R   M   M

700                 710                 720                 730                 740                 750                 760                 770                 780
GAA ACC CAG ACC TCC ACT TGG TTT GGC TTC AAC GGC ACC AGG GCC GAG AAC AGG ACC TAC ATC TAC TGG CAC GGC AGG GAC AAC AGG
E   T   Q   T   S   T   W   F   G   F   N   G   T   R   A   E   N   R   T   Y   I   Y   W   H   G   R   D   N   R

790                 800                 810                 820                 830                 840                 850                 860                 870
ACC ATC ATC TCC CTG AAC AAG TAC TAC AAC CTG ACC ATG AAG TGC AGA AGG CCC GGC AAC AAA ACC GTG CTG CCA GTG ACC ATC ATG
T   I   I   S   L   N   K   Y   Y   N   L   T   M   K   C   R   R   P   G   N   K   T   V   L   P   V   T   I   M

880                 890                 900                 910                 920                 930                 940                 950
TCC GGC CTG GTG TTT CAC AGC CAG CCA GTG AAC GAA AGG CCC AAC CAG GCT TGG TGT TGG TTC GGC GGA AAT TGG AAG GAC GCC ATC
S   G   L   V   F   H   S   Q   P   V   N   E   R   P   N   Q   A   W   C   W   F   G   G   N   W   K   D   A   I

960                 970                 980                 990                 1,000               1,010               1,020               1,030               1,040
AAA GAA GTG AAG CAG ACC ATC GTG AAG CAC CCC AGA TAC ACC GGC ACC AAC AAC ACC GAC AAG ATC AAC CTG ACA GCC CCA AGA GGC
K   E   V   K   Q   T   I   V   K   H   P   R   Y   T   G   T   N   N   T   D   K   I   N   L   T   A   P   R   G

1,050               1,060               1,070               1,080               1,090               1,100               1,110               1,120               1,130
GGA GAT CCC GAA GTG ACC TTT ATG TGG ACC AAC TGC AGG GGC GAG TTC CTG TAC TGC AAG ATG AAC TGG TTC CTG AAC TGG GTC GAA
G   D   P   E   V   T   F   M   W   T   N   C   R   G   E   F   L   Y   C   K   M   N   W   F   L   N   W   V   E

1,140               1,150               1,160               1,170               1,180               1,190               1,200               1,210
GAT AGG GAC CTG ACC ACA CAG AGG CCC AAA GAG AGG CAT AGA AGA AAC TAC GTG CCC TGC CAC ATC AGG CAG ATC ATC AAC ACC TGG
D   R   D   L   T   T   Q   R   P   K   E   R   H   R   R   N   Y   V   P   C   H   I   R   Q   I   I   N   T   W

1,220               1,230               1,240               1,250               1,260               1,270               1,280               1,290               1,300
CAC AAA GTG GGC AAG AAC GTG TAC CTG CCA CCT AGA GAG GGC GAC CTG ACC TGC AAT TCT ACC GTG ACC AGC CTG ATC GCT AAC ATC
H   K   V   G   K   N   V   Y   L   P   P   R   E   G   D   L   T   C   N   S   T   V   T   S   L   I   A   N   I

1,310               1,320               1,330               1,340               1,350               1,360               1,370               1,380               1,390
GAC TGG ACC GAC GGC AAC CAG ACC AAT ATC ACC ATG TCT GCC GAG GTG GCC GAG CTG TAC AGA CTG GAA CTG GGA GAC TAC AAG CTG
D   W   T   D   G   N   Q   T   N   I   T   M   S   A   E   V   A   E   L   Y   R   L   E   L   G   D   Y   K   L

1,400               1,410               1,420               1,430               1,440               1,450               1,460               1,470               1,476
GTG GAA ATC ACC CCA ATC GGA CTG GCC CCA ACC GAC GTG AAA AGA TAT ACC ACC GGC GGC ACC TCC AGA AAC AAG AGA TGA TGA
V   E   I   T   P   I   G   L   A   P   T   D   V   K   R   Y   T   T   G   G   T   S   R   N   K   R   *   *
```

Supplemental Table 3

```
1                   10                  20                  30                  40                  50                  60                  70                  80                  90                  100
ATG GGC GGC GCC GCC GCC CGG CTG GGC GCC GTG ATC CTG TTC GTG GTG ATC GTG GGC CTG CAC GGC GTG CGG GGC AAG TAC GCC CTG GCC GAC GCC AGC CTG
 M   G   G   A   A   A   R   L   G   A   V   I   L   F   V   V   I   V   G   L   H   G   V   R   G   K   Y   A   L   A   D   A   S   L

110                 120                 130                 140                 150                 160                 170                 180                 190                 200
AAG ATG GCC GAC CCC AAC CGG TTC CGG GGC AAG GAC CTG CCC GTG CTG GAC CAG CTG GCT AGC ATC TAC TGC ACC CAG TAC GTG ACC GTG TTC TAC GGC GTG
 K   M   A   D   P   N   R   F   R   G   K   D   L   P   V   L   D   Q   L   A   S   I   Y   C   T   Q   Y   V   T   V   F   Y   G   V

210                 220                 230                 240                 250                 260                 270                 280                 290                 300
CCC GCC TGG CGG AAC GCC ACC ATC CCT CTG TTC TGC GCC ACC AAG AAC CGG GAC ACC TGG GGC ACC ACC CAG TGC CTG CCC GAC AAC GGC GAC TAC AGC GAG
 P   A   W   R   N   A   T   I   P   L   F   C   A   T   K   N   R   D   T   W   G   T   T   Q   C   L   P   D   N   G   D   Y   S   E

310                 320                 330                 340                 350                 360                 370                 380                 390                 400
CTG GCC CTG AAC GTG ACC GAG AGC TTC GAC GCC TGG GAG AAC ACC GTG ACC GAG CAG GCC ATC GAG GAC GTG TGG CAG CTG TTC GAA ACC AGC ATC AAG CCC
 L   A   L   N   V   T   E   S   F   D   A   W   E   N   T   V   T   E   Q   A   I   E   D   V   W   Q   L   F   E   T   S   I   K   P

410                 420                 430                 440                 450                 460                 470                 480                 490                 500                 510
TGC GTG AAG CTG AGC CCC CTG TGC ATC ACC ATG CGG TGC AAC AAG AGC GAG ACA GAT AAG TGG GGC CTG ACC AAG AGC AGC ACC ACC ACC GCC AGC ACC ACA
 C   V   K   L   S   P   L   C   I   T   M   R   C   N   K   S   E   T   D   K   W   G   L   T   K   S   S   T   T   T   A   S   T   T

520                 530                 540                 550                 560                 570                 580                 590                 600                 610
ACC ACC ACA GCC CCT GCC AAG ATC GAC ATG GTG AAC GAG ACA AGC AGC TGC ATC ACC CAC GAC AAC TGC ACC GGC CTG GAA CAG GAA CAG ATG ATC GGC TGC
 T   T   T   A   P   A   K   I   D   M   V   N   E   T   S   S   C   I   T   H   D   N   C   T   G   L   E   Q   E   Q   M   I   G   C

620                 630                 640                 650                 660                 670                 680                 690                 700                 710
AAG TTC AAC ATG ACC GGC CTG AAG CGG GAC AAG ACC AAA GAG TAC AAC GAA ACC TGG TAC AGC ACC GAC CTG GTG TGC GAG CAG GGC AAC TCC ACC GAC AAC
 K   F   N   M   T   G   L   K   R   D   K   T   K   E   Y   N   E   T   W   Y   S   T   D   L   V   C   E   Q   G   N   S   T   D   N

720                 730                 740                 750                 760                 770                 780                 790                 800                 810
GAG AGC CGG TGC TAC ATG AAC CAC TGC AAC ACC AGC ATC ATC CAG GAA AGC TGC GAC AAG CAC TAC TGG GAC ACC ATC CGG TTC CGG TAC TGC GCC CCT CCT
 E   S   R   C   Y   M   N   H   C   N   T   S   I   I   Q   E   S   C   D   K   H   Y   W   D   T   I   R   F   R   Y   C   A   P   P

820                 830                 840                 850                 860                 870                 880                 890                 900                 910
GGC TAC GCC CTG CTG AGA TGC AAC GAC ACC AAC TAC AGC GGC TTC ATG CCC AAG TGC AGC AAG GTG GTG GTG TCC AGC TGC ACC CGG ATG ATG GAA ACC CAG
 G   Y   A   L   L   R   C   N   D   T   N   Y   S   G   F   M   P   K   C   S   K   V   V   V   S   S   C   T   R   M   M   E   T   Q

920                 930                 940                 950                 960                 970                 980                 990                 1,000               1,010               1,020
ACC AGC ACT TGG TTT GGC TTC AAC GGC ACC AGA GCC GAG AAC CGG ACC TAC ATC TAC TGG CAC GGC CGG GAC AAC CGG ACC ATC ATC AGC CTG AAC AAG TAC
 T   S   T   W   F   G   F   N   G   T   R   A   E   N   R   T   Y   I   Y   W   H   G   R   D   N   R   T   I   I   S   L   N   K   Y

1,030               1,040               1,050               1,060               1,070               1,080               1,090               1,100               1,110               1,120
TAC AAC CTG ACC ATG AAG TGC AGA AGG CCC GGC AAC AAG ACC GTG CTG CCC GTG ACC ATC ATG AGC GGC CTG GTG TTC CAC AGC CAG CCC GTG AAC GAG CGG
 Y   N   L   T   M   K   C   R   R   P   G   N   K   T   V   L   P   V   T   I   M   S   G   L   V   F   H   S   Q   P   V   N   E   R

1,130               1,140               1,150               1,160               1,170               1,180               1,190               1,200               1,210               1,220
CCC AAC CAG GCT TGG TGT TGG TTC GGC GGC AAC TGG AAG GAC GCC ATC AAA GAA GTG AAG CAG ACC ATC GTG AAG CAC CCC CGG TAC ACC GGC ACC AAC AAC
 P   N   Q   A   W   C   W   F   G   G   N   W   K   D   A   I   K   E   V   K   Q   T   I   V   K   H   P   R   Y   T   G   T   N   N

1,230               1,240               1,250               1,260               1,270               1,280               1,290               1,300               1,310               1,320
ACC GAC AAG ATC AAC CTG ACC GCC CCC AGA GGC GGC GAC CCC GAA GTG ACC TTC ATG TGG ACC AAC TGC AGA GGC GAG TTC CTG TAC TGC AAG ATG AAC TGG
 T   D   K   I   N   L   T   A   P   R   G   G   D   P   E   V   T   F   M   W   T   N   C   R   G   E   F   L   Y   C   K   M   N   W

1,330               1,340               1,350               1,360               1,370               1,380               1,390               1,400               1,410               1,420
TTC CTG AAC TGG GTG GAA GAT CGG GAC CTG ACC ACC CAG CGG CCC AAA GAG CGG CAC AGA CGG AAC TAC GTG CCC TGC CAC ATC CGG CAG ATC ATC AAC ACC
 F   L   N   W   V   E   D   R   D   L   T   T   Q   R   P   K   E   R   H   R   R   N   Y   V   P   C   H   I   R   Q   I   I   N   T

1,430               1,440               1,450               1,460               1,470               1,480               1,490               1,500               1,510               1,520               1,530
TGG CAC AAA GTG GGC AAG AAC GTG TAC CTG CCC CCC AGA GAG GGC GAT CTG ACC TGC AAC AGC ACC GTG ACC AGC CTG ATC GCC AAC ATC GAC TGG ACC GAC
 W   H   K   V   G   K   N   V   Y   L   P   P   R   E   G   D   L   T   C   N   S   T   V   T   S   L   I   A   N   I   D   W   T   D

1,540               1,550               1,560               1,570               1,580               1,590               1,600               1,610               1,620               1,630
GGC AAC CAG ACC AAC ATC ACC ATG AGC GCC GAG GTG GCC GAG CTG TAC CGG CTG GAA CTG GGC GAC TAC AAG CTG GTG GAA ATC ACC CCC ATC GGC CTG GCC
 G   N   Q   T   N   I   T   M   S   A   E   V   A   E   L   Y   R   L   E   L   G   D   Y   K   L   V   E   I   T   P   I   G   L   A

1,640               1,650               1,660               1,670               1,680               1,689
CCC ACC GAC GTG AAG AGA TAC ACC ACC GGC GGC ACC AGC CGG AAC AAG AGA TGA TGA
 P   T   D   V   K   R   Y   T   T   G   G   T   S   R   N   K   R   *   *
```

Supplemental Table 4

```
1          10         20         30         40         50         60         70         80         90         100        110
ATG GGC TGC CTG GGC AAC CAG CTG CTG ATC GCC ATC CTG CTG CTG TCG GTG TAC GGC ATC TAC TGC ACC CAG TAC GTG ACC GTG TTC TAC GGC GTG CCT GCC TGG CGG AAT GCC ACC
 M   G   C   L   G   N   Q   L   L   I   A   I   L   L   L   S   V   Y   G   I   Y   C   T   Q   Y   V   T   V   F   Y   G   V   P   A   W   R   N   A   T

120        130        140        150        160        170        180        190        200        210        220        230
ATC CCG CTG TTC TGC GCC ACC AAG AAC AGA GAC ACC TGG GGC ACC ACA CAG TGC CTG CCC GAC AAC GGC GAT TAC AGC GAG CTG GCC CTG AAC GTG ACC GAG AGC TTC GAC GCC TGG
 I   P   L   F   C   A   T   K   N   R   D   T   W   G   T   T   Q   C   L   P   D   N   G   D   Y   S   E   L   A   L   N   V   T   E   S   F   D   A   W

240        250        260        270        280        290        300        310        320        330        340        350
GAG AAC ACC GTG ACC GAG CAG GCC ATC GAG GAC GTG TGG CAG CTG TTC GAG ACC ATC AAG CCC TGC GTG AAG CTG TCC CCT CTC TGT ATC ACA ATG CGC TGT AAC AAG AGC GAG
 E   N   T   V   T   E   Q   A   I   E   D   V   W   Q   L   F   E   T   S   I   K   P   C   V   K   L   S   P   L   C   I   T   M   R   C   N   K   S   E

360        370        380        390        400        410        420        430        440        450        460
ACA GAC AAG TGG GGC CTG ACC AAG TCG AGC ACC ACG ACC GCG AGC ACA ACC ACT ACG ACG GCG CCT GCC AAG ATC GAC ATG GTG AAC GAG ACA AGC AGC TGC ATC ACG CAC GAC AAC
 T   D   K   W   G   L   T   K   S   S   T   T   T   A   S   T   T   T   T   T   A   P   A   K   I   D   M   V   N   E   T   S   S   C   I   T   H   D   N

470        480        490        500        510        520        530        540        550        560        570        580
TGC ACC GGC CTG GAA CAG GAA CAG ATG ATC GGC TGC AAG TTC AAC ATG ACC GGC CTG AAG CGG GAC AAG ACC AAA GAG TAC AAC GAA ACC TGG TAC AGC ACC GAC CTG GTG TGC GAG
 C   T   G   L   E   Q   E   Q   M   I   G   C   K   F   N   M   T   G   L   K   R   D   K   T   K   E   Y   N   E   T   W   Y   S   T   D   L   V   C   E

590        600        610        620        630        640        650        660        670        680        690        700
CAG GGC AAC TCC ACC GAC AAC GAG AGC CGG TGC TAC ATG AAC CAC TGC AAC ACC AGC ATC ATC CAG GAA AGC TGC GAC AAG CAC TAC TGG GAC ACC ATC CGG TTC AGA TAC TGC GCG
 Q   G   N   S   T   D   N   E   S   R   C   Y   M   N   H   C   N   T   S   I   I   Q   E   S   C   D   K   H   Y   W   D   T   I   R   F   R   Y   C   A

710        720        730        740        750        760        770        780        790        800        810
CCT CCT GGC TAC GCC CTG CTG AGA TGC AAC GAC ACC AAC TAC AGC GGC TTC ATG CCC AAG TGC AGC AAG GTG GTG GTG TCC AGC TGC ACC CGG ATG ATG GAA ACC CAG ACC AGC ACT
 P   P   G   Y   A   L   L   R   C   N   D   T   N   Y   S   G   F   M   P   K   C   S   K   V   V   V   S   S   C   T   R   M   M   E   T   Q   T   S   T

820        830        840        850        860        870        880        890        900        910        920        930
TGG TTT GGC TTC AAC GGC ACC AGA GCC GAG AAC CGG ACC TAC ATC TAC TGG CAC GGC CGG GAC AAC CGG ACC ATC ATC AGC CTG AAC AAG TAC TAC AAC CTG ACC ATG AAG TGC AGA
 W   F   G   F   N   G   T   R   A   E   N   R   T   Y   I   Y   W   H   G   R   D   N   R   T   I   I   S   L   N   K   Y   Y   N   L   T   M   K   C   R

940        950        960        970        980        990        1,000      1,010      1,020      1,030      1,040      1,050
AGG CCC GGC AAC AAG ACC GTG CTG CCC GTG ACC ATC ATG AGC GGC CTG GTG TTC CAC TCG CAG CCC GTC AAC GAG AGG CCC AAC CAG GCT TGG TGT TGG TTC GGC GGC AAC TGG AAG
 R   P   G   N   K   T   V   L   P   V   T   I   M   S   G   L   V   F   H   S   Q   P   V   N   E   R   P   N   Q   A   W   C   W   F   G   G   N   W   K

1,060      1,070      1,080      1,090      1,100      1,110      1,120      1,130      1,140      1,150      1,160      1,170
GAC GCC ATC AAA GAA GTG AAG CAG ACC ATC GTG AAG CAC CCC CGG TAC ACC GGC ACC AAC AAC ACC GAC AAG ATC AAC CTG ACC GCC CCG AGA GGC GGC GAT CCC GAA GTG ACC TTC
 D   A   I   K   E   V   K   Q   T   I   V   K   H   P   R   Y   T   G   T   N   N   T   D   K   I   N   L   T   A   P   R   G   G   D   P   E   V   T   F

1,180      1,190      1,200      1,210      1,220      1,230      1,240      1,250      1,260      1,270      1,280
ATG TGG ACC AAC TGC AGA GGC GAG TTC CTG TAC TGC AAG ATG AAC TGG TTC CTG AAC TGG GTG GAG GAC CGG GAC CTC ACC ACC CAG CGG CCC AAA GAG CGG CAC CGG AGA AAC TAC
 M   W   T   N   C   R   G   E   F   L   Y   C   K   M   N   W   F   L   N   W   V   E   D   R   D   L   T   T   Q   R   P   K   E   R   H   R   R   N   Y

1,290      1,300      1,310      1,320      1,330      1,340      1,350      1,360      1,370      1,380      1,390      1,400
GTG CCC TGC CAC ATC CGG CAG ATC ATC AAC ACC TGG CAC AAA GTG GGC AAG AAC GTG TAC CTG CCG CCC AGA GAG GGC GAC CTG ACC TGC AAC AGC ACC GTG ACC AGC CTG ATC GCC
 V   P   C   H   I   R   Q   I   I   N   T   W   H   K   V   G   K   N   V   Y   L   P   P   R   E   G   D   L   T   C   N   S   T   V   T   S   L   I   A

1,410      1,420      1,430      1,440      1,450      1,460      1,470      1,480      1,490      1,500      1,510      1,520
AAC ATC GAC TGG ACC GAC GGC AAC CAG ACC AAC ATC ACC ATG AGC GCG GAG GTG GCC GAG CTG TAC AGA CTG GAA CTG GGC GAC TAC AAA CTG GTG GAG ATC ACC CCG ATC GGC CTG
 N   I   D   W   T   D   G   N   Q   T   N   I   T   M   S   A   E   V   A   E   L   Y   R   L   E   L   G   D   Y   K   L   V   E   I   T   P   I   G   L

1,530      1,540      1,550      1,560      1,570      1,580      1,590      1,600      1,610      1,620      1,630
GCC CCC ACC GAC GTG AAG AGA TAC ACC ACC GGC GGA ACA AGT AGA AAT AAG AGA GGC GTG TTC GTC CTG GGC TTC CTG GGC TTT CTG GCC ACC GCC GGA TCT GCC ATG GGA GCC GCC
 A   P   T   D   V   K   R   Y   T   T   G   G   T   S   R   N   K   R   G   V   F   V   L   G   F   L   G   F   L   A   T   A   G   S   A   M   G   A   A

1,640      1,650      1,660      1,670      1,680      1,690      1,700      1,710      1,720      1,730      1,740      1,750
AGC CTG ACA CTC ACA GCT CAG AGC AGA ACA CTG CTG GCC GGC ATT GTC CAG CAG CAG CAG CAG CTC CTC GAC GTG GTG AAG CGG CAG CAG GAA CTG CTG AGA CTG ACC GTG TGG GGC
 S   L   T   L   T   A   Q   S   R   T   L   L   A   G   I   V   Q   Q   Q   Q   Q   L   L   D   V   V   K   R   Q   Q   E   L   L   R   L   T   V   W   G

1,760      1,770      1,780      1,790      1,800      1,810      1,820      1,830      1,840      1,850      1,860      1,870
ACC AAG AAC CTG CAG ACC AGA GTG ACC GCC ATC GAG AAG TAC CTG AAG GAC CAG GCC CAG CTG AAT GCC TGG GGC TGC GCC TTC AGA CAA GTC TGC CAC ACA ACC GTG CCT TGG CCC
 T   K   N   L   Q   T   R   V   T   A   I   E   K   Y   L   K   D   Q   A   Q   L   N   A   W   G   C   A   F   R   Q   V   C   H   T   T   V   P   W   P

1,880      1,890      1,900      1,910      1,920      1,930      1,940      1,950      1,960      1,970      1,980
AAC GCC TCC CTG ACC CCC GAC TGG AAC AAC GAC ACC TGG CAG GAA TGG GAG CGG AAA GTC GAT TTC CTG GAA GAG AAC ATC ACC GCC CTG CTG GAA GAG GCC CAG ATC CAG CAG GAA
 N   A   S   L   T   P   D   W   N   N   D   T   W   Q   E   W   E   R   K   V   D   F   L   E   E   N   I   T   A   L   L   E   E   A   Q   I   Q   Q   E

1,990      2,000      2,010      2,020      2,030      2,040      2,050      2,060      2,070      2,080      2,090      2,100
AAG AAC ATG TAC GAG CTG CAG AAG CTG AAC AGC TGG GAC GTG TTC GGC AAT TGG TTC GAC CTG GCC AGC TGG ATC CGC TAC ATC CAG TAC GGC ATC TAC ATC GTG GTG GGA GTC ATT
 K   N   M   Y   E   L   Q   K   L   N   S   W   D   V   F   G   N   W   F   D   L   A   S   W   I   R   Y   I   Q   Y   G   I   Y   I   V   V   G   V   I

2,110      2,120      2,130      2,140      2,150      2,160      2,170      2,180      2,190      2,200      2,210      2,220
CTC CTC CGG ATC GTG ATC TAC ATT GTG CAG ATG CTG GCC AAG CTG CGG CAG GGC TAC AGA CCC GTG TTC AGC AGC CCC CCC AGC TAC TCG CAG CAG ACC CAC ATT CAG CAG GAT CCG
 L   L   R   I   V   I   Y   I   V   Q   M   L   A   K   L   R   Q   G   Y   R   P   V   F   S   S   P   P   S   Y   S   Q   Q   T   H   I   Q   Q   D   P

2,230      2,240      2,250      2,260      2,270      2,280      2,290      2,300      2,310      2,320      2,330      2,340
GCT CTC CCT ACA AGA GAG GGC AAA GAG GGA GAT GGA GGA GAG TCG GGC GGC AAT AGC TCC TGG CCC TGG CAG ATC GAG TAC ATC CAC TTT CTG ATC CGC CAG CTC ATT AGA CTG CTG
 A   L   P   T   R   E   G   K   E   G   D   G   G   E   S   G   G   N   S   S   W   P   W   Q   I   E   Y   I   H   F   L   I   R   Q   L   I   R   L   L

2,350      2,360      2,370      2,380      2,390      2,400      2,410      2,420      2,430      2,440      2,450
ACC TGG CTG TTC AAC AAC TGC CGG ACC CTG CTG TCC AGA GCC TAC CAG ATC CTG CAG CCC ATC CTG CAG AGA CTG TCT GCG GCC CTG CAG CGG ATC AGA GAG GTG CTG CGG ACC GAG
 T   W   L   F   N   N   C   R   T   L   L   S   R   A   Y   Q   I   L   Q   P   I   L   Q   R   L   S   A   A   L   Q   R   I   R   E   V   L   R   T   E

2,460      2,470      2,480      2,490      2,500      2,510      2,520      2,530      2,540      2,550      2,560      2,570
CTG ACC TAC CTG CAG TAC GGC TGG TCC TAC TTC CAC GAG GCC GTG CAG GCT GGG TGG AGA AGC GCC ACA GAG ACA CTG GCT GGC GCC TGG GGC GAT CTG TGG GAG ACA CTG CGG AGA
 L   T   Y   L   Q   Y   G   W   S   Y   F   H   E   A   V   Q   A   G   W   R   S   A   T   E   T   L   A   G   A   W   G   D   L   W   E   T   L   R   R

2,580      2,590      2,600      2,610      2,620      2,630      2,640 2,643
GGC GGC AGA TGG ATC CTG GCC ATC CCC AGA AGA ATC CGG CAG GGC CTG GAA CTG ACA CTG CTG TGA TAA
 G   G   R   W   I   L   A   I   P   R   R   I   R   Q   G   L   E   L   T   L   L   *   *
```

Supplemental Table 5

```
1         10        20        30        40        50        60        70        80        90       100       110       120       130       140
ATG GGA TGT CTG GGA AAT CAG CTG CTG ATC GCC ATC CTG CTG CTG TCC GTG TAC GGA ATC TAC TGC ACC CAG TAC GTG ACC GTG TTC TAC GGC GTG CCA GCT TGG AGA AAC GCC ACC ATT CCA CTG TTC TGC GCC ACC AAG
 M   G   C   L   G   N   Q   L   L   I   A   I   L   L   L   S   V   Y   G   I   Y   C   T   Q   Y   V   T   V   F   Y   G   V   P   A   W   R   N   A   T   I   P   L   F   C   A   T   K

      150       160       170       180       190       200       210       220       230       240       250       260       270       280
AAC AGG GAC ACC TGG GGA ACA ACC CAG TGC CTG CCA GAC AAT GGC GAT TAC TCT GAG CTG GCC CTG AAC GTG ACC GAG TCT TTC GAT GCC TGG GAG AAC ACC GTG ACC GAA CAG GCC ATT GAG GAC GTG TGG CAG CTG TTC
 N   R   D   T   W   G   T   T   Q   C   L   P   D   N   G   D   Y   S   E   L   A   L   N   V   T   E   S   F   D   A   W   E   N   T   V   T   E   Q   A   I   E   D   V   W   Q   L   F

      290       300       310       320       330       340       350       360       370       380       390       400       410       420
GAA ACC TCC ATC AAG CCC TGC GTG AAG CTG TCC CCA CTG TGC ATC ACC ATG AGG TGC AAC AAG TCC GAA ACC}{CAG ATG ATC GGC TGC AAG TTC AAC ATG ACC GGC CTG AAG AGG GAC AAG ACC AAA GAG TAC AAC GAA ACC
 E   T   S   I   K   P   C   V   K   L   S   P   L   C   I   T   M   R   C   N   K   S   E   T   Q   M   I   G   C   K   F   N   M   T   G   L   K   R   D   K   T   K   E   Y   N   E   T

      430       440       450       460       470       480       490       500       510       520       530       540       550       560
TGG TAC TCC ACC GAC CTC GTG TGC GAG CAG GGA AAC TCT ACC GAC AAC GAG TCC AGG TGC TAC ATG AAC CAC TGC AAC ACC AGC ATC ATC CAA GAG TCC TGC GAC AAG CAC TAC TGG GAC ACC ATC AGG TTC AGA TAC TGC
 W   Y   S   T   D   L   V   C   E   Q   G   N   S   T   D   N   E   S   R   C   Y   M   N   H   C   N   T   S   I   I   Q   E   S   C   D   K   H   Y   W   D   T   I   R   F   R   Y   C

      570       580       590       600       610       620       630       640       650       660       670       680       690       700
GCC CCA CCA GGA TAC GCC CTG CTG AGA TGC AAC GAC ACC AAC TAC TCC GGC TTC ATG CCC AAG TGC TCC AAG GTG GTG GTG TCC TCC TGC ACC AGG ATG ATG GAA ACC CAG ACC TCC ACT TGG TTT GGC TTC AAC GGC ACC
 A   P   P   G   Y   A   L   L   R   C   N   D   T   N   Y   S   G   F   M   P   K   C   S   K   V   V   V   S   S   C   T   R   M   M   E   T   Q   T   S   T   W   F   G   F   N   G   T

      710       720       730       740       750       760       770       780       790       800       810       820       830       840
AGG GCC GAG AAC AGG ACC TAC ATC TAC TGG CAC GGC AGG GAC AAC AGG ACC ATC ATC TCC CTG AAC AAG TAC TAC AAC CTG ACC ATG AAG TGC AGA AGG CCC GGC AAC AAA ACC GTG CTG CCA GTG ACC ATC ATG TCC GGC
 R   A   E   N   R   T   Y   I   Y   W   H   G   R   D   N   R   T   I   I   S   L   N   K   Y   Y   N   L   T   M   K   C   R   R   P   G   N   K   T   V   L   P   V   T   I   M   S   G

      850       860       870       880       890       900       910       920       930       940       950       960       970       980
CTG GTG TTT CAC AGC CAG CCA GTG AAC GAA AGG CCC AAC CAG GCT TGG TGT TGG TTC GGC GGA AAT TGG AAG GAC GCC ATC AAA GAA GTG AAG CAG ACC ATC GTG AAG CAC CCC AGA TAC ACC GGC ACC AAC AAC ACC GAC
 L   V   F   H   S   Q   P   V   N   E   R   P   N   Q   A   W   C   W   F   G   G   N   W   K   D   A   I   K   E   V   K   Q   T   I   V   K   H   P   R   Y   T   G   T   N   N   T   D

      990      1,000     1,010     1,020     1,030     1,040     1,050     1,060     1,070     1,080     1,090     1,100     1,110     1,120
AAG ATC AAC CTG ACA GCC CCA AGA GGC GGA GAT CCC GAA GTG ACC TTT ATG TGG ACC AAC TGC AGG GGC GAG TTC CTG TAC TGC AAG ATG AAC TGG TTC CTG AAC TGG GTC GAA GAT AGG GAC CTG ACC ACA CAG AGG CCC
 K   I   N   L   T   A   P   R   G   G   D   P   E   V   T   F   M   W   T   N   C   R   G   E   F   L   Y   C   K   M   N   W   F   L   N   W   V   E   D   R   D   L   T   T   Q   R   P

    1,130     1,140     1,150     1,160     1,170     1,180     1,190     1,200     1,210     1,220     1,230     1,240     1,250     1,260
AAA GAG AGG CAT AGA AGA AAC TAC GTG CCC TGC CAC ATC AGG CAG ATC ATC AAC ACC TGG CAC AAA GTG GGC AAG AAC GTG TAC CTG CCA CCT AGA GAG GGC GAC CTG ACC TGC AAT TCT ACC GTG ACC AGC CTG ATC GCT
 K   E   R   H   R   R   N   Y   V   P   C   H   I   R   Q   I   I   N   T   W   H   K   V   G   K   N   V   Y   L   P   P   R   E   G   D   L   T   C   N   S   T   V   T   S   L   I   A

    1,270     1,280     1,290     1,300     1,310     1,320     1,330     1,340     1,350     1,360     1,370     1,380     1,390     1,400     1,410
AAC ATC GAC TGG ACC GAC GGC AAC CAG ACC AAT ATC ACC ATG TCT GCC GAG GTG GCC GAG CTG TAC AGA CTG GGA GAC TAC AAG CTG GTG GAA ATC ACC CCA ATC GGA CTG GCC CCA ACC GAC GTG AAA AGA TAT
 N   I   D   W   T   D   G   N   Q   T   N   I   T   M   S   A   E   V   A   E   L   Y   R   L   E   L   G   D   Y   K   L   V   E   I   T   P   I   G   L   A   P   T   D   V   K   R   Y

    1,420     1,430     1,440     1,450     1,460     1,470     1,480     1,490     1,500     1,510     1,520     1,530     1,540     1,550
ACC ACC GGC GGC ACC TCC AGA AAC AAG AGA GGC GTG TTC GTT CTG GGC TTC CTG GGA TTT CTG GCC ACA GCC GGA TCT GCC ATG GGA GCT GCT TCT CTG ACA CTG ACC GCT CAG TCT AGA ACC CTG CTG GCT GGA ATC GTG
 T   T   G   G   T   S   R   N   K   R   G   V   F   V   L   G   F   L   G   F   L   A   T   A   G   S   A   M   G   A   A   S   L   T   L   T   A   Q   S   R   T   L   L   A   G   I   V

    1,560     1,570     1,580     1,590     1,600     1,610     1,620     1,630     1,640     1,650     1,660     1,670     1,680     1,690
CAG CAG CAG CAA CAG CTG CTG GAC GTG GTC AAG AGG CAG CAA GAA CTG CTG AGA CTG ACC GTG TGG GGC ACC AAG AAT CTG CAG ACC AGA GTG ACC GCC ATC GAG AAG TAC CTG AAG GAT CAG GCC CAG CTG AAT GCC TGG
 Q   Q   Q   Q   Q   L   L   D   V   V   K   R   Q   Q   E   L   L   R   L   T   V   W   G   T   K   N   L   Q   T   R   V   T   A   I   E   K   Y   L   K   D   Q   A   Q   L   N   A   W

    1,700     1,710     1,720     1,730     1,740     1,750     1,760     1,770     1,780     1,790     1,800     1,810     1,820     1,830
GGA TGC GCC TTT AGA CAA GTG TGC CAT ACC ACC GTG CCT TGG CCA AAT GCC AGT CTG ACC CCT GAC TGG AAC AAC GAC ACA TGG CAA GAG TGG GAG AGA AAG GTG GAC TTC CTG GAA GAG AAC ATC ACC GCT CTG CTG GAA
 G   C   A   F   R   Q   V   C   H   T   T   V   P   W   P   N   A   S   L   T   P   D   W   N   N   D   T   W   Q   E   W   E   R   K   V   D   F   L   E   E   N   I   T   A   L   L   E

    1,840     1,850     1,860     1,870     1,880     1,890     1,900     1,910     1,920     1,930     1,940     1,950     1,960     1,970
GAG GCC CAG ATC CAG CAA GAG AAG AAT ATG TAC GAG CTG CAG AAG CTG AAC TCC TGG GAC GTG TTC GGC AAT TGG TTC GAC CTG GCC TCC TGG ATC AGA TAT ATC CAG TAC GGC ATC TAC ATC GTC GTG GGC GTG ATC CTG
 E   A   Q   I   Q   Q   E   K   N   M   Y   E   L   Q   K   L   N   S   W   D   V   F   G   N   W   F   D   L   A   S   W   I   R   Y   I   Q   Y   G   I   Y   I   V   V   G   V   I   L

    1,980     1,990     2,000     2,010     2,020     2,030     2,040     2,050     2,060     2,070     2,080     2,090     2,100     2,110
CTG AGG ATC GTG ATC TAT ATC GTG CAG ATG CTG GCC AAG CTG AGG CAG GGC TAC AGA CCA GTG TTC TCC TCT CCA CCA TCC TAC TCT CAG CAG ACC CAC ATC CAA CAG GAT CCC GCT CTG CCC ACC AGA GAA GGC AAA GAA
 L   R   I   V   I   Y   I   V   Q   M   L   A   K   L   R   Q   G   Y   R   P   V   F   S   S   P   P   S   Y   S   Q   Q   T   H   I   Q   Q   D   P   A   L   P   T   R   E   G   K   E

    2,120     2,130     2,140     2,150     2,160     2,170     2,180     2,190     2,200     2,210     2,220     2,230     2,240     2,250
GGC GAC GGC GGA GAG TCC GGT GGA AAC TCT TCT TGG CCC TGG CAG ATC GAG TAT ATC CAC TTC CTG ATC CGC CAG CTG ATC AGA CTG CTG ACC TGG CTG TTC AAC AAC TGT AGG ACC CTG CTG TCC AGG GCC TAC CAG ATC
 G   D   G   G   E   S   G   G   N   S   S   W   P   W   Q   I   E   Y   I   H   F   L   I   R   Q   L   I   R   L   L   T   W   L   F   N   N   C   R   T   L   L   S   R   A   Y   Q   I

    2,260     2,270     2,280     2,290     2,300     2,310     2,320     2,330     2,340     2,350     2,360     2,370     2,380     2,390
CTG CAG CCA ATC CTG CAG AGA CTG TCT GCT GCC CTG CAG AGG ATC AGA GAG GTG CTG AGA ACC GAG CTG ACC TAC CTG CAG TAC GGC TGG TCT TAC TTC CAT GAA GCT GTG CAG GCT GGA TGG CGC TCT GCC ACA GAA ACA
 L   Q   P   I   L   Q   R   L   S   A   A   L   Q   R   I   R   E   V   L   R   T   E   L   T   Y   L   Q   Y   G   W   S   Y   F   H   E   A   V   Q   A   G   W   R   S   A   T   E   T

    2,400     2,410     2,420     2,430     2,440     2,450     2,460     2,470     2,480     2,490     2,500     2,508
CTT GCT GGT GCT TGG GGC GAT CTG TGG GAA ACA CTT AGA CGC GGC GGA AGA TGG ATC CTG GCT ATC CCC AGA AGA ATC AGG CAG GGC CTC GAA CTG ACA CTG CTG TGA TGA
 L   A   G   A   W   G   D   L   W   E   T   L   R   R   G   G   R   W   I   L   A   I   P   R   R   I   R   Q   G   L   E   L   T   L   L   *   *
```

Supplemental Table 6

```
1          10         20         30         40         50         60         70         80         90         100        110        120        130
ATG GGA TGT CTG GGA AAT CAG CTG CTG ATC GCC ATC CTG CTG CTG TCC GTG TAC GGA ATC TAC TGC ACC CAG TAC GTG ACC GTG TTC TAC GGC GTG CCA GCT TGG AGA AAC GCC ACC ATT CCA CTG TTC TGC GCC
 M   G   C   L   G   N   Q   L   L   I   A   I   L   L   L   S   V   Y   G   I   Y   C   T   Q   Y   V   T   V   F   Y   G   V   P   A   W   R   N   A   T   I   P   L   F   C   A

    140        150        160        170        180        190        200        210        220        230        240        250        260        270
ACC AAG AAC AGG GAC ACC TGG GGA ACA ACC CAG TGC CTG CCA GAC AAT GGC GAT TAC TCT GAG CTG GCC CTG AAC GTG ACC GAG TCT TTC GAT GCC TGG GAG AAC ACC GTG ACC GAA CAG GCC ATT GAG GAC GTG
 T   K   N   R   D   T   W   G   T   T   Q   C   L   P   D   N   G   D   Y   S   E   L   A   L   N   V   T   E   S   F   D   A   W   E   N   T   V   T   E   Q   A   I   E   D   V

            280        290        300        310        320        330        340        350        360        370        380        390        400
TGG CAG CTG TTC GAA ACC TCC ATC AAG CCC TGC GTG AAG CTG TCC CCA CTG TGC ATC ACC ATG AGG TGC AAC AAG TCC GAA ACC}GGA CCA GGC{CAG ATG ATC GGC TGC AAG TTC AAC ATG ACC GGC CTG AAG AGG
 W   Q   L   F   E   T   S   I   K   P   C   V   K   L   S   P   L   C   I   T   M   R   C   N   K   S   E   T   G   P   G   Q   M   I   G   C   K   F   N   M   T   G   L   K   R

    410        420        430        440        450        460        470        480        490        500        510        520        530        540
GAC AAG ACC AAA GAG TAC AAC GAA ACC TGG TAC TCC ACC GAC CTC GTG TGC GAG CAG GGA AAC TCT ACC GAC AAC GAG TCC AGG TGC TAC ATG AAC CAC TGC AAC ACC AGC ATC ATC CAA GAG TCC TGC GAC AAG
 D   K   T   K   E   Y   N   E   T   W   Y   S   T   D   L   V   C   E   Q   G   N   S   T   D   N   E   S   R   C   Y   M   N   H   C   N   T   S   I   I   Q   E   S   C   D   K

            550        560        570        580        590        600        610        620        630        640        650        660        670
CAC TAC TGG GAC ACC ATC AGG TTC AGA TAC TGC GCC CCA CCA GGA TAC GCC CTG CTG AGA TGC AAC GAC ACC AAC TAC TCC GGC TTC ATG CCC AAG TGC TCC AAG GTG GTG GTG TCC TCC TGC ACC AGG ATG ATG
 H   Y   W   D   T   I   R   F   R   Y   C   A   P   P   G   Y   A   L   L   R   C   N   D   T   N   Y   S   G   F   M   P   K   C   S   K   V   V   V   S   S   C   T   R   M   M

    680        690        700        710        720        730        740        750        760        770        780        790        800        810
GAA ACC CAG ACC TCC ACT TGG TTT GGC TTC AAC GGC ACC AGG GCC GAG AAC AGG ACC TAC ATC TAC TGG CAC GGC AGG GAC AAC AGG ACC ATC ATC TCC CTG AAC AAG TAC TAC AAC CTG ACC ATG AAG TGC AGA
 E   T   Q   T   S   T   W   F   G   F   N   G   T   R   A   E   N   R   T   Y   I   Y   W   H   G   R   D   N   R   T   I   I   S   L   N   K   Y   Y   N   L   T   M   K   C   R

            820        830        840        850        860        870        880        890        900        910        920        930        940
AGG CCC GGC AAC AAA ACC GTG CTG CCA GTG ACC ATC ATG TCC GGC CTG GTG TTT CAC AGC CAG CCA GTG AAC GAA AGG CCC AAC CAG GCT TGG TGT TGG TTC GGC GGA AAT TGG AAG GAC GCC ATC AAA GAA GTG
 R   P   G   N   K   T   V   L   P   V   T   I   M   S   G   L   V   F   H   S   Q   P   V   N   E   R   P   N   Q   A   W   C   W   F   G   G   N   W   K   D   A   I   K   E   V

    950        960        970        980        990        1,000      1,010      1,020      1,030      1,040      1,050      1,060      1,070      1,080
AAG CAG ACC ATC GTG AAG CAC CCC AGA TAC ACC GGC ACC AAC AAC ACC GAC AAG ATC AAC CTG ACA GCC CCA AGA GGC GGA GAT CCC GAA GTG ACC TTT ATG TGG ACC AAC TGC AGG GGC GAG TTC CTG TAC TGC
 K   Q   T   I   V   K   H   P   R   Y   T   G   T   N   N   T   D   K   I   N   L   T   A   P   R   G   G   D   P   E   V   T   F   M   W   T   N   C   R   G   E   F   L   Y   C

            1,090      1,100      1,110      1,120      1,130      1,140      1,150      1,160      1,170      1,180      1,190      1,200      1,210
AAG ATG AAC TGG TTC CTG AAC TGG GTC GAA GAT AGG GAC CTG ACC ACA CAG AGG CCC AAA GAG AGG CAT AGA AGA AAC TAC GTG CCC TGC CAC ATC AGG CAG ATC ATC AAC ACC TGG CAC AAA GTG GGC AAG AAC
 K   M   N   W   F   L   N   W   V   E   D   R   D   L   T   T   Q   R   P   K   E   R   H   R   R   N   Y   V   P   C   H   I   R   Q   I   I   N   T   W   H   K   V   G   K   N

    1,220      1,230      1,240      1,250      1,260      1,270      1,280      1,290      1,300      1,310      1,320      1,330      1,340      1,350
GTG TAC CTG CCA CCT AGA GAG GGC GAC CTG ACC TGC AAT TCT ACC GTG ACC AGC CTG ATC GCT AAC ATC GAC TGG ACC GAC GGC AAC CAG ACC AAT ATC ACC ATG TCT GCC GAG GTG GCC GAG CTG TAC AGA CTG
 V   Y   L   P   P   R   E   G   D   L   T   C   N   S   T   V   T   S   L   I   A   N   I   D   W   T   D   G   N   Q   T   N   I   T   M   S   A   E   V   A   E   L   Y   R   L

            1,360      1,370      1,380      1,390      1,400      1,410      1,420      1,430      1,440      1,450      1,460      1,470      1,480
GAA CTG GGA GAC TAC AAG CTG GTG GAA ATC ACC CCA ATC GGA CTG GCC CCA ACC GAC GTG AAA AGA TAT ACC ACC GGC GGC ACC TCC AGA AAC AAG AGA GGC GTG TTC GTT CTG GGC TTC CTG GGA TTT CTG GCC
 E   L   G   D   Y   K   L   V   E   I   T   P   I   G   L   A   P   T   D   V   K   R   Y   T   T   G   G   T   S   R   N   K   R   G   V   F   V   L   G   F   L   G   F   L   A

    1,490      1,500      1,510      1,520      1,530      1,540      1,550      1,560      1,570      1,580      1,590      1,600      1,610      1,620
ACA GCC GGA TCT GCC ATG GGA GCT GCT TCT CTG ACA CTG ACC GCT CAG TCT AGA ACC CTG CTG GCT GGA ATC GTG CAG CAG CAG CAA CAG CTG CTG GAC GTG GTC AAG AGG CAG CAA GAA CTG CTG AGA CTG ACC
 T   A   G   S   A   M   G   A   A   S   L   T   L   T   A   Q   S   R   T   L   L   A   G   I   V   Q   Q   Q   Q   Q   L   L   D   V   V   K   R   Q   Q   E   L   L   R   L   T

            1,630      1,640      1,650      1,660      1,670      1,680      1,690      1,700      1,710      1,720      1,730      1,740      1,750
GTG TGG GGC ACC AAG AAT CTG CAG ACC AGA GTG ACC GCC ATC GAG AAG TAC CTG AAG GAT CAG GCC CAG CTG AAT GCC TGG GGA TGC GCC TTT AGA CAA GTG TGC CAT ACC ACC GTG CCT TGG CCA AAT GCC AGT
 V   W   G   T   K   N   L   Q   T   R   V   T   A   I   E   K   Y   L   K   D   Q   A   Q   L   N   A   W   G   C   A   F   R   Q   V   C   H   T   T   V   P   W   P   N   A   S

    1,760      1,770      1,780      1,790      1,800      1,810      1,820      1,830      1,840      1,850      1,860      1,870      1,880      1,890
CTG ACC CCT GAC TGG AAC AAC GAC ACA TGG CAA GAG TGG GAG AGA AAG GTG GAC TTC CTG GAA GAG AAC ATC ACC GCT CTG CTG GAA GAG GCC CAG ATC CAG CAA GAG AAG AAT ATG TAC GAG CTG CAG AAG CTG
 L   T   P   D   W   N   N   D   T   W   Q   E   W   E   R   K   V   D   F   L   E   E   N   I   T   A   L   L   E   E   A   Q   I   Q   Q   E   K   N   M   Y   E   L   Q   K   L

            1,900      1,910      1,920      1,930      1,940      1,950      1,960      1,970      1,980      1,990      2,000      2,010      2,020
AAC TCC TGG GAC GTG TTC GGC AAT TGG TTC GAC CTG GCC TCC TGG ATC AGA TAT ATC CAG TAC GGC ATC TAC ATC GTC GTG GGC GTG ATC CTG CTG AGG ATC GTG ATC TAT ATC GTG CAG ATG CTG GCC AAG CTG
 N   S   W   D   V   F   G   N   W   F   D   L   A   S   W   I   R   Y   I   Q   Y   G   I   Y   I   V   V   G   V   I   L   L   R   I   V   I   Y   I   V   Q   M   L   A   K   L

    2,030      2,040      2,050      2,060      2,070      2,080      2,090      2,100      2,110      2,120      2,130      2,140      2,150      2,160
AGG CAG GGC TAC AGA CCA GTG TTC TCC TCT CCA CCA TCC TAC TCT CAG CAG ACC CAC ATC CAA CAG GAT CCC GCT CTG CCC ACC AGA GAA GGC AAA GAA GGC GAC GGC GGA GAG TCC GGT GGA AAC TCT TCT TGG
 R   Q   G   Y   R   P   V   F   S   S   P   P   S   Y   S   Q   Q   T   H   I   Q   Q   D   P   A   L   P   T   R   E   G   K   E   G   D   G   G   E   S   G   G   N   S   S   W

            2,170      2,180      2,190      2,200      2,210      2,220      2,230      2,240      2,250      2,260      2,270      2,280      2,290
CCC TGG CAG ATC GAG TAT ATC CAC TTC CTG ATC CGC CAG CTG ATC AGA CTG CTG ACC TGG CTG TTC AAC AAC TGT AGG ACC CTG CTG TCC AGG GCC TAC CAG ATC CTG CAG CCA ATC CTG CAG AGA CTG TCT GCT
 P   W   Q   I   E   Y   I   H   F   L   I   R   Q   L   I   R   L   L   T   W   L   F   N   N   C   R   T   L   L   S   R   A   Y   Q   I   L   Q   P   I   L   Q   R   L   S   A

    2,300      2,310      2,320      2,330      2,340      2,350      2,360      2,370      2,380      2,390      2,400      2,410      2,420      2,430
GCC CTG CAG AGG ATC AGA GAG GTG CTG AGA ACC GAG CTG ACC TAC CTG CAG TAC GGC TGG TCT TAC TTC CAT GAA GCT GTG CAG GCT GGA TGG CGC TCT GCC ACA GAA ACA CTT GCT GGT GCT TGG GGC GAT CTG
 A   L   Q   R   I   R   E   V   L   R   T   E   L   T   Y   L   Q   Y   G   W   S   Y   F   H   E   A   V   Q   A   G   W   R   S   A   T   E   T   L   A   G   A   W   G   D   L

            2,440      2,450      2,460      2,470      2,480      2,490      2,500      2,510      2,517
TGG GAA ACA CTT AGA CGC GGC GGA AGA TGG ATC CTG GCT ATC CCC AGA AGA ATC AGG CAG GGC CTC GAA CTG ACA CTG CTG TGA TGA
 W   E   T   L   R   R   G   G   R   W   I   L   A   I   P   R   R   I   R   Q   G   L   E   L   T   L   L   *   *
```

Supplemental Table 7

Vaccine	ADCC Target					
	WT		DV1		DV1gpg	
	Mean titers	Risk	Mean titers	Risk	Mean titers	Risk
WT	1.8×10^5	R = –0.5511 p = 0.0431	6.1×10^4	R = 0.5941 p = 0.0306	2.6×10^5	NS
DV1	1×10^5	NS	2.4×10^5	R = 0.758 p = 0.0028	1.9×10^2	NS
DV1gpg	9.4×10^4	R = 0.6109 p = 0.029	2.5×10^5	R = 0.5103 p = 0.078	8.6×10^3	NS

Supplemental Table 8

		ID50 in TZM-bl cells[1]								IC80 in TZM-bl cells
		SIVmac251.6	SIVmac251 CS/RhPBMC	SIVmac251CS/RhPBMC	SIVmac251CS.41	SIVmac251/M766/HPBMC	SIVmac239CS.23	SIVmac251/221S	SVA-MLV	SIVmac251/221S
Animal group	Animal ID	Tier 1A	Tier 1	Tier 2	Tier 2	Tier 1B	Tier 3		neg ctrl	
WT	DGJL	64819	7367	106	59	2018	0	15821	0	0
	DGTW	241937	38488	71	0	3673	0	21179	0	-8
	DGFC	34516	17340	256	0	719	0	43712	0	8
	DGFP	59814	20252	-75	0	505	0	6800	0	0
	DGCL	201976	43483	502	0	203	-5	11447	0	0
	DGKC	173708	43554	125	0	674	0	12434	0	0
	DGAP	161664	43573	219	5	1080	-2	9679	0	1
	DGPi	194345	43468	-174	0	256	0	40089	0	0
	HNL	68389	1093	16	0	1	-2	9787	0	0
	HZR	82348	43623	1183	0	585	-3	27237	0	0
	H21X	101093	785	125	0	205	-1	23	0	0
	H29P	383455	1307	-17	0	208	-10	43710	0	-7
	H28C	29484	1302	142	0	252	0	10379	0	0
	H28E	173544	4377	0	0	201	-8	43720	0	-6
ΔV1	DGBP	124876	43527	77	0	575	0	43709	0	4
	DGMW	166248	43533	79	0	535	0	43720	0	0
	DGHW	20146	7992	37	103	535	-2	2954	0	0
	DGLW	105104	43549	127	99	830	18	11598	0	-2
	DG70	259551	43476	284	11	662	0	29501	0	0
	DGHD	58078	4130	10	28	1161	-18	34630	0	0
	HRM	198593	13349	-46	46	977	-18	13093	0	0
	TA9	1028762	1183	32	40	820	15	43720	0	3
	ZL47	22610	383	-21	57	184	-21	1578	0	5
	ZL51	35840	456	131	0	853	0	145	0	-1
	H16R	86658	1230	79	0	310	0	10601	0	0
	H24J	362770	1436	-96	2	651	0	43714	3	-6
	H22G	117221	478	-162	0	144	0	14811	0	0
	H28D	41640	794	70	0	304	-31	3596	0	-4
ΔV1gpg	DG80	139818	862	240	0	321	2	3103	0	0
	DGVi	901739	672	8	0	337	-6	43702	0	-3
	DGBL	191328	14917	12	0	389	1	12367	0	0
	DGLL	389068	43462	-34	25	1131	16	43700	0	0
	DGEC	538986	43442	-2	0	5346	-18	43708	0	0
	DGFW	1113991	43540	146	168	306	2	43720	0	0
	HZE	13713	1782	-22	0	513	-6	1708	0	0
	HZG	187452	1231	60	0	821	28	43720	0	-23
	DG65	126760	471	-215	0	261	11	43720	0	11
	DGEJ	59989	1786	17	0	263	0	7854	0	0
	H16Y	24128	341	78	0	105	-11	8288	0	1
	H23E									
	H23F	146123	278	-32	0	143	-4	43712	0	0
	H28H	2343720	486	0	0	210	0	43708	0	-1

Supplemental Table 9

```
1   GCT AGC GTG CCA GTG TGG AAA GAG GCC GAC ACC ACA CTG TTC TGC GCC TCT GAT GCC AAG GCT CAC GAA ACC
        V   P   V   W   K   E   A   D   T   T   L   F   C   A   S   D   A   K   A   H   E   T

    GAG GTG CAC AAT GTG TGG GCT ACC CAC GCC TGT GTG CCC ACC GAT CCA AAT CCA CAA GAG ATC GAC CTG GAA
    E   V   H   N   V   W   A   T   H   A   C   V   P   T   D   P   N   P   Q   E   I   D   L   E

    AAC GTG ACC GAG AAC TTC AAC ATG TGG AAG AAC AAC ATG GTC GAG CAG ATG CAA GAG GAC GTG ATC TCC CTG
    N   V   T   E   N   F   N   M   W   K   N   N   M   V   E   Q   M   Q   E   D   V   I   S   L

    TGG GAC CAG TCT CTG AAG CCC TGT GTG AAG CTG ACC CCA CCA TGT GTG ACC CTG CAC TGC ACC AAC GCT AAC
    W   D   Q   S   L   K   P   C   V   K   L   T   P   P   C   V   T   L   H   C   T   N   A   N

    CTG ACC AAG GCC AAT CTG ACC AAC GTG AAC AAC AGG ACC AAT GTG TCC AAC ATC ATC GGC AAC ATC ACC GAC
    L   T   K   A   N   L   T   N   V   N   N   R   T   N   V   S   N   I   I   G   N   I   T   D

    GAA GTG CGC AAC TGC TCT TTC AAC ATG ACC ACC GAG CTG CGC GAC AAG AAA CAG AAG GTG CAC GCC CTG TTC
    E   V   R   N   C   S   F   N   M   T   T   E   L   R   D   K   K   Q   K   V   H   A   L   F

    TAC AAG CTG GAC ATC GTG CCC ATC GAG GAC AAC AAC GAC TCC TCC GAG TAC AGG CTG ATC AAC TGC AAC ACC
    Y   K   L   D   I   V   P   I   E   D   N   N   D   S   S   E   Y   R   L   I   N   C   N   T

    TCC GTG ATC AAG CAG CCC TGT CCA AAG ATC AGC TTC GAC CCC ATT CCA ATC CAC TAC TGC ACC CCA GCC GGA
    S   V   I   K   Q   P   C   P   K   I   S   F   D   P   I   P   I   H   Y   C   T   P   A   G

    TAC GCC ATC CTG AAG TGC AAC GAC AAG AAT TTC AAC GGC ACC GGA CCA TGC AAG AAC GTG TCC TCT GTG CAG
    Y   A   I   L   K   C   N   D   K   N   F   N   G   T   G   P   C   K   N   V   S   S   V   Q

    TGT ACC CAC GGC ATC AAG CCA GTG GTG TCT ACC CAG CTG CTG CTG AAC GGA TCT CTG GCC GAG GAA GAG ATC
    C   T   H   G   I   K   P   V   V   S   T   Q   L   L   L   N   G   S   L   A   E   E   E   I

    ATC ATC AGA TCC GAG AAC CTG ACC AAC AAC GCC AAG ACC ATC ATC GTG CAC CTG AAC AAG TCC GTG GTC ATC
    I   I   R   S   E   N   L   T   N   N   A   K   T   I   I   V   H   L   N   K   S   V   V   I

    AAC TGT ACC AGG CCA TCC AAC AAC ACC AGG ACC TCC ATC ACC ATC GGA CCC GGC CAG GTT TTC TAC AGG ACC
    N   C   T   R   P   S   N   N   T   R   T   S   I   T   I   G   P   G   Q   V   F   Y   R   T

    GGC GAC ATC ATC GGA GAC ATC AGA AAG GCC TAC TGC GAG ATC AAC GGA ACC GAG TGG AAC AAG GCC CTG AAG
    G   D   I   I   G   D   I   R   K   A   Y   C   E   I   N   G   T   E   W   N   K   A   L   K

    CAA GTG ACC GAA AAG CTC AAA GAG CAC TTC AAC AAC AAG CCC ATC ATC TTC CAG CCA CCA TCC GGC GGA GAT
    Q   V   T   E   K   L   K   E   H   F   N   N   K   P   I   I   F   Q   P   P   S   G   G   D

    CTG GAA ATC ACC ATG CAC CAC TTC AAC TGC AGA GGC GAG TTC TTC TAC TGC AAT ACC ACC AGG CTG TTC AAC
    L   E   I   T   M   H   H   F   N   C   R   G   E   F   F   Y   C   N   T   T   R   L   F   N

    AAT ACC TGT ATC GCC AAT GGC ACC ATC GAG GGC TGC AAC GGA AAT ATC ACC CTG CCA TGC AAA ATC AAG CAG
    N   T   C   I   A   N   G   T   I   E   G   C   N   G   N   I   T   L   P   C   K   I   K   Q

    ATC ATC AAT ATG TGG CAA GGC GCC GGA CAG GCT ATG TAC GCT CCA CCA ATC TCC GGC ACC ATC AAC TGC GTG
    I   I   N   M   W   Q   G   A   G   Q   A   M   Y   A   P   P   I   S   G   T   I   N   C   V

    TCC AAC ATC ACC GGA ATC CTG CTG ACA AGA GAT GGC GGA GCC ACA AAC AAC ACT AAC AAC GAA ACC TTC AGA
    S   N   I   T   G   I   L   L   T   R   D   G   G   A   T   N   N   T   N   N   E   T   F   R

    CCC GGC GGA GGC AAC ATC AAG GAC AAT TGG AGG AAC GAG CTG TAC AAG TAC AAG GTG GTG CAG ATC GAG CCA
    P   G   G   G   N   I   K   D   N   W   R   N   E   L   Y   K   Y   K   V   V   Q   I   E   P

    CTG GGA GTT GCC CCA ACC AGA GCC AAG AGA AGA GTG GTG GAA CGC GAG AAG AGA TGA TGA GAA TTC
    L   G   V   A   P   T   R   A   K   R   R   V   V   E   R   E   K   R   *   *
```

Supplemental Table 10

```
1                                                  10                                                 20                                                 30                                                 40                                                 50                                                 60                                                 70
GCT AGC GTG CCA GTG TGG AAA GAG GCC GAC ACC ACA CTG TTC TGC GCC TCT GAT GCC AAG GCT CAC GAA ACC
     V   P   V   W   K   E   A   D   T   T   L   F   C   A   S   D   A   K   A   H   E   T

                                                   80                                                 90                                                100                                                110                                                120                                                130                                                140
GAG GTG CAC AAT GTG TGG GCT ACC CAC GCC TGT GTG CCC ACC GAT CCA AAT CCA CAA GAG ATC GAC CTG GAA
 E   V   H   N   V   W   A   T   H   A   C   V   P   T   D   P   N   P   Q   E   I   D   L   E

                                                  150                                                160                                                170                                                180                                                190                                                200                                                210
AAC GTG ACC GAG AAC TTC AAC ATG TGG AAG AAC AAC ATG GTC GAG CAG ATG CAA GAG GAC GTG ATC TCC CTG
 N   V   T   E   N   F   N   M   W   K   N   N   M   V   E   Q   M   Q   E   D   V   I   S   L

                                                  220                                                230                                                240                                                250                                                260                                                270                                                280
TGG GAC CAG TCT CTG AAG CCC TGT GTG AAG CTG ACC CCA CCA TGT GTG ACC CTG CAC TGC ACC AAC GCT AAC
 W   D   Q   S   L   K   P   C   V   K   L   T   P   P   C   V   T   L   H   C   T   N   A   N

                                                  290                                                300                                                310                                                320                                                330                                                340                                                350                                                360
CTG GAA GTG CGC AAC TGC TCT TTC AAC ATG ACC ACC GAG CTG CGC GAC AAG AAA CAG AAG GTG CAC GCC CTG
 L   E   V   R   N   C   S   F   N   M   T   T   E   L   R   D   K   K   Q   K   V   H   A   L

                                                  370                                                380                                                390                                                400                                                410                                                420                                                430
TTC TAC AAG CTG GAC ATC GTG CCC ATC GAG GAC AAC AAC GAC TCC TCC GAG TAC AGG CTG ATC AAC TGC AAC
 F   Y   K   L   D   I   V   P   I   E   D   N   N   D   S   S   E   Y   R   L   I   N   C   N

                                                  440                                                450                                                460                                                470                                                480                                                490                                                500
ACC TCC GTG ATC AAG CAG CCC TGT CCA AAG ATC AGC TTC GAC CCC ATT CCA ATC CAC TAC TGC ACC CCA GCC
 T   S   V   I   K   Q   P   C   P   K   I   S   F   D   P   I   P   I   H   Y   C   T   P   A

                                                  510                                                520                                                530                                                540                                                550                                                560                                                570
GGA TAC GCC ATC CTG AAG TGC AAC GAC AAG AAT TTC AAC GGC ACC GGA CCA TGC AAG AAC GTG TCC TCT GTG
 G   Y   A   I   L   K   C   N   D   K   N   F   N   G   T   G   P   C   K   N   V   S   S   V

                                                  580                                                590                                                600                                                610                                                620                                                630                                                640
CAG TGT ACC CAC GGC ATC AAG CCA GTG GTG TCT ACC CAG CTG CTG CTG AAC GGA TCT CTG GCC GAG GAA GAG
 Q   C   T   H   G   I   K   P   V   V   S   T   Q   L   L   L   N   G   S   L   A   E   E   E

                                                  650                                                660                                                670                                                680                                                690                                                700                                                710                                                720
ATC ATC ATC AGA TCC GAG AAC CTG ACC AAC AAC GCC AAG ACC ATC ATC GTG CAC CTG AAC AAG TCC GTG GTC
 I   I   I   R   S   E   N   L   T   N   N   A   K   T   I   I   V   H   L   N   K   S   V   V

                                                  730                                                740                                                750                                                760                                                770                                                780                                                790
ATC AAC TGT ACC AGG CCA TCC AAC AAC ACC AGG ACC TCC ATC ACC ATC GGA CCC GGC CAG GTT TTC TAC AGG
 I   N   C   T   R   P   S   N   N   T   R   T   S   I   T   I   G   P   G   Q   V   F   Y   R

                                                  800                                                810                                                820                                                830                                                840                                                850                                                860
ACC GGC GAC ATC ATC GGA GAC ATC AGA AAG GCC TAC TGC GAG ATC AAC GGA ACC GAG TGG AAC AAG GCC CTG
 T   G   D   I   I   G   D   I   R   K   A   Y   C   E   I   N   G   T   E   W   N   K   A   L

                                                  870                                                880                                                890                                                900                                                910                                                920                                                930
AAG CAA GTG ACC GAA AAG CTC AAA GAG CAC TTC AAC AAC AAG CCC ATC ATC TTC CAG CCA CCA TCC GGC GGA
 K   Q   V   T   E   K   L   K   E   H   F   N   N   K   P   I   I   F   Q   P   P   S   G   G

                                                  940                                                950                                                960                                                970                                                980                                                990                                               1,000
GAT CTG GAA ATC ACC ATG CAC CAC TTC AAC TGC AGA GGC GAG TTC TTC TAC TGC AAT ACC ACC AGG CTG TTC
 D   L   E   I   T   M   H   H   F   N   C   R   G   E   F   F   Y   C   N   T   T   R   L   F

1,010                                             1,020                                             1,030                                             1,040                                             1,050                                             1,060                                             1,070                                             1,080
AAC AAT ACC TGT ATC GCC AAT GGC ACC ATC GAG GGC TGC AAC GGA AAT ATC ACC CTG CCA TGC AAA ATC AAG
 N   N   T   C   I   A   N   G   T   I   E   G   C   N   G   N   I   T   L   P   C   K   I   K

                                                 1,090                                             1,100                                             1,110                                             1,120                                             1,130                                             1,140                                             1,150
CAG ATC ATC AAT ATG TGG CAA GGC GCC GGA CAG GCT ATG TAC GCT CCA CCA ATC TCC GGC ACC ATC AAC TGC
 Q   I   I   N   M   W   Q   G   A   G   Q   A   M   Y   A   P   P   I   S   G   T   I   N   C

                                                 1,160                                             1,170                                             1,180                                             1,190                                             1,200                                             1,210                                             1,220
GTG TCC AAC ATC ACC GGA ATC CTG CTG ACA AGA GAT GGC GGA GCC ACA AAC AAC ACT AAC AAC GAA ACC TTC
 V   S   N   I   T   G   I   L   L   T   R   D   G   G   A   T   N   N   T   N   N   E   T   F

                                                 1,230                                             1,240                                             1,250                                             1,260                                             1,270                                             1,280                                             1,290
AGA CCC GGC GGA GGC AAC ATC AAG GAC AAT TGG AGG AAC GAG CTG TAC AAG TAC AAG GTG GTG CAG ATC GAG
 R   P   G   G   G   N   I   K   D   N   W   R   N   E   L   Y   K   Y   K   V   V   Q   I   E

                                                 1,300                                             1,310                                             1,320                                             1,330                                             1,340                                             1,350                                             1,360   1,365
CCA CTG GGA GTT GCC CCA ACC AGA GCC AAG AGA AGA GTG GTG GAA CGC GAG AAG AGA TGA TGA GAA TTC
 P   L   G   V   A   P   T   R   A   K   R   R   V   V   E   R   E   K   R   *   *
```

Supplemental Table 11

```
1                   10                  20                  30                  40                  50                  60                  70
GCT AGC GTG CCA GTG TGG AAA GAG GCC GAC ACC ACA CTG TTC TGC GCC TCT GAT GCC AAG GCT CAC GAA ACC
     V   P   V   W   K   E   A   D   T   T   L   F   C   A   S   D   A   K   A   H   E   T

80                  90                  100                 110                 120                 130                 140
GAG GTG CAC AAT GTG TGG GCT ACC CAC GCC TGT GTG CCC ACC GAT CCA AAT CCA CAA GAG ATC GAC CTG GAA
 E   V   H   N   V   W   A   T   H   A   C   V   P   T   D   P   N   P   Q   E   I   D   L   E

150                 160                 170                 180                 190                 200                 210
AAC GTG ACC GAG AAC TTC AAC ATG TGG AAG AAC AAC ATG GTC GAG CAG ATG CAA GAG GAC GTG ATC TCC CTG
 N   V   T   E   N   F   N   M   W   K   N   N   M   V   E   Q   M   Q   E   D   V   I   S   L

220                 230                 240                 250                 260                 270                 280
TGG GAC CAG TCT CTG AAG CCC TGT GTG AAG CTG ACC CCA CCA TGT GTG ACC CTG CAC TGC AAC AAG AGC GAA}
 W   D   Q   S   L   K   P   C   V   K   L   T   P   P   C   V   T   L   H   C   N   K   S   E

290                 300                 310                 320                 330                 340                 350                 360
{ACC CAG ATG ATC GGC TGC TCT TTC AAC ATG ACC ACC GAG CTG CGC GAC AAG AAA CAG AAG GTG CAC GCC CTG
 T   Q   M   I   G   C   S   F   N   M   T   T   E   L   R   D   K   K   Q   K   V   H   A   L

370                 380                 390                 400                 410                 420                 430
TTC TAC AAG CTG GAC ATC GTG CCC ATC GAG GAC AAC AAC GAC TCC TCC GAG TAC AGG CTG ATC AAC TGC AAC
 F   Y   K   L   D   I   V   P   I   E   D   N   N   D   S   S   E   Y   R   L   I   N   C   N

440                 450                 460                 470                 480                 490                 500
ACC TCC GTG ATC AAG CAG CCC TGT CCA AAG ATC AGC TTC GAC CCC ATT CCA ATC CAC TAC TGC ACC CCA GCC
 T   S   V   I   K   Q   P   C   P   K   I   S   F   D   P   I   P   I   H   Y   C   T   P   A

510                 520                 530                 540                 550                 560                 570
GGA TAC GCC ATC CTG AAG TGC AAC GAC AAG AAT TTC AAC GGC ACC GGA CCA TGC AAG AAC GTG TCC TCT GTG
 G   Y   A   I   L   K   C   N   D   K   N   F   N   G   T   G   P   C   K   N   V   S   S   V

580                 590                 600                 610                 620                 630                 640
CAG TGT ACC CAC GGC ATC AAG CCA GTG GTG TCT ACC CAG CTG CTG CTG AAC GGA TCT CTG GCC GAG GAA GAG
 Q   C   T   H   G   I   K   P   V   V   S   T   Q   L   L   L   N   G   S   L   A   E   E   E

650                 660                 670                 680                 690                 700                 710                 720
ATC ATC ATC AGA TCC GAG AAC CTG ACC AAC AAC GCC AAG ACC ATC ATC GTG CAC CTG AAC AAG TCC GTG GTC
 I   I   I   R   S   E   N   L   T   N   N   A   K   T   I   I   V   H   L   N   K   S   V   V

730                 740                 750                 760                 770                 780                 790
ATC AAC TGT ACC AGG CCA TCC AAC AAC ACC AGG ACC TCC ATC ACC ATC GGA CCC GGC CAG GTT TTC TAC AGG
 I   N   C   T   R   P   S   N   N   T   R   T   S   I   T   I   G   P   G   Q   V   F   Y   R

800                 810                 820                 830                 840                 850                 860
ACC GGC GAC ATC ATC GGA GAC ATC AGA AAG GCC TAC TGC GAG ATC AAC GGA ACC GAG TGG AAC AAG GCC CTG
 T   G   D   I   I   G   D   I   R   K   A   Y   C   E   I   N   G   T   E   W   N   K   A   L

870                 880                 890                 900                 910                 920                 930
AAG CAA GTG ACC GAA AAG CTC AAA GAG CAC TTC AAC AAC AAG CCC ATC ATC TTC CAG CCA CCA TCC GGC GGA
 K   Q   V   T   E   K   L   K   E   H   F   N   N   K   P   I   I   F   Q   P   P   S   G   G

940                 950                 960                 970                 980                 990                 1,000
GAT CTG GAA ATC ACC ATG CAC CAC TTC AAC TGC AGA GGC GAG TTC TTC TAC TGC AAT ACC ACC AGG CTG TTC
 D   L   E   I   T   M   H   H   F   N   C   R   G   E   F   F   Y   C   N   T   T   R   L   F

1,010               1,020               1,030               1,040               1,050               1,060               1,070               1,080
AAC AAT ACC TGT ATC GCC AAT GGC ACC ATC GAG GGC TGC AAC GGA AAT ATC ACC CTG CCA TGC AAA ATC AAG
 N   N   T   C   I   A   N   G   T   I   E   G   C   N   G   N   I   T   L   P   C   K   I   K

1,090               1,100               1,110               1,120               1,130               1,140               1,150
CAG ATC ATC AAT ATG TGG CAA GGC GCC GGA CAG GCT ATG TAC GCT CCA CCA ATC TCC GGC ACC ATC AAC TGC
 Q   I   I   N   M   W   Q   G   A   G   Q   A   M   Y   A   P   P   I   S   G   T   I   N   C

1,160               1,170               1,180               1,190               1,200               1,210               1,220
GTG TCC AAC ATC ACC GGA ATC CTG CTG ACA AGA GAT GGC GGA GCC ACA AAC AAC ACT AAC AAC GAA ACC TTC
 V   S   N   I   T   G   I   L   L   T   R   D   G   G   A   T   N   N   T   N   N   E   T   F

1,230               1,240               1,250               1,260               1,270               1,280               1,290
AGA CCC GGC GGA GGC AAC ATC AAG GAC AAT TGG AGG AAC GAG CTG TAC AAG TAC AAG GTG GTG CAG ATC GAG
 R   P   G   G   G   N   I   K   D   N   W   R   N   E   L   Y   K   Y   K   V   V   Q   I   E

1,300               1,310               1,320               1,330               1,340               1,350               1,360   1,365
CCA CTG GGA GTT GCC CCA ACC AGA GCC AAG AGA AGA GTG GTG GAA CGC GAG AAG AGA TGA TGA GAA TTC
 P   L   G   V   A   P   T   R   A   K   R   R   V   V   E   R   E   K   R   *   *
```

Supplemental Tables

Table S1. DNA and protein sequence of SIV gp120$_{\Delta V1}$, Related to Figure 3. The tPA signal peptide that is cleaved in the mature protein (blue) and the position where the V1 region has been deleted in the immunogen (orange) are shown.

Table S2. DNA and protein sequence of SIVgp120$_{\Delta V1gpg}$, Related to Figure 3. The tPA signal peptide that is cleaved in the mature protein (blue) and the GPG sequence inserted in the immunogen (orange) are shown.

Table S3. DNA and protein sequence of SIVgp120$_{WT}$, Related to Figure 3. The HSV-1 gD leader sequence that is cleaved in the mature protein (red) and the V1 region deleted in the ΔV1 immunogen (orange) are shown.

Table S4. DNA and protein sequence of SIVgp160$_{WT}$, Related to Figure 3. The V1 region deleted in the ΔV1 immunogen is shown in orange.

Table S5. DNA and protein sequence of SIVgp160$_{\Delta V1}$, Related to Figure 3. The position where the V1 region has been deleted in the immunogen is shown in orange.

Table S6. DNA and protein sequence of SIVgp160$_{\Delta V1gpg}$, Related to Figure 3. The GPG sequence inserted in the immunogen is shown in orange.

Table S7. ADCC titers and risk of SIV$_{mac251}$ acquisition in the immunized groups, Related to Figure 4. Summary of ADCC activity measured in the immunized groups using the WT, ΔV1, and ΔV1gpg antigens to coat CEM cells.

Table S8. Serum neutralizing activity against tier 1, 2, and 3 SIV, Related to Figure 5 and Figure S8. The data represented are serum neutralizing activity of samples collected at week 17 subtracted from neutralizing activity of samples collected at baseline.

Table S9. DNA and protein sequence of HIV AE.A244 D11gp120$_{WT}$, Related to Figure 6. The V1 stem sequence is shown in blue and the V1 region is shown in orange.

Table S10. DNA and protein sequence of HIV AE.A244 D11gp120 $\Delta V1_a$, Related to Figure 6. Deletion of V1 is represented by brackets.

Table S11. DNA and protein sequence of HIV AE.A244 D11gp120 $\Delta V1_b$, Related to Figure 6. Deletion of V1 is represented by brackets.

Transparent Methods

Animal Studies

All animals used in this study were colony-bred rhesus macaques (*Macaca mulatta*), obtained from either Covance Research Products (Alice, Texas, USA) or the NIAID colony at Morgan Island, South Carolina, USA. The animals were housed and handled in accordance with the standards of the Association for the Assessment and Accreditation of Laboratory Animal Care International.

The first cohort of animals consisted of a total of 78 vaccinated animals, immunized with four different vaccine regimens, ALVAC-SIV/gp120+alum, ALVAC-SIV/gp120+MF59, DNA-SIV/ALVAC-SIV/gp120+alum or Ad26-SIV/ALVAC-SIV/gp120+alum, and 53 naïve controls, as previously reported (Vaccari et al., 2018; Vaccari et al., 2016). As a source of B cells for the molecular cloning of monoclonal antibodies, we used PBMCs from animal P770, a colony-bred rhesus macaque (*Macaca mulatta*) included in the study described in ref 8. Briefly, P770 was immunized at weeks 0, 4, 12, and 24 with intramuscular inoculations of 10^8 plaque-forming units (PFU) of ALVAC (vCP2432) expressing SIV *gag-pro* genes and gp120TM (Sanofi Pasteur). The sequence of the SIV genes was that of M766r, a mucosal transmitted founder variant of SIV_{mac251}. At weeks 12 and 24, the animal was administered a protein boost of 200 µg each of monomeric $SIV_{mac251\text{-}M766}$ gp120-gD and SIV_{smE660} gp120-gD CG7V, both formulated in alum, and administered in the thighs opposite to vCP2432 administration. Four weeks after the final immunization, the animal was challenged with 10 low-dose intrarectal 120 $TCID_{50}$ SIV_{mac251} administrations. At week 53, P770 underwent a second round of 9 immunizations with the combination of vCP2432 and 200 µg each of monomeric $SIV_{mac251\text{-}M766}$ gp120-gD and SIV_{smE660} gp120-gD CG7V, both formulated in alum, and administered in opposite thighs, every five weeks up to week 93. Starting at week 131, the animal was challenged weekly for 10 weeks using 120 $TCID_{50}$ of the same SIV_{mac251} challenge stock used at week 28 (**Fig. S2**). Animal P770 remained uninfected.

The second cohort included three groups of 14 animals each, vaccinated intramuscularly with 1 mg of SIVp57Gag DNA together with 2 mg of either SIV $gp160_{WT}$, $\Delta V1$, or $\Delta V1_{gpg}$ DNA at weeks 0 and 4. All

animals were administered ALVAC-SIV alone at week 8, and ALVAC-SIV simultaneously with a gp120+alum SIV_{mac251} $gp120_{M766}$ monovalent boost at week 12. Of note, a prior vaccine regimen using two inoculations of SIV-DNA (2 mg each of gp160 *env* and *gag*) and two of ALVAC-SIV administered simultaneously with a bivalent gp120+alum boosts SIV_{mac251} $gp120_{M766}$ and $SIV_{SM\ E660}$ $gp120_{GC7V}$ proteins) demonstrated 52% efficacy in macaques (Vaccari et al., 2018). Curiously, the decreased risk of SIV_{mac251} acquisition in that study correlated not with the homologous cyclic V2 peptide from $SIV_{mac251,}$ but rather with the heterologous $V2_{E543}$ from the SIV_{SME660} strain, suggesting that the V2 conformation may be more important than the primary amino acid sequence. Briefly, the DNA doses were formulated in sterile PBS in a final volume of 1.4mL containing 1 mg of SIVp57Gag DNA together with 2 mg of either SIV $gp160_{WT}$, $\Delta V1$, or $\Delta V1_{gpg}$, or SIV gp160 wild type DNA. Half of the dose was injected in each thigh, intramuscularly.

At weeks 8 and 12, all animals received an intramuscular immunization of 10^8 pfu of ALVAC-SIV vCP2432. At week 12, they received SIV M766 $gp120_{WT}$, $\Delta V1$, or $\Delta V1_{gpg}$ protein formulated in alum and administered in the contralateral thigh. Beginning five weeks after the last immunization (week 17), all vaccinated animals and a group of 18 naïve control animals, were exposed intrarectally to one weekly dose of SIV_{mac251} (stock day 8 from 2010) $TCID_{50}$ 400 (calculated in Rhesus 221 cells). Viral load was evaluated weekly and animals testing negative for SIV RNA in plasma were re-exposed, for a maximum of 11 weekly challenges.

Gp160 DNA Vaccine Preparation

The sequence of SIV *env* was obtained from M766r, a transmitted founder variant of SIV_{mac251} (M766.B9 GeneBank access code: KX089585.1). For the SIV gp160 DNA vaccinations, the $SIV_{mac251\text{-}M766r}$ *env* was codon optimized (Geneart) and cloned into pCLucF, downstream of the CMV promoter, replacing the luciferase gene. A Kozak sequence (gccgccaccATGg) was inserted at the start codon, and duplicate stop codons were included. For the SIV $gp160_{WT}$, the native signal peptide was replaced with a modified human tissue plasminogen activator signal (tPA) peptide (MDAMKRGLCCVLLLCGAVFVTTTEA). The gp160 (gp160 numbering based on SIV_{mac251}: from I20 to L88; or numbering based on SIV_{mac239}: I20 to

L879) was cloned in frame with the signal. For the SIV gp160 ΔV1 and ΔV1gpg mutants, the native signal peptide was utilized, and the V1 region (V1 region numbering based on $SIV_{mac251:}$ from D119 through E165; V1 region numbering based on SIV_{mac239}: from D119 through E163) was deleted. For ΔV1gpg, the deleted V1 region was replaced with Gly-Pro-Gly.

For the protein vaccinations, $SIV_{mac251\text{-}M766}$ gp120s were expressed in Chinese Hamster Ovary (CHO) cells. The codon optimized M766r *env* was terminated at R527, based on SIV_{mac251} numbering , (or R525 based on SIV_{mac239} numbering) with duplicate stop codons. The ΔV1 and ΔV1gpg have the same V1 region mutations as described for the gp160 mutants. The native signal peptide was deleted prior to I20 and was replaced with the herpes simplex virus type 1 glycoprotein D (HSV-1 gD) leader sequence (MGGAAARLGAVILFVVIVGLHGVRGKYALADASLKMADPNRFRGKDLPVLDQL) for the WT construct. For the ΔV1 and ΔV1gpg mutants, the signal peptide was replaced with the modified tPA signal. The WT gene was cloned into pSWTIPK3 (Advanced BioScience Laboratories, Inc.) downstream of the CMV promoter and Kozak sequence. Protein was expressed in stably transfected and cloned suspension-adapted CHO-S cells (Life Technologies). The ΔV1 and ΔV1gpg mutant genes were cloned into pSWTIPK3 (Advanced BioScience Laboratories, Inc.) downstream of the CMV promoter and Kozak sequence. Proteins were expressed in transiently transfected CHO-S cells using polyethyleneimine (PEI). Proteins were purified from the conditioned cell culture supernatant using a lectin-affinity chromatography (*Galanthus nivalis* lectin agarose; Vector Labs, Inc.) capture step, followed by anion exchange chromatography (Q-Sepharose; GE Healthcare Life Sciences) operated in flow through mode. Proteins were buffer exchanged into Dulbecco's phosphate buffered saline (DPBS) and filtered with 0.22μm filter.

Cloning of monoclonal antibodies from vaccinated and protected animal P770

The protein scaffold 1J08 has previously been shown to exhibit the SIV Env V1/V2 domain in the conformation naturally found on the native V1/V2 protomer basing on stable expression, clash score, and solvent accessibility. It was used here to identify V1/V2-specific B-cell clones and produced as previously described by Mason, *et al.* (Mason et al., 2016). The expression vector pVRC8400 encoding the C-

terminal His-tagged, averaged 1J08-scaffolded $SIV_{mac251\text{-}M766r}$ or SIV_{smE543} V1/V2 sequences (GenScript) was used to transfect 293Freestyle (293F) cells with the 293fectin transfection reagent (Invitrogen) following the company's instructions. Six days post-transfection, cell culture supernatants were harvested and filtered through a 0.22 µm filter and supplemented with protease inhibitor tablets (Roche). The constructs were passed through a NiSepharose excel affinity column (GE Healthcare) and further purified with size exclusion chromatography (SEC) on a HiLoad 16/600 200 pg Superdex column (GE Healthcare).

The mAbs NCI05 and NCI09 were cloned from the hyperimmunized, protected rhesus macaque P770 following the methods described by Mason, *et al.* (Mason et al., 2016). Briefly, frozen PBMCs taken from this animal at week 85 (two weeks after the 7th hyperimmunization) were thawed and stained to allow the identification of $CD20^+$ (clone 2H7, Cy55PerCP, BioLegend, San Diego, California, USA), $CD3^-$ (clone SP34-2, Brilliant Violet 421, BD Biosciences, San Jose, California, USA), $CD4^-$ (clone OKT4, Brilliant Violet 421, BioLegend), $CD8^-$ (clone RPA-T8, Brilliant Violet 421, BioLegend), $CD14^-$ (clone M5E2, Brilliant Violet 421, BioLegend), IgG^+ (G18-145, Alexa flour 680, BD Biosciences), and IgM^- (clone G20-127, FITC, BD Biosciences). After staining, the cells were washed twice with PBS and resuspended in 200 µl of PBS containing 1J08 $SIV_{mac251\text{-}M766}$ V1/V2 conjugated to APC and 1J08 SIV_{smE543} V1/V2 conjugated to PE, and then incubated in the dark for 15 min at room temperature (RT). The cells were then washed in PBS, analyzed, and sorted with a modified 3-laser FACSAria cell sorter using the FACSDiva software (BD Biosciences). Cells that were positive for binding to only SIV_{smE543}/V1/V2 or to both SIV_{smE543} and SIV_{mac251}/V1/V2 were singularly sorted into 96-well plates containing lysis solution. Flow cytometric data was analyzed with FlowJo 9.7.5.

Total RNA was reverse-transcribed in each well, and the rhesus immunoglobulin heavy (H), light kappa (Lκ), and light lambda (Lλ) chain variable domain genes were amplified by nested PCR. Positive amplification products as analyzed on 2% agarose gel (Embi-Tec) were sequenced, and those that were identified as carrying either Igγ, IgLκ, or IgLλ sequences were re-amplified with sequence-specific primers carrying unique restriction sites using the first-round nested PCR products as a template. Resulting PCR

products were run on a 1% agarose gel, purified with QIAGEN Gel Extraction Kit (QIAGEN), and eluted with 25µl of nuclease-free water (Quality Biological). Purified PCR products were then digested and ligated into rhesus Igγ, IgLκ, and IgLλ expression vectors containing a multiple cloning site upstream of the rhesus Igγ, Igκ, or Igλ constant regions. The vectors were designed by Dr. Saunders and kindly provided by Dr. Mascola of the NIH Vaccine Research Center (Bethesda, Maryland, USA). Full-length IgG were expressed by co-transfecting 293F cells with equal amounts of paired heavy and light chain plasmids, then purified using Protein A Sepharose beads (GE Healthcare) according to the manufacturer's instructions.

V2 mAbs binding to SIV_{mac239} infected A66 cells

The ability of mAbs to bind to SIV_{mac239} envelope expressed on the surface of infected A66 cells was evaluated by indirect surface staining using methods similar to those previously described[51]. Briefly, mock-infected and SIVmac239-infected A66 cells expressing NHP CD4 and CCR5 were incubated with test anti-SIV V2 (NCI05 and NCI09) or different control antibodies (JV16 antibody: SIV-mac239-infected pigtail polyclonal serum; NHP-SN: negative-control serum from a naïve Rhesus macaque; CH65: a human anti-Flu mAb with engineered NHP Fc region; Ab903793: Rhesus mAb isolated from HIV-1 immunized NHP, Rh IgG mAb a Rhesus monoclonal IgG isotype) for 2h at 37˚C, then stained Live/Dead Aqua to eliminate dead cells from analysis. BD Cytofix/Cytoperm was then used to wash and permeabilize cells. Cells were washed again and stained with secondary Phycoerythrin (PE)-conjugated anti-rhesus IgG (Goat anti-Rhesus IgG, catalog # 6200-09; Southern Biotech) and FITC-conjugated anti-p24 (KC57, Beckman Coulter) to select for infected cells. We analysed the results obtained in the live, $p24^+$, $FITC^+$ population. Final results are reported as the percentage of FITC-positive cells and FITC MFI among the p24-positive events, having subtracted background secondary antibody binding and signal received from mock-infected cells. Assays were carried out in duplicate for each sample.

Capture of SIV_{mac251} virions by MNPs coated with V2 mAbs

Virions from SIV_{mac251} preparation were captured with 15 nm magnetic nanoparticles (MNPs) coupled to NCI05, NC09, mouse IgG, or Rhesus recombinant IgG1 (NHP Reagent Resource, clone DSPR1) mAbs as previously described (Arakelyan et al., 2013). Briefly, carboxyl-terminated iron oxide nanoparticles (Ocean Nanotech, San Diego) were coated with 1 mg of mAbs according to manufacturer's protocol via two step carbodiimide reaction. In order to capture virions, MNPs coated with mAbs (3.9×10^{12}) in 60 µl were incubated with 100µl of viral preparation (10 ng/ml based on p27 content) for 1 h at 37°C. Captured virions were separated on MACS magnetic columns attached to an OctoMacs magnet (Miltenyi Biotech, Bergisch Gladbach, Germany), washed 4 times with 600 µl (0.5% bovine serum albumin, 2mM EDTA in PBS), and eluted in 100 µl PBS. The SIV RNA levels were measured by droplet digital PCR (ddPCR).

ELISA Monoclonal antibody (mAb) binding and in vitro *competition assays*

The ITS41 mAbs was isolated from an SIV_{smE660}-infected rhesus macaque. ITS41 recognizes the EQEQMISCKFTNMTGL peptide (sequence based on SIV_{mac239}) that is part of the V1 epitope as previously reported (Mason et al.). The monoclonal antibodies, NCI04, NCI06, NCI05, and NCI09 were generated in the present work. Binding of SIV-specific mAbs to viral proteins or synthetic peptides was measured by enzyme-linked immunosorbent assay (ELISA). Plates were coated overnight at 4ºC with 50 µl, 100 ng/well of antigen in PBS, then blocked with 300 µl/well of 1% PBS-BSA for 1 h at 37ºC. When cyclic V2 (cV2) was tested, plates were coated at 4ºC overnight with 200 ng/well of streptavidin (Sigma-Aldrich) in bicarbonate buffer, pH 9.6, then incubated with biotinylated cV2 peptide (produced by JPT Peptide Technologies) for 1 h at 37ºC and blocked with 0.5% milk in 1× PBS, 0.1% Tween 20, pH 7.4, overnight at 4ºC. Coated, blocked plates were incubated with 40 µl/well of serial dilutions of mAbs in 1% PBS-BSA for 1 h at 37ºC. Then, 40 µl/well of a polyclonal preparation of Horseradish peroxidase conjugated goat anti-monkey IgG antibody (Abcam) were added to the plate at 1:30,000 and incubated for 1 h at 37ºC. Plates were washed between each step with 0.05% Tween 20 in PBS. Plates were developed using either 3,3´or ,5,5´- tetramethylbenzidine (TMB; Thermo Fisher Scientific, Waltham, Massachusetts, USA) and read at 450 nm. When testing binding to linear peptides, cyclic V2, or 1J08 V1/V2 scaffolds, a ratio of the molecular weights of these constructs to the native glycoprotein monomer was calculated to obtain coating with the same number of epitopes/well. Competition assays of anti-V2

mAbs were performed by enzyme-linked immunosorbent assay (ELISA) as described by Mason, *et al.* (Mason et al.), and Sautto, *et al.* (Sautto et al., 2012). Briefly, plates were coated with 100 ng/well of purified proteins $SIV_{mac251\text{-}M766}$/gp120 (Advanced BioScience Laboratories, Inc.) and SIV_{smE660} 1J08 V1/V2 scaffold (Fazi et al., 2002; Mason et al., 2016), and blocked with 1% PBS/BSA. Serial dilutions of unbiotinylated competitor mAbs in 1% PBS-BSA were then added to the wells for 15 min prior to the addition of biotinylated probe mAbs at a concentration to yield ~50% saturating OD450. After incubation with streptavidin-HRP (KPL) for 1 h at 37ºC, signal was developed through incubation with 3 TMB substrate (Thermo Fisher Scientific) and optical density (OD) read at 450 nm. Two negative (1% PBS/BSA or serial dilutions of anti-CD4bs mAb ITS01) and one positive (serial dilutions of unbiotinylated probe mAb) controls of competition were included in each assay.

V1 and V2 mAbs competition assay to SIVmac251 infected PBMC

Peripheral blood mononuclear cells (PBMCs) from Rhesus macaques were isolated by centrifugation of EDTA whole blood on a Ficoll-Paque Plus gradient. $CD8^+$ T cells were depleted using CD8 beads (Miltenyi Bio Beads) and stimulated for three days in PHA followed by *in vitro* infection with SIV_{mac251}. Cells were maintained in RPMI containing 15% FBS, 1% Penicillin Streptomycin, 1% glutamine, and 40 IU/mL of IL-2 for at least 3 days at 37ºC, 5% CO_2, and P27 levels were assayed by ELISA to measure productive viral replication. Following at least 3 days of culture, infected or naïve cells from the same animal were centrifuged in PBS and resuspended to $1x10^6$ cells/mL, and $1x10^6$ cells were pelleted in separate FACS tubes.

To assess competition between anti-V1a and V2 antibodies, the cell pellets were resuspended in 100 µL of a 1:1 PBS serial dilution of ITS41 mAb starting at 2.5µg/mL and incubated for 30 min at RT. Cells were washed in 1 mL PBS and centrifuged at 2,000 RPM for 6 min, resuspended in 50 µL of PBS containing 1.9 µg of NCI09 mAb directly conjugated with AlexaFluor 647 (Thermo Fisher Scientific), and incubated in the dark for 30 min at RT. Cells were washed and incubated in the dark for 30 min at RT with 150 µL of antibody solution containing CD3-AlexaFluor 700 (BD Pharmingen, clone SP34-2, Cat. #557917), CD4-

PerCP-Cy5.5 (BD Pharmingen, Cat. #552838), and LIVE/DEAD Fixable Aqua Dead Cell Stain (Thermo Fisher Scientific) in PBS. Cells were washed and fixed in 300 µL of PBS containing 1% formaldehyde overnight. Samples were acquired with LSR-II or FACS Symphony flow cytometers and analyzed with FlowJo 10.5.0 (Treestar, Inc., Ashland, Oregon, USA).

Binding of gp120 mutant proteins to V1 and V2 mAbs

The ability of the gp120 mutants (WT, ΔV1, or $\Delta V1_{gpg}$) to be bound by V1 and V2 mAbs was measured by ELISA. ELISA plates were coated overnight with 40 µl, 100 ng of $SIV_{mac251\text{-}M766}$/gp120 mutants ($gp120_{WT}$, ΔV1, or $\Delta V1_{gpg}$) in PBS, washed once with PBS, and blocked with 100 µl of 1% BT3 (150mM NaCl, 50mM Tris-HCl, 1mM EDTA, 3.3% fetal bovine serum, 2% bovine albumin, 0.07% Tween-20) for 3 h at 37ºC. NCI06, NCI05 or NCI09 mAb were serial diluted in BT3 in a 4-point 10-fold dilution. Starting at 20000ng/mL, 40 µl were added to the plate and incubated for 1 h at 37ºC. The plates were washed three times with PBS 0.05% Tween 20, pH 7.4, and incubated with anti-monkey HRP (cat. #ab112767, Abcam) 1:10,000 in PBS for 1 h at 37ºC. Plates were developed using TMB (Thermo Fisher Scientific) and optical density (O.D.) read at 450 nm.

Binding of gp120 mutant proteins to CD4 molecule

The ability of the gp120 mutants (WT, ΔV1, or $\Delta V1_{gpg}$) to bind to the CD4 molecule was measured by ELISA. ELISA plates were coated overnight with 40 µl, 100 ng of $SIV_{mac251\text{-}M766}$/gp120 mutants ($gp120_{WT}$, ΔV1, or $\Delta V1_{gpg}$) in PBS, washed once with PBS, and blocked with 100 µl of 1% BT3 (150mM NaCl, 50mM Tris-HCl, 1mM EDTA, 3.3% fetal bovine serum, 2% bovine albumin, 0.07% Tween-20) for 3 h at 37ºC. CD4-Ig (1 mg/ml) were serial diluted in BT3 in an 8-point 4-fold dilution. Starting at 20 µg/mL, 40 µl were added to the plate and incubated for 1 h at 37ºC. The plates were washed three times with PBS 0.05% Tween 20, pH 7.4, and incubated with anti-monkey HRP (cat. #ab112767, Abcam) 1:10,000 in PBS for 1 h at 37ºC. Plates were developed using TMB (Thermo Fisher Scientific) and optical density (O.D.) read at 450 nm.

Immunoprecipitation and western blot

600 ng of wild type, ΔV1 $SIV_{mac251-M766}$/gp120 and ΔV1gpg $SIV_{mac251-M766}$/gp120 were incubated with 3.5 µg of NCI05 or NCI09 mAbs, respectively, in 400 µL of IP wash buffer (50 mM Tris, 120 mM NaCl, 5 mM EDTA, 0.1% NP40) on a rotator for 2 h at RT. Antibody-protein complexes were precipitated by incubation with 30 µL of washed Protein G-Agarose beads (Roche) on a rotator for 2 h at RT. Beads were washed twice, resuspended in 100 µL of 2x sample buffer with 10% β-mercaptoethanol, and boiled for 5 min at 100ºC. 25 µL of each supernatant was analyzed by western blot analysis with NCI05, NCI09, and rabbit α-gp120.

100 ng of $SIV_{mac251-M766}$/gp120 mutant (WT, ΔV1or ΔV1gpg) proteins were boiled for 5 min at 100ºC with 2x sample buffer with 10% β-mercaptoethanol. The denatured proteins or 25µl of immunoprecipitated proteins were separated by SDS-PAGE (NuPAGE™ 4-12% Bis-Tris Protein Gels, 1.0 mm, cat. #NP0321PK2, Thermo Fisher Scientific) for approximately 1 h at 100A and transferred to a 7.0 cm x 8.4 cm, 0.45 µm pore size, hydrophobic PVDF (Immobilon-P PVDF cat. #IPVH07850, Millipore Sigma Millipore), previously activated with methanol for 1 min. Proteins were transferred for 1 h at 140 mA. The membranes were incubated overnight at 4ºC with primary antibodies to NCI09 or NCI05 or ITS41 (1:2,000) in PBS containing 0.1% Tween 20 and 0.25% milk. Membranes were washed in PBS 0.1% Tween and exposed to a horseradish peroxidase-conjugated goat secondary anti-monkey antibody (1:10,000; Abcam #ab112767). Immunoreactivity proteins were visualized by chemiluminescence using a ChemiDoc™ Imaging System (Biorad). Densitometric analysis was performed using Image Lab Software.

The immune precipitation of the HIV gp120 proteins (AE.A244 D11gp120 WT or ΔV1) were performed with the same methodology described above. The antibodies used for immunoprecipitation were PG9, an anti-V2 antibody that recognizes V2 in β-Barrel conformation (Liao et al., 2013) (Anti-HIV-1 gp120 Monoclonal (PG9) was obtained from IAVI, cat# 12149, through the NIH AIDS Reagent Program, Division of AIDS, NIAID, NIH (Walker et al., 2009)) or CH58, an anti-V2 antibody that recognizes V2 in the α-helix

conformation (Liao et al., 2013) (CH58 was obtained from Drs. Barton F. Haynes and Hua-Xin Liao through the NIH AIDS Reagent Program, Division of AIDS, NIAID, NIH (Bonsignori et al., 2012; Liao et al., 2013)). Western blot was performed as describe above. The membranes were incubated either with CH58, 697-30D (Anti-HIV-1 gp120 Monoclonal (697-30D) was obtained from Dr. Susan Zolla-Pazner through the NIH AIDS Reagent Program, Division of AIDS, NIAID, NIH (Gorny et al., 1994)) or Rabbit gp120 SIV_{mac251} antiserum (cat# 5413, Advanced bioscience laboratories).

IgG plasma titers to gp120

Gp120 total IgG antibodies were measured by ELISA. ELISA plates (Nunc Maxisorp 96 well plate) were coated with 100 µl of 500 ng/ml $SIV_{mac251\text{-}M766}$ gp120 protein /well in 50 mM sodium bicarbonate buffer pH 9.6 and incubated overnight at 4ºC. Plates were blocked with 200 µl PBS Superblock (Thermo Fisher Scientific) for 1 h at RT. Plasma samples were serial-diluted with sample diluent (Avioq), and 100 µl of diluted plasma was added to the wells. Plates were covered and incubated for 1 h at 37ºC, washed 6 times with PBS Tween 20 (0.05%), and incubated with 100 µl anti-human HRP diluted at 1:120,000 in sample diluent (Avioq) for 1 h covered at 37ºC. The plates were washed 6 times. Plates were developed using 100 µl K-Blue Aqueous substrate (Neogen) to all wells and incubated for 30 min at RT. The reaction was stopped by the addition of 100 µl 2N Sulfuric acid to all wells and the plate was read at 450 nm on a Molecular Devices E-max plate reader.

Pepscan

Plasma samples were assayed by PEPSCAN analysis using SIV_{mac251} gp120 linear peptides as previously described (Demberg et al., 2013). ELISA plates (Nunc Maxisorp) were coated with 100 ng of each of the 1 to 89 overlapping peptides (with 15 amino acids each encompassing the entire SIV_{mac251} gp120 sequence) in 50 mM $NaHCO_3$, pH 9.6, per well, incubated overnight at 4ºC, and blocked with 200 µl of Pierce SuperBlock blocking buffer in PBS for 1 h at RT. Serum samples were diluted at 1:50 in sample diluent (Avioq), and 100 µl were added to the plate and incubated for 1 h at 37ºC. Plates were washed 6 times with PBS Tween 20 (0.05%) and incubated with 100 µl anti-human HRP diluted at

1:120,000 in sample diluent (Avioq) to all wells and incubated, covered, for 1 h at 37ºC. The plates were again washed 6 times and developed using 100 µl K-Blue Aqueous substrate (Neogen) to all wells and incubated 30 min at RT. The reaction was stopped by adding 100 µl 2N Sulfuric acid to all wells and read plate at 450 nm on a Molecular Devices E-max plate reader.

Neutralization activity of monoclonal antibodies

SIV pseudoviruses were produced as previously described (Abagyan and Totrov, 1994). Briefly, a luciferase reporter plasmid containing essential HIV genes was used in combination with a plasmid encoding for SIV gp160 to yield pseudo viruses exposing SIV Env on their surface. The plasmids used encoded SIV gp160, clones $SIV_{smE660.CP3C}$, $SIV_{smE660.CR54}$, $SIV_{mac251.H9}$, and $SIV_{mac251.30}$. Single-round infection of TZM-bl was detected quantitatively in relative light units (RLU). Virus neutralization was measured as the 50% inhibitory concentration of mAb necessary to cause a 50% reduction in RLU as compared to virus control wells after the subtraction of background RLU.

SIV-specific mucosal IgG-binding by antibody multiplex assay

Rectal mucosal env-SIV IgG was measured from rectal mucosa swabs collected at 2 weeks before vaccination and at week 14. Swabs were collected from animals in the WT, ΔV1, or ΔV1gpg groups by custom SIV binding antibody multiplex assays (SIV-BAMA) as previously described (Tomaras et al., 2013). Samples were processed, examined for blood contamination, and measured for semiquantitative evaluation of hemoglobin. The total IgG concentration was measured by a custom macaque total IgG ELISA using purified IgG (DBM5) from an SIV-infected macaque (Mason et al., 2016) as a positive control to calculate SIV antibody concentration. Antibodies against native V1/V2 epitopes were quantified by binding assays against scaffolded SIV V1/V2 antigens expressed as gp70 fusion proteins related to the CaseA2 antigen used in the RV144 correlate study (provided by A. Pinter, New Jersey Medical School, Newark, New Jersey, USA) (Pitisuttithum et al., 2006). These proteins contained the glycosylated, disulfide-bonded V1/V2 regions of SIV_{mac239}, SIV_{mac251}, and SIV_{smE660} (corresponding to AA 120–204 of HXB2 Env), fused to residue 263 of the Fr-MuLV SU (gp70) protein. The positive control for each antigen

was tracked via Levey–Jennings charts. Binding magnitude is reported as Specific Activity, calculated by the median fluorescence intensity (MFI) × dilution divided by total IgG (concentration in μg/ml).

$\alpha_4\beta_7$ integrin adhesion assay

We used a static adhesion assay to characterize the interaction between gp120 and $\alpha_4\beta_7$ based on the method developed by Dr. Peachman and colleagues (Peachman et al., 2015) in which RPMI8866 cells, which express $\alpha_4\beta_7$ on the cell surface, were allowed to adhere to the recombinant Env proteins (partly deglycosylated), V1/V2 scaffolds, or synthetic cyclic V2 peptides. The $\alpha_4\beta_7$-expressing RPMI8866 cell line was derived from a human B cell lymphoma, and expresses $\alpha_4\beta_7$, but no detectable CD4. Cells were grown in media containing retinoic acid, which increased the levels of both expression and clustering of $\alpha_4\beta_7$. In some assays, we included anti-integrin (Vedolizumab) and anti-gp120 mAbs or plasma as adhesion inhibitors. For plasma samples considered the cut-off of 15% of binding inhibition, combined with the condition that the percentage of inhibition from induced by plasma from week 17 should be at least 2x higher than the baseline. This cell-based assay measured adhesion between two multivalent surfaces.

Antibody binding measured by surface plasmon resonance

To characterize the interaction between gp120 and $\alpha_4\beta_7$, we developed a novel surface-plasmon resonance (SPR) -based assay that utilized dextran surfaces coated with recombinant Env proteins, V1/V2 scaffolds, or synthetic cyclic V2 peptides (Lertjuthaporn et al., 2018). The analyte that reacted with these surfaces was a recombinant soluble $\alpha_4\beta_7$ heterodimer in which the carboxy-terminal transmembrane and cytoplasmic tail domains of both chains were removed and replaced by short peptides that function as an "α_4 chain acid-β_7 chain base coiled-coil clasp" (Nishiuchi et al., 2006). This acid-base clasp was joined by a disulfide bond that served to stabilize the heterodimer. In one iteration of this assay, we employed short, linear peptides derived from V2 as competitive inhibitors.

Antibody-dependent neutrophil phagocytosis (ADNP)

ΔV1gp120 was biotinylated following manufacturer's instructions (Thermo Fisher Scientific) and incubated with yellow-green streptavidin-fluorescent beads (Molecular Probes) for 2 h at 37ºC. Here, 10 µl of a 100-fold dilution of beads–protein were incubated for 2 h at 37ºC with 100 µl diluted plasma samples before the addition of effector cells (50,000 cells/well). Fresh peripheral blood leukocytes from one healthy donor were used as effector cells after red blood cell lysis with ACK lysing buffer (Thermo Fisher Scientific). After 1 h incubation at 37ºC, the cells were washed, surface stained, fixed with 4% formaldehyde solution (Tousimis, Rockville, Maryland), and their fluorescence was evaluated on an LSRII (BD Biosciences). Anti-human CD3 AF700 (clone UCHT1) and anti-human CD14 APC-Cy7 (clone MϕP9) antibodies obtained from BD Biosciences, and anti-human CD66b Pacific Blue (clone G10F5) antibodies from Biolegend were used for flow cytometry. The phagocytic score was calculated by multiplying the percentage of bead-positive neutrophils (SSC high, $CD3^-$ $CD14^-$ $CD66^+$) by the geometric mean fluorescence intensity of the bead-positive cells and dividing by 10^4.

Antibody-dependent cell phagocytosis (ADCP)

ΔV1gp120 was biotinylated following manufacturer's instructions (Thermo Fisher Scientific) and incubated with yellow-green streptavidin-fluorescent beads (Molecular Probes) for 2 h at 37ºC. Here, 10µl of a 100-fold dilution of beads–protein were incubated for 2 h at 37ºC with 100 µl diluted plasma samples before the addition of THP-1 effector cells (25,000 cells/well). After 18 h of incubation at 37ºC, the cells were washed and fixed with 4% formaldehyde solution (Tousimis, Rockville, Maryland, USA), and fluorescence was evaluated on an LSRII (BD Biosciences). The phagocytic score was calculated by multiplying the percentage of bead-positive cells by the geometric mean fluorescence intensity of the bead-positive cells and dividing by 10^4.

ADCC against SIV_{mac251} infected cells

ADCC activity directed against SIV_{mac251}-infected target cells was determined by the ADCC-Luc assay as previously described (Pollara et al., 2011; Pollara et al., 2019). CEM.NKRCCR5 target cells were infected

with SIV_{mac251}. The infectious molecular clone virus encoding Renilla luciferase for 48 h and was then incubated with PBMC effector cells (30:1 effector cell/target cell ratio) and serum dilutions in half-area opaque flat bottom plates (Corning Life Sciences, Corning, New York, USA), in duplicate wells, for 6 h at 37°C and 5% CO2. ADCC activity, reported as percent specific killing, was calculated from the change in relative light units (RLU; ViviRen luciferase assay; Promega) resulting from the loss of intact target cells in wells containing effector cells, target cells, and serum samples compared to RLU in control wells containing target cells and effector cells alone according to the following formula: percent specific killing (number of RLU of target and effector well number of RLU of test well)/number of RLU of target and effector well. Adjusted percentages of specific ADCC killing were determined after subtracting the background activity observed for matched prevaccination samples and were reported as reciprocal dilution.

ADCC CEM-based assay.

We tested the percentage of CEM that reacted with the anti-V2 NCI05 and NCI09 mAbs coated with the gp120 immunogens. EGFP-CEM-NKr-CCR5-SNAP cells were incubated with 50 µg of gp120 protein WT, ΔV1, or ΔV1gpg for 2 h at 37ºC. After wash, coated cells were incubated with 5 µg/ml of NCI05 or NCI09 antibody at RT for 30 mins. The cells were washed and incubated with secondary IgG anti-monkey antibody conjugated with PE. Uncoated target cells in the presence of NCI05 or NCI09 and secondary antibody were used as negative control. Cells were acquired on a SORP LSR II (BD Biosciences) and analyzed using FlowJo Software (FlowJo, Ashland, OR).

ADCC activity was assessed as previously described using EGFP-CEM-NKr-CCR5-SNAP cells that constitutively express GFP as targets (Orlandi et al., 2016). Briefly, one million target cells were incubated with 50 µg of gp120 protein wild type, ΔV1, or ΔV1-gpg for 2 h at 37ºC. After this coating, the target cells were washed and labeled with SNAP-Surface® Alexa Fluor® 647 (New England Biolabs, Connecticut, USA S9136S) per manufacturer recommendations for 30 min at RT. Plasma samples, heat inactivated at 56ºC for 30 min, were serially diluted (7 ten-fold dilutions starting at 1:10) and 100 µl were added to wells

of a 96-well V-bottom plate (Millipore Sigma). 5000 target cells (50 µl) and 250,000 human PBMCs (50 µl) were added as effectors to each well to give an effector/target (E/T) ratio of 50:1. The plate was incubated at 37ºC for 2 h followed by two PBS washes. The cells were resuspended in 200 µl of a 2% PBS–paraformaldehyde solution and acquired on an LSRII equipped with a high throughput system (BD Biosciences, San Jose, California, USA). Specific killing was measured by loss of GFP from the SNAP-Alexa647^{+} target cells. Target and effector cells cultured in the presence of R10 medium were used as background. Anti-SIVmac gp120 monoclonal antibody KK17 (NIH AIDS reagent program) was used as a positive control. Normalized percent killing was calculated as: (killing in the presence of plasma – background)/ (killing in the presence of KK17- background) X100. The ADCC endpoint titer is defined as the reciprocal dilution at which the percent ADCC killing was greater than the mean percent killing of the background wells containing medium only with target and effector cells, plus three standard deviations.

Inhibition of ADCC CEM-based assay by monoclonal F(ab')$_2$ of NCI05 and NCI09

F(ab')$_2$ fragments were prepared from NCI04, NCI05 or NCI09 mAb using Pierce f(ab')2 Micro Preparation Kit (Cat#44688, Thermo scientific) following the manufacturer's instructions. A SDS-page gel with the recovered F(ab')$_2$ was run and Silver stained (Cat# LC6070, Silver Quest staining Kit, Invitrogen) according to the manufacturer's instructions, to assure the purity of the F(ab')$_2$ fragments. Target cells, coated with gp120 as indicated and labeled with SNAP-Surface® Alexa Fluor® 647, were incubated for 1 h at 37ºC with 6 ten-fold serial dilutions, beginning at 1 µg of purified F(ab')$_2$ fragments from NCI04, NCI05, or NCI09 monoclonal antibodies. Cells incubated without F(ab')$_2$ served as control. These target cells were subsequently used in the ADCC assay as described above.

Competitive ADCC assay

ITS41, a V1 monoclonal antibody, was used to compete with NCI05 or NCI09 -mediated ADCC activity. NCI04 monoclonal antibody served as an additional control. Six serial ten-fold dilutions of ITS41 and NCI04 were performed in a 96 well V-bottom plate beginning at 50 µg. In addition, 1 µg of the NCI05 or NCI09 antibody was added to each well. Target cells coated with the wild type gp120 protein and labeled

with SNAP-Alexa647 together with effector cells were added as described above for the ADCC assay. ADCC activity in both the presence and absence of competing antibodies was then determined. The experiment was repeated 3 times.

Serum neutralizing antibodies in the immunized animals

The levels of Neutralizing antibodies were measured in the plasma of animals from the three vaccinated group (WT, ΔV1, and ΔV1gpg) at baseline and week 17 (5 weeks after the last immunization) as a reduction in luciferase reporter gene expression after a single round of infection in TZM-b1 cells as described previously. TZM-bl cells were obtained from the NIH AIDS Research and Reference Reagent Program, contributed by John Kappes and Xiaoyun Wu. Test samples were serial diluted (3-fold dilution in duplicate) and incubated with 200 $TCID_{50}$ of virus in a total volume of 150 µl for 1 h at 37°C in 96-well flat-bottom culture plates. TZM-bl cells were trypsinized and added to each well (10,000 cells in 100 µl of growth medium containing 20 µg/ml DEAE dextran). A set of wells with cells and virus was used as virus control, and another set of wells with cells only was used as background control. After 48 h incubation, the cells were lysed by the addition of Britelite (PerkinElmer Life Sciences, Waltham, Massachusetts, USA), and three quarters of the cell lysate were transferred to a 96-well black solid plate (Corning Costar, Tewksbury, Massachusetts, USA) for luminescence measurement. Neutralization titers are defined as the dilution at which relative luminescence units were reduced by 50% or 80% compared to that in virus control wells after subtraction of background relative luminescence units. Neutralization was tested against the virus $SIV_{mac251.6}$ and $SIV_{mac239CS.23}$ (pseudoviruses produced in 293T cells), $SIV_{mac251CS/RhPBMC}$, $SIV_{mac251/M766/HPBMC}$ (replication competent viruses grown in activated human PBMCs and MLV), and $SIV_{mac251/221S}$.

$CD4^+$ T cell phenotypes

The levels of $CD4^+$ T cell subsets were measured in blood at week 17. PBMCs were stained with the following: PerCPCy5.5 anti-CD4 (L200; cat. #552838, 5 µl), AlexaFluor 700 anti-CD3 (SP34-2, cat. #557917, 0.2 mg/ml), and BV650 anti-CCR5 (3A9, 5 µl) PeCy5 anti-CD95 (DX2, #559773, 5 µl) from

BD Biosciences; PE-eFluor 610 anti-CD185 (CXCR5; MU5UBEE, #61-9185-42 5 µl) from eBiocence (San Diego, California, USA); APC Cy7 anti-CXCR3 (G025H7, cat. #353721, 5µl) and BV605 anti-CCR6 (G034E3, cat. #353419, 5 µl) from BioLegend (San Diego, California, USA); FITC anti-Ki67 (cat. #556026, 8µl, BD Biosciences), and APC anti-α4β7, provided by the NIH Nonhuman Primate Reagent Resource (R24 OD010976, and NIAID contract HHSN272201300031C). Gating was done on live $CD3^+CD4^+$ cells and on vaccine-induced $Ki67^+$ cells. CXCR3 and CCR6 expression was used to identify Th1 or Th2 populations, as previously described (Vaccari et al., 2018).

Measurement of viral RNA, DNA

SIV_{mac251} RNA in plasma was quantified by nucleic acid sequence-based amplification, as previously described (Romano et al., 1997). SIV DNA was quantified in mucosal tissues 3 weeks after infection by a real-time qPCR assay with sensitivity up to ten copies × 10^6 cells, as previously described (Lee et al., 2010).

Structural Analysis

The variable region of the NCI09 heavy chain was synthesized and cloned into a pVRC8400 vector containing an HRV3C cleavage site in the hinge region as previously described (McLellan et al., 2011). Heavy and light chain plasmids were co-expressed in 1 liter of Expi293F cells. IgG was purified from the supernatant through binding to a protein A Plus Agarose (Pierce) column and eluted with IgG Binding Buffer (Thermo Fisher Scientific). Antibodies were buffer-exchanged to PBS, then 10 mg of IgG were cleaved with HRV3C protease. The digested IgG was then passed over a 2 ml protein A Plus column to remove the Fc fragment. The Fab was further purified over a Superdex 200 gel filtration column in buffer containing 5 mM HEPES 7.5, 50 mM NaCl, and 0.02% NaN_3. To form NCI09-V2 peptide complexes, 5 mg of purified fab at a concentration of 2 mg/ml were incubated at RT for 30 min with a five-fold molar excess of SIV V2 peptide, synthesized by GenScript, and the complex was then concentrated down to 10 mg/ml using 10,000 MWCO Ultra centrifugal filter units (EMD Millipore). Antibody-peptide complexes were then screened against 576 crystallization conditions using a Mosquito crystallization robot mixing

0.1 µl of protein complex with 0.1 µl of the crystallization screening reservoir. Larger crystals were then grown by the vapor diffusion method in a sitting drop at 20ºC by mixing 1 µl of protein complex with 1 µl of reservoir solution (22% [w/v] PEG 4000, 0.1 M Na Acetate, pH 4.6). Crystals were flash-frozen in liquid nitrogen supplemented with 20% ethylene glycol as a cryoprotectant. Data were collected at 1.00 Å using the SER-CAT beamline ID-22 of the Advanced Photon Source, Argonne National Laboratory. Diffraction data were processed with an HKL-2000 (HKL Research). A molecular replacement solution obtained from Phenix (www.phenix-online.org) contained one Fab molecule per asymmetric unit in space group $P2_12_12_1$. Model building was carried out using COOT software (https://www2.mrc-lmb.cam.ac.uk/personal/pemsley/coot/) and was refined with Phenix. The Ramachandran plot determined by Molprobity http://molprobity.biochem.duke.edu) shows 98.2% of all residues in favored regions, and 100% of all residues in allowed regions for the complex structure.

Probe peptide design, mutational analysis and ELISA with gp120 mutants

Peptides specific for the epitopes in the region near the $\alpha_4\beta_7$ receptor site in the V2 loop of SIV_{mac251} and SIV_{mac543} (V2c) and distinct from the epitope targeted by NCI09 (V2b) were designed by NMR-validated, *ab initio* computational folding (Abagyan and Totrov, 1994; Aiyegbo et al., 2017; Almond and Cardozo, 2010; Almond et al., 2012) of overlapping fragments of amino acid segments 5 to 17 units in length from position 165 in the V2 loop to position 184 (Hxbc2 numbering). Optimal characteristics were considered as folding into an α-helix, and helical stability was assessed by the energy spectrum of the folding. The optimal fragment from SIV_{mac251} was 14 amino acids in length with sequence DKTKEYNETWYSTD, and its equivalent fragment from SIV_{SME543} was DKKIEYNETWYSRD. These peptide sequences were designed into probes suitable for ELISA by adding an N-terminal biotin and tri-glycine linker (biotin-GGG-V2c sequence) and synthesized commercially (Genemed Inc., San Francisco, California, USA). The point mutants described in the text were also synthesized commercially. ELISA assays for peptide reactivity were performed as previously described (Almond et al., 2012; Cardozo et al., 2014). Briefly, streptavidin coated plates were incubated for 3 h at RT in wash buffer (TBS, 0.1% BSA, 0.05% Tween – 20) with the biotinylated peptides at 100 µL/well, followed by an overnight incubation at 4ºC with serum samples or NCI05 at a concentration of 1:50 for the serum, and 1 µg/mL for the NCI05 mAb in 100 µL/well of wash

buffer. Plates were incubated for 2 h at RT with goat, anti-monkey IgG conjugated with alkaline phosphatase at 0.5µg/mL in 100µL/well of wash buffer. Plates were incubated with alkaline phosphatase substrate in developing buffer (PBS, 1M DEA, 0.24M MgCl2.6H2O, pH 9.8) and read at OD 405 nm.

HIV AE.A244 D11 gp120 ΔV1 protein expression.

The sequence of AE.A244 D11 gp120 recombinant protein was obtained from the CRFO1_AE Env gp120 subunit, derived from an individual chronically infected with HIV. The first 11 amino acids at the N-terminus of the mature Env protein have been deleted, as described by Alam *et al.* (Alam et al., 2013). For the purpose of this study, we designed an HIV gp120 mutant protein with deletion of the V1 region (TKANLTNVNNRTNVSNIIGNITD) identified here as AE.A244 D11gp120 $\Delta V1_a$. The protein/DNA sequence is represented in Table S9. The A244 WT and A244 $\Delta V1_a$ mutant genes were cloned into pSWTIPK3 (Advanced BioScience Laboratories, Inc.) downstream of the CMV promoter and Kozak sequence. Proteins were expressed in transiently transfected CHO-S cells using polyethyleneimine (PEI). Proteins were purified from the conditioned cell culture supernatant using a lectin-affinity chromatography (*Galanthus nivalis* lectin agarose; Vector Labs, Inc.) capture step, followed by anion exchange chromatography (Q-Sepharose; GE Healthcare Life Sciences) operated in flow-through mode. Proteins were buffer exchanged into Dulbecco's phosphate buffered saline (DPBS) and filtered with 0.22 µm filter.

Statistical analysis

Statistical analysis was performed using the Wilcoxon signed-rank test or Mann–Whitney test to compare continuous factors between two paired or unpaired groups, respectively. Comparison between multiple groups was done with the non-parametrical Kruskal-Wallis test with Dunn's multiple comparison test or the 2-way ANOVA test with Tukey's or Dunn's multiple comparison tests. Comparisons of differences between groups in the number of challenges before viral acquisition were assessed using the log-rank (Mantel–Cox) test of the discrete-time proportional hazards model. The average per-risk challenge of viral acquisition was estimated as the total number of observed infections divided by the number of

administered challenges. Correlation analyses were performed using the non-parametric Spearman rank correlation method with exact permutation two-tailed P values calculated.

Full wwPDB X-ray Structure Validation Report (i)

Dec 23, 2020 – 04:05 PM EST

PDB ID	:	6VRY
Title	:	Structure of NCI09 fab in complex with SIV V2 peptide
Authors	:	Gorman, J.; Ahmadi, M.; Kwong, P.D.
Deposited on	:	2020-02-10
Resolution	:	1.40 Å(reported)

This is a Full wwPDB X-ray Structure Validation Report for a publicly released PDB entry.

We welcome your comments at *validation@mail.wwpdb.org*
A user guide is available at
https://www.wwpdb.org/validation/2017/XrayValidationReportHelp
with specific help available everywhere you see the (i) symbol.

The following versions of software and data (see references (i)) were used in the production of this report:

MolProbity	:	4.02b-467
Mogul	:	1.8.5 (274361), CSD as541be (2020)
Xtriage (Phenix)	:	1.13
EDS	:	2.16
Percentile statistics	:	20191225.v01 (using entries in the PDB archive December 25th 2019)
Refmac	:	5.8.0158
CCP4	:	7.0.044 (Gargrove)
Ideal geometry (proteins)	:	Engh & Huber (2001)
Ideal geometry (DNA, RNA)	:	Parkinson et al. (1996)
Validation Pipeline (wwPDB-VP)	:	2.16

1 Overall quality at a glance (i)

The following experimental techniques were used to determine the structure:
X-RAY DIFFRACTION

The reported resolution of this entry is 1.40 Å.

Percentile scores (ranging between 0-100) for global validation metrics of the entry are shown in the following graphic. The table shows the number of entries on which the scores are based.

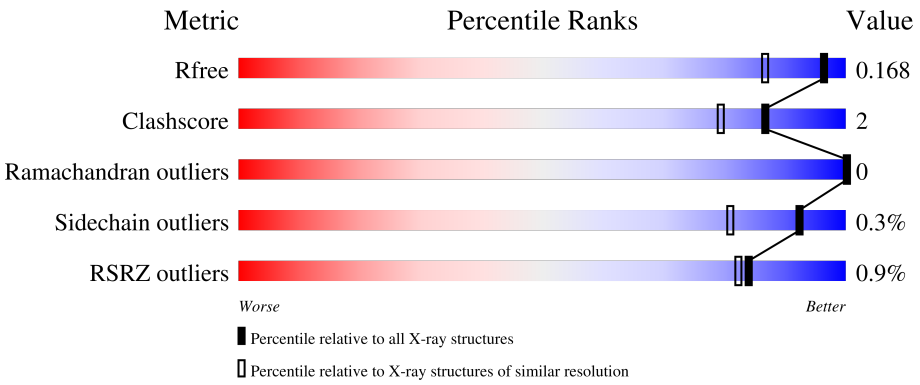

Metric	Whole archive (#Entries)	Similar resolution (#Entries, resolution range(Å))
R_{free}	130704	1714 (1.40-1.40)
Clashscore	141614	1812 (1.40-1.40)
Ramachandran outliers	138981	1763 (1.40-1.40)
Sidechain outliers	138945	1762 (1.40-1.40)
RSRZ outliers	127900	1674 (1.40-1.40)

The table below summarises the geometric issues observed across the polymeric chains and their fit to the electron density. The red, orange, yellow and green segments of the lower bar indicate the fraction of residues that contain outliers for >=3, 2, 1 and 0 types of geometric quality criteria respectively. A grey segment represents the fraction of residues that are not modelled. The numeric value for each fraction is indicated below the corresponding segment, with a dot representing fractions <=5% The upper red bar (where present) indicates the fraction of residues that have poor fit to the electron density. The numeric value is given above the bar.

Mol	Chain	Length	Quality of chain
1	L	214	.% 91% 9%
2	G	16	69% 31%
3	H	236	.% 94% • 5%
4	A	4	100%

2 Entry composition (i)

There are 5 unique types of molecules in this entry. The entry contains 7693 atoms, of which 3501 are hydrogens and 0 are deuteriums.

In the tables below, the ZeroOcc column contains the number of atoms modelled with zero occupancy, the AltConf column contains the number of residues with at least one atom in alternate conformation and the Trace column contains the number of residues modelled with at most 2 atoms.

- Molecule 1 is a protein called NCI09 light chain.

Mol	Chain	Residues	Atoms						ZeroOcc	AltConf	Trace
			Total	C	H	N	O	S			
1	L	214	3365	1069	1668	278	343	7	0	13	0

- Molecule 2 is a protein called SIV V2 peptide.

Mol	Chain	Residues	Atoms					ZeroOcc	AltConf	Trace
			Total	C	H	N	O			
2	G	11	202	61	102	18	21	0	1	0

There is a discrepancy between the modelled and reference sequences:

Chain	Residue	Modelled	Actual	Comment	Reference
G	173	ASN	-	expression tag	UNP P08810

- Molecule 3 is a protein called NCI09 heavy chain.

Mol	Chain	Residues	Atoms						ZeroOcc	AltConf	Trace
			Total	C	H	N	O	S			
3	H	225	3409	1090	1697	276	338	8	0	7	0

- Molecule 4 is an oligosaccharide called beta-D-mannopyranose-(1-4)-2-acetamido-2-deoxy-beta-D-glucopyranose-(1-4)-[alpha-L-fucopyranose-(1-6)]2-acetamido-2-deoxy-beta-D-glucopyranose.

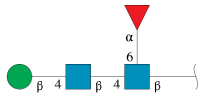

Mol	Chain	Residues	Atoms					ZeroOcc	AltConf	Trace
			Total	C	H	N	O			
4	A	4	83	28	34	2	19	0	0	0

- Molecule 5 is water.

Mol	Chain	Residues	Atoms		ZeroOcc	AltConf
			Total	O		
5	L	300	300	300	0	0
			Total	O		
5	G	26	26	26	0	0
			Total	O		
5	H	308	308	308	0	0

3 Residue-property plots (i)

These plots are drawn for all protein, RNA, DNA and oligosaccharide chains in the entry. The first graphic for a chain summarises the proportions of the various outlier classes displayed in the second graphic. The second graphic shows the sequence view annotated by issues in geometry and electron density. Residues are color-coded according to the number of geometric quality criteria for which they contain at least one outlier: green = 0, yellow = 1, orange = 2 and red = 3 or more. A red dot above a residue indicates a poor fit to the electron density (RSRZ > 2). Stretches of 2 or more consecutive residues without any outlier are shown as a green connector. Residues present in the sample, but not in the model, are shown in grey.

• Molecule 1: NCI09 light chain

Chain L:

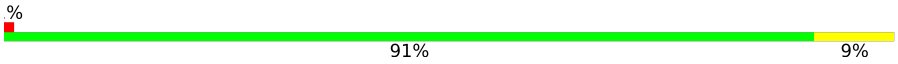

• Molecule 2: SIV V2 peptide

Chain G:

• Molecule 3: NCI09 heavy chain

Chain H:

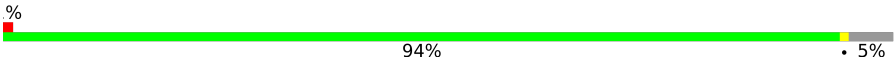

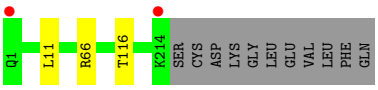

• Molecule 4: beta-D-mannopyranose-(1-4)-2-acetamido-2-deoxy-beta-D-glucopyranose-(1-4)-[alpha-L-fucopyranose-(1-6)]2-acetamido-2-deoxy-beta-D-glucopyranose

Chain A:

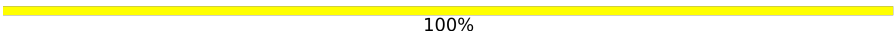

4 Data and refinement statistics (i)

Property	Value	Source
Space group	P 21 21 21	Depositor
Cell constants a, b, c, α, β, γ	65.76Å 72.09Å 100.83Å 90.00° 90.00° 90.00°	Depositor
Resolution (Å)	31.26 – 1.40 31.26 – 1.40	Depositor EDS
% Data completeness (in resolution range)	88.0 (31.26-1.40) 88.0 (31.26-1.40)	Depositor EDS
R_{merge}	0.04	Depositor
R_{sym}	(Not available)	Depositor
$< I/\sigma(I) >$ [1]	4.40 (at 1.40Å)	Xtriage
Refinement program	PHENIX (1.14_3260: ???)	Depositor
R, R_{free}	0.147 , 0.168 0.147 , 0.168	Depositor DCC
R_{free} test set	4175 reflections (5.00%)	wwPDB-VP
Wilson B-factor (Å^2)	13.7	Xtriage
Anisotropy	0.016	Xtriage
Bulk solvent k_{sol}(e/Å^3), B_{sol}(Å^2)	0.46 , 52.7	EDS
L-test for twinning[2]	$< \|L\| > = 0.49$, $< L^2 > = 0.32$	Xtriage
Estimated twinning fraction	No twinning to report.	Xtriage
F_o,F_c correlation	0.97	EDS
Total number of atoms	7693	wwPDB-VP
Average B, all atoms (Å^2)	20.0	wwPDB-VP

Xtriage's analysis on translational NCS is as follows: *The largest off-origin peak in the Patterson function is 5.02% of the height of the origin peak. No significant pseudotranslation is detected.*

[1]Intensities estimated from amplitudes.

[2]Theoretical values of $< |L| >$, $< L^2 >$ for acentric reflections are 0.5, 0.333 respectively for untwinned datasets, and 0.375, 0.2 for perfectly twinned datasets.

5 Model quality (i)

5.1 Standard geometry (i)

Bond lengths and bond angles in the following residue types are not validated in this section: BMA, NAG, FUC

The Z score for a bond length (or angle) is the number of standard deviations the observed value is removed from the expected value. A bond length (or angle) with $|Z| > 5$ is considered an outlier worth inspection. RMSZ is the root-mean-square of all Z scores of the bond lengths (or angles).

Mol	Chain	Bond lengths		Bond angles	
		RMSZ	$\#\|Z\| >5$	RMSZ	$\#\|Z\| >5$
1	L	0.50	0/1772	0.69	0/2410
2	G	0.51	0/103	0.69	0/133
3	H	0.52	0/1777	0.71	0/2425
All	All	0.51	0/3652	0.70	0/4968

There are no bond length outliers.

There are no bond angle outliers.

There are no chirality outliers.

There are no planarity outliers.

5.2 Too-close contacts (i)

In the following table, the Non-H and H(model) columns list the number of non-hydrogen atoms and hydrogen atoms in the chain respectively. The H(added) column lists the number of hydrogen atoms added and optimized by MolProbity. The Clashes column lists the number of clashes within the asymmetric unit, whereas Symm-Clashes lists symmetry-related clashes.

Mol	Chain	Non-H	H(model)	H(added)	Clashes	Symm-Clashes
1	L	1697	1668	1664	13	0
2	G	100	102	101	0	0
3	H	1712	1697	1697	2	0
4	A	49	34	43	0	0
5	G	26	0	0	0	0
5	H	308	0	0	1	4
5	L	300	0	0	4	4
All	All	4192	3501	3505	15	4

The all-atom clashscore is defined as the number of clashes found per 1000 atoms (including hydrogen atoms). The all-atom clashscore for this structure is 2.

All (15) close contacts within the same asymmetric unit are listed below, sorted by their clash magnitude.

Atom-1	Atom-2	Interatomic distance (Å)	Clash overlap (Å)
3:H:11:LEU:HD22	3:H:116[A]:THR:HG22	1.92	0.51
3:H:116[A]:THR:HG21	5:H:403:HOH:O	2.13	0.49
1:L:2:ILE:HG12	1:L:27:GLN:HG2	1.94	0.49
1:L:110[B]:VAL:HG21	1:L:199:GLN:OE1	2.14	0.47
1:L:15:PRO:HD3	1:L:107:LYS:O	2.15	0.47
1:L:24:ARG:NE	1:L:70:GLU:OE2	2.42	0.46
1:L:67[A]:SER:HB2	5:L:482:HOH:O	2.17	0.44
1:L:147:GLN:OE1	1:L:154[B]:LEU:HG	2.18	0.43
1:L:16:GLY:HA2	1:L:77:SER:OG	2.19	0.43
1:L:185:ASP:HA	1:L:188:LYS:HE2	2.01	0.43
1:L:147:GLN:HG2	1:L:154[B]:LEU:HD11	2.02	0.42
1:L:72[B]:THR:CG2	5:L:417:HOH:O	2.68	0.42
1:L:72[B]:THR:HG22	5:L:417:HOH:O	2.19	0.42
1:L:168[B]:SER:OG	5:L:402:HOH:O	2.22	0.41
1:L:125:LEU:O	1:L:183:LYS:HD2	2.21	0.40

All (4) symmetry-related close contacts are listed below. The label for Atom-2 includes the symmetry operator and encoded unit-cell translations to be applied.

Atom-1	Atom-2	Interatomic distance (Å)	Clash overlap (Å)
5:L:645:HOH:O	5:H:540:HOH:O[3_554]	1.84	0.36
5:L:659:HOH:O	5:H:552:HOH:O[3_554]	2.02	0.18
5:L:612:HOH:O	5:H:507:HOH:O[2_544]	2.06	0.14
5:L:656:HOH:O	5:H:555:HOH:O[4_444]	2.10	0.10

5.3 Torsion angles (i)

5.3.1 Protein backbone (i)

In the following table, the Percentiles column shows the percent Ramachandran outliers of the chain as a percentile score with respect to all X-ray entries followed by that with respect to entries of similar resolution.

The Analysed column shows the number of residues for which the backbone conformation was analysed, and the total number of residues.

Mol	Chain	Analysed	Favoured	Allowed	Outliers	Percentiles
1	L	225/214 (105%)	217 (96%)	8 (4%)	0	100 100

Continued on next page...

Continued from previous page...

Mol	Chain	Analysed	Favoured	Allowed	Outliers	Percentiles	
2	G	10/16 (62%)	10 (100%)	0	0	100	100
3	H	230/236 (98%)	227 (99%)	3 (1%)	0	100	100
All	All	465/466 (100%)	454 (98%)	11 (2%)	0	100	100

There are no Ramachandran outliers to report.

5.3.2 Protein sidechains (i)

In the following table, the Percentiles column shows the percent sidechain outliers of the chain as a percentile score with respect to all X-ray entries followed by that with respect to entries of similar resolution.

The Analysed column shows the number of residues for which the sidechain conformation was analysed, and the total number of residues.

Mol	Chain	Analysed	Rotameric	Outliers	Percentiles	
1	L	198/186 (106%)	198 (100%)	0	100	100
2	G	11/15 (73%)	11 (100%)	0	100	100
3	H	200/203 (98%)	199 (100%)	1 (0%)	88	74
All	All	409/404 (101%)	408 (100%)	1 (0%)	92	82

All (1) residues with a non-rotameric sidechain are listed below:

Mol	Chain	Res	Type
3	H	66	ARG

Sometimes sidechains can be flipped to improve hydrogen bonding and reduce clashes. All (1) such sidechains are listed below:

Mol	Chain	Res	Type
1	L	27	GLN

5.3.3 RNA (i)

There are no RNA molecules in this entry.

5.4 Non-standard residues in protein, DNA, RNA chains (i)

There are no non-standard protein/DNA/RNA residues in this entry.

5.5 Carbohydrates (i)

4 monosaccharides are modelled in this entry.

In the following table, the Counts columns list the number of bonds (or angles) for which Mogul statistics could be retrieved, the number of bonds (or angles) that are observed in the model and the number of bonds (or angles) that are defined in the Chemical Component Dictionary. The Link column lists molecule types, if any, to which the group is linked. The Z score for a bond length (or angle) is the number of standard deviations the observed value is removed from the expected value. A bond length (or angle) with $|Z| > 2$ is considered an outlier worth inspection. RMSZ is the root-mean-square of all Z scores of the bond lengths (or angles).

Mol	Type	Chain	Res	Link	Bond lengths			Bond angles		
					Counts	RMSZ	$\#\|Z\| > 2$	Counts	RMSZ	$\#\|Z\| > 2$
4	NAG	A	1	1,4	14,14,15	0.95	1 (7%)	17,19,21	0.55	0
4	NAG	A	2	4	14,14,15	0.62	1 (7%)	17,19,21	0.64	0
4	BMA	A	3	4	11,11,12	0.82	0	15,15,17	1.06	1 (6%)
4	FUC	A	4	4	10,10,11	0.89	0	14,14,16	1.07	2 (14%)

In the following table, the Chirals column lists the number of chiral outliers, the number of chiral centers analysed, the number of these observed in the model and the number defined in the Chemical Component Dictionary. Similar counts are reported in the Torsion and Rings columns. '-' means no outliers of that kind were identified.

Mol	Type	Chain	Res	Link	Chirals	Torsions	Rings
4	NAG	A	1	1,4	-	0/6/23/26	0/1/1/1
4	NAG	A	2	4	-	0/6/23/26	0/1/1/1
4	BMA	A	3	4	-	2/2/19/22	0/1/1/1
4	FUC	A	4	4	-	-	0/1/1/1

All (2) bond length outliers are listed below:

Mol	Chain	Res	Type	Atoms	Z	Observed(Å)	Ideal(Å)
4	A	1	NAG	O5-C1	-3.51	1.38	1.43
4	A	2	NAG	O5-C1	-2.23	1.40	1.43

All (3) bond angle outliers are listed below:

Mol	Chain	Res	Type	Atoms	Z	Observed(^{o})	Ideal(^{o})
4	A	3	BMA	C1-O5-C5	3.22	116.55	112.19
4	A	4	FUC	C1-O5-C5	2.27	117.92	112.78
4	A	4	FUC	C1-C2-C3	2.25	112.43	109.67

There are no chirality outliers.

All (2) torsion outliers are listed below:

Mol	Chain	Res	Type	Atoms
4	A	3	BMA	C4-C5-C6-O6
4	A	3	BMA	O5-C5-C6-O6

There are no ring outliers.

No monomer is involved in short contacts.

5.6 Ligand geometry (i)

There are no ligands in this entry.

5.7 Other polymers (i)

There are no such residues in this entry.

5.8 Polymer linkage issues (i)

There are no chain breaks in this entry.

6 Fit of model and data (i)

6.1 Protein, DNA and RNA chains (i)

In the following table, the column labelled '#RSRZ> 2' contains the number (and percentage) of RSRZ outliers, followed by percent RSRZ outliers for the chain as percentile scores relative to all X-ray entries and entries of similar resolution. The OWAB column contains the minimum, median, 95th percentile and maximum values of the occupancy-weighted average B-factor per residue. The column labelled 'Q< 0.9' lists the number of (and percentage) of residues with an average occupancy less than 0.9.

Mol	Chain	Analysed	<RSRZ>	#RSRZ>2	OWAB(Å^2)	Q<0.9
1	L	214/214 (100%)	-0.38	2 (0%) 84 82	8, 15, 34, 60	0
2	G	11/16 (68%)	-0.45	0 100 100	12, 18, 28, 32	0
3	H	225/236 (95%)	-0.51	2 (0%) 84 82	8, 15, 27, 49	0
All	All	450/466 (96%)	-0.44	4 (0%) 84 82	8, 15, 31, 60	0

All (4) RSRZ outliers are listed below:

Mol	Chain	Res	Type	RSRZ
3	H	1	GLN	5.0
1	L	214	CYS	4.9
3	H	214	LYS	2.9
1	L	212	GLY	2.5

6.2 Non-standard residues in protein, DNA, RNA chains (i)

There are no non-standard protein/DNA/RNA residues in this entry.

6.3 Carbohydrates (i)

In the following table, the Atoms column lists the number of modelled atoms in the group and the number defined in the chemical component dictionary. The B-factors column lists the minimum, median, 95th percentile and maximum values of B factors of atoms in the group. The column labelled 'Q< 0.9' lists the number of atoms with occupancy less than 0.9.

Mol	Type	Chain	Res	Atoms	RSCC	RSR	B-factors(Å^2)	Q<0.9
4	BMA	A	3	11/12	0.70	0.33	38,48,55,59	0
4	FUC	A	4	10/11	0.76	0.29	40,49,56,59	0
4	NAG	A	2	14/15	0.83	0.29	30,45,54,64	0
4	NAG	A	1	14/15	0.90	0.23	20,30,59,59	0

6.4 Ligands (i)

There are no ligands in this entry.

6.5 Other polymers (i)

There are no such residues in this entry.